“Submerged Vinegar Fermentation in Small Scale Culture Systems”

Von der Fakultät für Maschinenwesen
der Rheinisch-Westfälischen Technischen Hochschule Aachen
zur Erlangung des akademischen Grades
eines Doktors der Naturwissenschaften
genehmigte Dissertation

vorgelegt von

Tino Schlepütz

Berichter: Universitätsprofessor Dr.-Ing. Jochen Büchs
Universitätsprofessor Dr. rer. nat. Uwe Deppenmeier

Tag der mündlichen Prüfung: 27.08.2013

Diese Dissertation ist auf den Internetseiten der Hochschulbibliothek online verfügbar.



Dedicated to John Paul Gerhards

* 19th March 1987

† 10th February 2013

Acknowledgements

The current thesis was made at the Institute for Biochemical Engineering (AVT.BioVT) of the RWTH Aachen University. I am grateful to all the persons who made this dissertation possible.

I thank Prof. Dr.-Ing. Jochen Büchs for being my supervisor and examiner of this thesis. He gave me the opportunity to prepare my dissertation at AVT.BioVT. He was always open-minded and contributed very good ideas to my work. I thank him for his support, the productive discussions we had and his trust in me during all the time.

I thank Prof. Dr. rer. nat. Uwe Deppenmeier for his readiness to be the second examiner of this thesis.

I send warm thanks to all the students who helped me with my work: Rudolph Klementz, Sebastian Tobies, John Paul Gerhards, Nina Wilbertz, Kornelius Schweinfurth and Susanne Schwechheimer. They considerably contributed to the success of this work. Especially, I want to thank John who became a really good friend. We had so much fun and made such great plans. Unfortunately, these plans ceased much too early.

Moreover, I thank all the colleagues and students at AVT.BioVT and AVT.EPT (Enzyme Process Technology) for the nice atmosphere and their friendly aid. Without them the work would not have made that much fun. I give special thanks to Priya Philip and Tobias Ladner for proof reading this manuscript. Likewise, my thanks belong to all the staff of the electronic and mechanical workshop for always willingly producing my special devices as well as to our software developer for programming assistance.

I want to thank all my friends, not mentioned by name but knowing that they are meant, for their encouragements and fine distractions.

My deepest gratitude belongs of course to my girlfriend Tina Kitsche who was always there for me. She cheered me up and made my life easier. I thank her for her patience with me.

Last but not least my heartfelt thank belongs to my parents Inge and Hermann-Josef as well as my brother Marco for their enduring support not only during my doctoral studies.

Publications

Parts of this thesis have been published previously.

Peer reviewed articles:

1) Schlepütz T., Gerhards J. P. and Büchs J. “Ensuring constant oxygen supply during inoculation is essential to obtain reproducible results with obligatory aerobic acetic acid bacteria in vinegar production” Process Biochemistry, 2013: 48 (3) 398-405

2) Schlepütz T. and Büchs J. “Investigation of vinegar production using a novel shaken repeated batch culture system” Biotechnology Progress, 2013: (in press)

3) Schlepütz T. and Büchs J. “Scale-down of vinegar production into microtiter plates using a custom-made lid” Journal of Bioscience and Bioengineering, 2013: (submitted)

Conferences:

1) Schlepütz T. and Büchs J. „Scale-down der obligat aeroben Essigfermentation unter industriellen Konzentrationsverhältnissen“ DECHEMA Vortrags- und Diskussions-tagung: Bioverfahrenstechnik an Grenzflächen, 05/31/2011-06/01/2011, Potsdam, Germany; oral presentation

2) Schlepütz T. and Büchs J. 2012. “Small Scale Cultivation of Acetic Acid Bacteria for Vinegar Production” 3rd Third International Conference on Acetic Acid Bacteria Vinegar and Other Products, 04/17/2012-04/20/2012, Córdoba, Spain; poster presentation; abstract in: Acetic Acid Bacteria 2012:1 (1S) 30

Table of Contents

Nomenclature ..... **IV**

Abbreviations IV

Formula symbols IV

List of Figures ..... **VIII**

List of Tables ..... **X**

I Abstract **1**

II Deutsche Zusammenfassung **3**

1 Introduction **5**

1.1 Vinegar production by acetic acid bacteria 5

1.2 Repeated batch processes 8

1.3 Small scale cultivation methods 8

1.4 Objectives and Overview 12

2 Theory **13**

2.1 Introduction of the proposed shaken repeated batch culture system 13

2.2 Theoretical comparison of repeated batch in conventional bioreactor and the proposed flushing repeated batch in ShaRBS 14

2.2.1 Conventional repeated batch processes 15

2.2.2 Flushing repeated batch fermentation 16

2.3 Development of an oxygen analysis for the ShaRBS 18

2.3.1 Oxygen partial pressure in the headspace of ShaRBS during vinegar fermentation 18

2.3.2 Online calibration of oxygen sensor on ShaRBS 20

2.4 Design of custom-made lid for vinegar fermentation in microtiter plates 22

2.4.1 Oxygen balance in microtiter plate with custom-made lid 22

2.4.2 Oxygen balance of bioreactor for vinegar fermentation 25

2.4.3 Scale-down of vinegar fermentation from 9 L-bioreactor to microtiter plate 26

3 Materials and Methods 28

3.1 Chemicals 28

3.2 Devices 28

3.3 Setup of ShaRBS 29

3.4 Characterization of the ethanol sensors of the ShaRBS 31

3.5 Determination of oxygen partial pressure and oxygen transfer rate in ShaRBS 31

3.6 Fermentation 32

3.6.1 Preculture fermentation in 9 L-bioreactor 32

3.6.2 Shake flask fermentations in RAMOS 32

3.6.3 ShaRBS fermentations 35

3.6.4 Microtiter plate fermentations 36

3.7 Shut off experiment in bubble column 38

3.8 Gas chromatography 38

4 Results and Discussion 39

4.1 Vinegar fermentation in batch mode on shake flask scale 39

4.1.1 Shake flask fermentations according to the traditional procedure of inoculation 39

4.1.2 Shake flask fermentations according to the aerated inoculation scheme 41

4.1.2.1 Comparison of traditional procedure of inoculation with the aerated inoculation scheme 41

4.1.2.2 Influence of filling volume and aeration rate on oxygen mass transfer characteristic in shake flasks 43

4.1.2.3 Comparison of aeration with air or pure oxygen during inoculation 45

4.1.3 Respiration characteristics of acetic acid bacteria in shake flasks for vinegar fermentation 46

4.1.4 Shut off experiment in bubble column 47

4.2 Vinegar fermentation in repeated batch mode on shake flask scale 49

4.2.1 Conventional and flushing repeated batch vinegar fermentation 49

4.2.2 Ethanol sensor characteristics in ShaRBS for vinegar fermentation 53

4.2.3 Flushing repeated batch fermentation for vinegar fermentation in ShaRBS 55

4.2.4 Oxygen dependency of the ethanol sensors and co-monitoring of oxygen partial pressure in headspace during fermentation in ShaRBS 59
4.2.5 Online calibration of oxygen sensor on ShaRBS 61
4.2.6 Determination of oxygen transfer rate in SharRBS 68
4.3 Scale-down of vinegar fermentation into microtiter plates 69
4.3.1 Vinegar fermentation in Flowerplate under typical shaking conditions 69
4.3.2 Determination of fermentation conditions in the 9 L-bioreactor for vinegar production 71
4.3.3 Determination of experimental parameters for vinegar fermentation in the microtiter plate 73
4.3.4 Model based estimation of vinegar fermentation in Flowerplate with custom-made lid 75
4.3.5 Experimental vinegar fermentation in a Flowerplate with a custom-made lid 76
5 Conclusion 81
6 Outlook 82
7 Appendix 85
7.1 Recapitulation of the used models for vinegar fermentation 85
7.2 Concentration changes due to filling a reactor 86
7.3 Calculation of diffusion coefficient of oxygen in air 87
8 References 91

Nomenclature

Abbreviations

A/H	Area-to-Height ratio (of bore hole in microtiter plat lid)
COSBIOS	Continuous Operated Shaken BIOreactor System
Eq., Eqs.	Equation(s)
IS	Insertion Sequence
RAMOS	Respiration Activity Monitoring System
Ref.	Reference
ShaRBS	Shaken Repeated Batch System

Formula symbols

Latin symbols

A	Acetic acid concentration [g/L]
A	Cross-sectional area of borehole in microtiter plate lid [mm^2]
$A_{t_{fl}}$	Acetic acid concentration at end of flushing (start of batch) [g/L]
A_{well}	Cross-sectional area of microtiter plate well [mm^2]
A_0	Acetic acid concentration at beginning of filling/flushing (end of batch) [g/L]
b	Intercept [bar]
c	Concentration of any compound [g/L]
CF	Calibration factor [mV/bar]
c_f	Concentration of any compound in ethanol substrate solution for filling [g/L]
c_{fl}	Concentration of any compound in ethanol substrate solution for flushing [g/L]
$c_{O_2,g}$	Oxygen concentration of the gas at the gas-liquid interface [mol/L]
$c_{O_2,in}$	Molar oxygen concentration of the aeration stream [mol/L]
$c_{O_2,l}$	Oxygen concentration of the liquid at the gas-liquid interface [mol/L]
$c_{O_2,out}$	Molar oxygen concentration of gas phase (reactor headspace) or exhaust gas stream [mol/L]
$c_{t_{fl}}$	Concentration of any compound at end of flushing (start of batch) [g/L]
c_0	Concentration of any compound at beginning of filling/flushing (end of batch) [g/L]
$C_{1,i}$	Constant 1 to calculate molar density
$C_{2,i}$	Constant 2 to calculate molar density
$C_{3,i}$	Constant 3 to calculate molar density

$C_{4,i}$	Constant 4 to calculate molar density
D	Dilution rate [h^{-1}]
D	Diameter of borehole in microtiter plate lid [mm]
D_a	Absolute draining rate [L/h]
D_{e,O_2}	Effective diffusion coefficient of oxygen [cm^2/s]
D_i	Diffusion coefficient of component i in multicomponent gas mixture [cm^2/s]
D_{ij}	Binary diffusion coefficient of component i with respect to component j [cm^2/s]
$D_{O_{2,air}}$	Diffusion coefficient of oxygen in air [cm^2/s]
D_{O_2,CO_2}	Binary diffusion coefficient of oxygen with respect to carbon dioxide [cm^2/s]
D_{O_2,N_2}	Binary diffusion coefficient of oxygen with respect to nitrogen [cm^2/s]
D^*	Draining rate [h^{-1}]
E	Ethanol concentration [g/L, mol/L]
E_0	Ethanol concentration at beginning of filling/flushing (end of batch) [g/L]
E_f	Ethanol concentration of ethanol substrate solution for filling [g/L]
E_{fl}	Ethanol concentration of ethanol substrate solution for flushing [g/L]
$E_{t_{fl}}$	Ethanol concentration at end of flushing (start of batch) [g/L]
F	Filling rate [L/h]
H	Height of microtiter plate lid [mm]
H_{well}	Height of microtiter plate well [mm]
K_{IA}	Acetic acid inhibition constant [g/L]
K_{IO}	Oxygen inhibition constant [mg/L]
K_{IE}	Ethanol inhibition constant [g/L]
k_La	Volumetric mass transfer coefficient [h^{-1}]
k_{lid,O_2}	Mass transfer coefficient of oxygen [mol/h]
K_{SA}	Acetic acid activation constant [g/L]
K_{SE}	Ethanol saturation constant [g/L]
K_{SO}	Oxygen activation constant [mg/L]
M_E	Molecular weight of ethanol [g/mol]
M_i	Molecular weight of component i [g/mol]
M_j	Molecular weight of component j [g/mol]
n	Shaking frequency [rpm]
N	Number of components in multicomponent gas mixture
$n_{O_2,out}$	Amount of oxygen in the gas phase (reactor headspace) or exhaust gas stream [mol]
O	Oxygen concentration [mg/L]

O_{max}	Maximal influence of oxygen on growth
O_{opt}	Optimal dissolved oxygen concentration for growth [mg/L]
$OTR_{bioreactor}$	Oxygen transfer rate in bioreactor [mol/L/h]
$OTR_{g/l}$	Oxygen transfer rate from the gas to the liquid phase [mol/L/h]
OTR_{lid}	Oxygen transfer rate through borehole in microtiter plate lid [mol/L/h]
OUR	Oxygen uptake rate [mol/L/h]
p_{abs}	Absolute pressure [bar]
$p_{CO_2,air}$	Partial pressure of carbon dioxide [bar]
p_{H_2O}	Partial pressure of water in water saturated air [bar]
p_i	Partial pressure of component i in multicomponent gas mixture [bar]
p_j	Partial pressure of component j in multicomponent gas mixture [bar]
$p_{N_2,air}$	Partial pressure of nitrogen [bar]
$p_{O_2,air}$	Oxygen partial pressure of dry air [bar, %]
$p_{O_2,g}$	Oxygen partial pressure in gas phase of microtiter plate well [bar, %]
$p_{O_2,in}$	Oxygen partial pressure of aeration stream [bar, %]
$p_{O_2,out}$	Oxygen partial pressure of reactor headspace and exhaust gas stream [bar, %]
$\dot{q}_{in}$	Volume specific aeration rate [L/L/h, vvh]
$\dot{q}_{out}$	Volume specific exhaust rate [L/L/h, vvh]
R	Ideal gas constant [J/mol/K]
S_{O_2}	Oxygen solubility of the fermentation medium [mol/L/bar]
t	Time [h]
T	Absolute temperature [K]
$T_{b,i}$	Normal boiling point [K]
t_{fl}	Duration of flush phase [h]
T_{ij}^*	Reduced temperature [K]
t_0	Time of beginning of filling/flushing [h]
U	Sensor voltage [mV]
V	Filling volume of reactor [L]
V_f	Added volume of feed solution [L]
V_g	Volume of the gas phase (reactor headspace) [L]
$\dot{V}_{in}$	Volumetric aeration stream [L/h]
V_l	Volume of the fermentation liquid [L]
$V_{lb,i}$	Molar volume of component i in the liquid state at normal boiling point [cm^3/mol]

V_m	Molar gas volume [L/mol]
V_{max}	Maximum filling volume of reactor [L]
$\dot{V}_{out}$	Volumetric exhaust gas stream [L/h]
V_{rel}	Relative filling volume of the reactor
$V_{rel,0}$	Relative filling volume of the reactor at beginning of filling
V_{well}	Total well volume [µL]
V_0	Filling volume of the reactor at beginning of filling [L]
X	Biomass concentration [g/L]
Y_{EA}	Stoichiometric coefficient for conversion of ethanol into acetic acid [g/g]
Y'_{XE}	Yield coefficient for biomass from ethanol [mg/g]

Greek symbols

δ_i	Dimensionless polarity parameter of component i
δ_{ij}	Dimensionless polarity parameter between component i and j
μ	Growth rate [h^{-1}]
μ_i	Dipole moment of component i [Debyes]
μ_{max}	Maximal growth rate [h^{-1}]
μ^*_{max}	Maximal growth rate at optimal dissolved oxygen concentration [h^{-1}]
$\rho_{lb,i}$	Molar density of component i in the liquid state at normal boiling point [mol/cm^3]
σ_i	Zero energy collision diameter of component i [Å]
σ_{ij}	Characteristic length of intermolecular potential between component i and j [Å]
σ_j	Zero energy collision diameter of component j [Å]
$\Omega_{D_{ij}}$	Dimensionless diffusion collision integral between component i and j
$\Omega^*_{D_{ij}}$	Reduced dimensionless diffusion collision integral between component i and j

List of Figures

Figure 1: Scheme of repeated batch in conventional bioreactor and ShaRBS. 14
Figure 2: Oxygen balance in a ShaRBS reactor. 19
Figure 3: Oxygen supply in microtiter plate well during fermentation. 23
Figure 4: Determination of borehole dimensions in microtiter plate lid for vinegar fermentation. 27
Figure 5: Schematic diagram of the ShaRBS device for parallel vinegar fermentation. 29
Figure 6: ShaRBS device for parallel vinegar fermentation. 30
Figure 7: Inoculation schemes for shaken bacterial cultures. 33
Figure 8: Mobile bubble column for inoculation of shaken acetic acid bacteria cultures for vinegar fermentation. 34
Figure 9: BioLector device for measurement of dissolved oxygen tension in micortiter plates. 36
Figure 10: Inoculation scheme for vinegar fermentation in microtiter plates. 37
Figure 11: Oxygen transfer rate in shake flasks of acetic acid bacteria inoculated according to a traditional procedure. 40
Figure 12: Oxygen transfer rate in shake flasks of acetic acid bacteria with reduced aeration rate typical for commercial vinegar production. 41
Figure 13: Oxygen transfer rate in shake flasks of acetic acid bacteria inoculated according to a traditional procedure or an aerated inoculation scheme. 42
Figure 14: Oxygen transfer rate in shake flasks of acetic acid bacteria inoculated according to an aerated inoculation scheme with different aeration rates. 44
Figure 15: Oxygen transfer rate in shake flasks of acetic acid bacteria inoculated according to an aerated inoculation scheme using either air or pure oxygen as supply gas in the bubble column. 46
Figure 16: Dissolved oxygen tension in a bubble column during shut off experiment. 48
Figure 17: Simulated repeated batch fermentations for the production of vinegar in conventional bioreactor and ShaRBS. 50
Figure 18: Draining and filling phase in conventional bioreactor compared to flush phase in ShaRBS in repeated batch vinegar fermentation. 52
Figure 19: Simulated oxygen partial pressure in the headspace of a ShaRBS reactor during vinegar fermentation. 54
Figure 20: Parallel repeated batch fermentations in ShaRBS. 56
Figure 21: Repeated batch vinegar fermentation in the ShaRBS with change of ethanol lots in the ethanol substrate solution. 58

Figure 22: Ethanol sensor voltage as a function of ethanol concentration and oxygen partial pressure. 59
Figure 23: Compensation of oxygen partial pressure dependency of ethanol sensor signal in repeated batch fermentation in ShaRBS. 60
Figure 24: Oxygen sensor calibration on ShaRBS during repeated batch fermentation. 62
Figure 25: R^2-values of linear fits for the determination of the calibration factor of the oxygen sensor on ShaRBS during fermentation. 63
Figure 26: Correlation of calibration factors of oxygen sensor on ShaRBS during fermentation determined at time points of flow change from low to high and high to low flow. 64
Figure 27: Calibration factor of oxygen sensor on ShaRBS during fermentation. 65
Figure 28: Determination of calibration factor with low R^2-value for the oxygen sensor on ShaRBS during repeated batch fermentation. 66
Figure 29: Repeated batch vinegar fermentation in ShaRBS with oxygen analytic during fermentation I. 67
Figure 30: Repeated batch vinegar fermentation in ShaRBS with oxygen analytic during fermentation II. 68
Figure 31: Dissolved oxygen tension in vinegar fermentation using a Flowerplate with a conventional gas-permeable seal. 70
Figure 32: Concentration changes during vinegar fermentation in Flowerplate with conventional gas-permeable seal. 71
Figure 33: Determination of fermentation conditions in a 9 L-bioreactor. 72
Figure 34: Calculated oxygen mass transfer coefficient for the microtiter plate lid. 74
Figure 35: Predicted fermentation conditions in the Flowerplate with a custom-made lid for vinegar fermentation. 75
Figure 36: Dissolved oxygen tension in vinegar fermentation using a Flowerplate with a custom-made lid. 77
Figure 37: Smoothed dissolved oxygen tension in Flowerplate with custom-made lid for vinegar fermentation. 78
Figure 38: Final conditions in the Flowerplate with a custom-made lid for vinegar fermentation. 80

List of Tables

Table 1: Initial conditions, parameters and results for modeled repeated batch vinegar fermentation in conventional bioreactor 51
Table 2: Initial conditions, parameters and results for modeled repeated batch vinegar fermentation in ShaRBS.....51
Table 3: Parameters of the model for vinegar fermentation.....85

I Abstract

Vinegar is an important food preservative and condiment. In industry, vinegar is widely produced by submerged fermentation. Although vinegar production is established on the large scale, small scale culture methods, in which bioprocesses are typically developed or optimized nowadays, are missing. To reinvestigate the established fermentation process and to gain profound knowledge for vinegar industry, the principal aim of this thesis was the development of suitable small scale culture methods and systems for submerged vinegar fermentation.

Since obligatory aerobic acetic acid bacteria in vinegar production suffer even from short oxygen depletion during traditional precultivation steps, the reproducibility of results in the main culture is insufficient. Thus, in the first part of this thesis a reproducible small scale cultivation method for obligatory aerobic acetic acid bacteria at industrially relevant high ethanol and acetic acid concentrations by ensuring constant oxygen transfer in the whole inoculation procedure was established. An acetic acid bacteria preculture was drained off from a laboratory-scale bioreactor into an aerated mobile bubble column and then transferred to an already shaking RAMOS shake flask device. Whereas the respiration curves of the traditionally processed acetic acid bacteria cultures were low and greatly diverged, those of the preculture transferred first into the bubble column and then into the already shaking flasks were high and coincided with one another. Furthermore, shutting off aeration in the mobile bubble column led to a rapid decrease in bacterial activity. In conclusion, traditional precultivation steps are not suitable for obligatory aerobic acetic acid bacteria in vinegar fermentation. Maintaining constant oxygen transfer is necessary to guarantee the reproducibility of main culture experiments with such bacteria.

In industry, vinegar is produced in repeated batch or repeated fed-batch processes. As yet, there was no small scale culture system for repeated batch bioprocesses. Therefore, in the second part of this thesis a new shaken culture system for parallel repeated batch vinegar fermentation was explored. A new operation mode – the flushing repeated batch – was developed. Parallel repeated batch vinegar fermentation could be established in shaken overflow vessels in a completely automated operation with only one pump per reactor. This flushing repeated batch was first theoretically investigated and then empirically tested. The ethanol concentration was online monitored during repeated batch fermentation by semiconductor gas sensors. It was shown that the switch from one ethanol substrate lot to different ethanol substrate lots resulted in prolonged lag phases and durations of the first batches. In the subsequent batches the length of the fermentations decreased considerably. This decrease in the respective lag phases indicates an adaptation of the acetic acid bacteria

mixed culture to the specific ethanol substrate lot. Consequently, flushing repeated batch fermentations on small scale are valuable for screening fermentation conditions and, thereby, improving industrial-scale bioprocesses such as vinegar fermentation in terms of process robustness, stability and productivity. To improve the shaken repeated batch system, the system was expanded with electrochemical oxygen sensors. The measurement of the oxygen partial pressure in the headspace of the shaken reactors allowed the compensation of the oxygen partial pressure dependency of the semiconductor ethanol gas sensors. Furthermore, the oxygen transfer rate in the repeated batch fermentation system could be determined during cultivation. The oxygen transfer rate was with 28 mmol/L/h in the same range as in batch cultivations in the RAMOS device. To calibrate the oxygen sensors online during cultivation, a method applying gas flow change was theoretically considered and practically implemented.

High-throughput cultures to optimize fermentation conditions are often conducted in microtiter plates. After the vinegar fermentation was accomplished in milliliter shake flask scale in batch as well as repeated batch mode, the vinegar fermentation was scaled-down to microliter scale in microtiter plates in the third part of this thesis. In order to minimize evaporation losses of ethanol and acetic acid in a 48-well microtiter plate during vinegar fermentation a new custom-made lid was developed. A diffusion model was used to calculate the dimensions of a hole in the lid to guarantee a suitable oxygen supply and level of ventilation. A reference fermentation was conducted in a 9 L-bioreactor to enable the calculation of the proper cultivation conditions in the microtiter plate. The minimum dissolved oxygen tensions in the microtiter plate were between 7.5 % and 23 % of air saturation and in the same range as in the 9 L-bioreactor. Evaporation losses of ethanol and acetic acid were less than 5 % after 47 h and considerably reduced compared to those of microtiter plate fermentations with a conventional gas-permeable seal. Furthermore, cultivation times in the microtiter plate were with about 40 h as long as in the 9 L-bioreactor. In conclusion, microtiter plate cultivations with the new custom-made lid provide a platform for high-throughput studies on vinegar fermentation. Results are comparable to those in the 9 L-bioreactor.

II Deutsche Zusammenfassung

Essig ist ein bedeutendes Konservierungs- und Würzmittel und wird industriell weitgehend durch submerse Fermentation hergestellt. Obwohl die Essigproduktion im großen Maßstab etabliert ist, fehlen Kleinkulturmethoden, in denen heutzutage Bioprozesse typischerweise entwickelt und optimiert werden. Um den etablierten Fermentationsprozess neu zu beforschen und profunde Erkenntnisse für die Essigindustrie zu gewinnen, war die Entwicklung von geeigneten Kleinkulturmethoden und Systemen für die submerse Essigfermentation das wesentliche Ziel dieser Arbeit.

Da die obligat aeroben Essigsäurebakterien in der Essigherstellung bei herkömmlichen Animpfschritten selbst unter kurzem Sauerstoffmangel leiden, ist die Reproduzierbarkeit der Ergebnisse aus der Hauptkultur unzureichend. Daher wurde im ersten Teil dieser Arbeit durch Gewährleistung eines ständigen Sauerstoffeintrags im gesamten Animpfprozess eine reproduzierbare Kleinkulturmethode für obligat aerobe Essigsäurebakterien unter industriell relevant hohen Ethanol- und Essigsäurekonzentration entwickelt. Die Vorkultur der Essigsäurebakterien wurde aus einem Laborbioreaktor in eine begaste, mobile Blasensäule abgelassen und dann in eine bereits schüttelnde RAMOS-Anlage überführt. Die Atmungskurven herkömmlich behandelter Essigsäurebakterienkulturen waren niedrig und wichen stark voneinander ab. Im Gegensatz dazu waren die Atmungskurven der Essigsäurebakterienkulturen, bei denen die Vorkultur zuerst in die Blasensäule und dann in die bereits schüttelnden Schüttelkolben überführt wurde, hoch und überlagerten sich. Das Abstellen der Begasung in der mobilen Blasensäule führte außerdem zu einem rapiden Abfall der Bakterienaktivität. Zusammenfassend sind herkömmliche Animpfverfahren für die Essigsäurebakterien in der Essigfermentation nicht geeignet. Das Aufrechthalten des Sauerstoffeintrags ist zwingend erforderlich, um die Reproduzierbarkeit der Hauptkulturexperimente mit diesen Bakterien zu gewährleisten.

Industriell wird Essig in Repeated-batch- oder Repeated-fed-batch-Verfahren hergestellt. Bisher gab es keine Kleinkultursysteme für Repeated-batch-Bioprozesse. Deshalb wurde im zweiten Teil dieser Arbeit ein neues geschütteltes Kultivierungssystem für die parallele Repeated-batch-Essigfermentation erforscht. Ein neuer Betriebsmodus – der „Flushing-repeated-Batch“ – wurde entwickelt. Die parallele Repeated-batch-Essigfermentation konnte vollkommen automatisiert in geschüttelten Überlaufgefäßen mit nur einer Pumpe pro Reaktor etabliert werden. Das Flushing-repeated-batch-Verfahren wurde zunächst theoretisch betrachtet und anschließend realisiert. Die Ethanolkonzentration wurde während der Repeated-batch-Fermentation online mit Halbleitergassensoren gemessen. Es wurde gezeigt, dass das Umstellen von einer Alkoholcharge auf andere Alkoholchargen in

verlängerten Lag-Phasen und Dauern der ersten Batch-Zyklen resultierte. In den nachfolgenden Batch-Zyklen nahmen die Fermentationszeiten beachtlich ab. Diese Abnahme der entsprechenden Lag-Phasen deutet auf eine Adaptation der gemischten Essigsäurebakterienkultur an die spezifische Alkoholcharge hin. Folglich sind Flushing-repeated-batch-Fermentationen in kleinem Maßstab nützlich, um Fermentationsbedingungen zu screenen und dabei Bioprozesse wie die Essigfermentation im industriellen Maßstab hinsichtlich der Prozessrobustheit, -stabilität und Produktivität zu verbessern. Zur Verbesserung des geschüttelten Repeated-batch-Systems wurde das System mit elektrochemischen Sauerstoffsensoren ausgestattet. Die Messung des Sauerstoff-partialdrucks im Kopfraum der Schüttelreaktoren erlaubte die Kompensation der Sauerstoffpartialdruckabhängigkeit der Ethanolhalbleitergassensoren. Weiterhin konnte die Sauerstofftransferrate im Repeated-batch-Fermentationssystem während der Kultivierung bestimmt werden. Die Sauerstofftransferrate war mit 28 mmol/L/h in der gleichen Größenordnung wie bei der Batch-Kultivierung in der RAMOS-Anlage. Zur Online-Kalibrierung der Sauerstoffsensoren während der Kultivierung wurde eine Methode mittels Umstellen der Begasungsrate theoretisch betrachtet und praktisch implementiert.

Hochdurchsatzkultivierung zur Verbesserung der Fermentationsbedingungen wird häufig in Mikrotiterplatten durchgeführt. Nachdem die Essigfermentation im Millilitermaßstab in Schüttelkolben sowohl im Batch- als auch Repeated-batch-Verfahren bewerkstelligt wurde, wurde die Essigfermentation im dritten Teil dieser Arbeit auf den Mikrolitermaßstab in Mikrotiterplatten herunterskaliert. Um die Verdunstungsverluste von Ethanol und Essigsäure in einer 48-well-Mikrotiterplatte während der Essigfermentation zu minimieren wurde ein neuer maßgeschneiderter Deckel entwickelt. Für die Berechnung der Dimensionen eines Deckellochs, das eine ausreichende Belüftung und Sauerstoffversorgung garantiert, wurde ein Diffusionsmodell verwendet. Eine Referenzfermentation in einem 9 L-Bioreaktor diente der Auslegung geeigneter Kultivierungsbedingungen in der Mikrotiterplatte. Die minimalen Gelöstsauerstoffanteile in der Mikrotiterplatte lagen zwischen 7,5 % und 23 % Luftsättigung und waren damit in der gleichen Größenordnung wie im 9 L-Bioreaktor. Die Verdunstungsverluste von Ethanol und Essigsäure waren nach 47 h kleiner als 5 % und damit im Vergleich zu einer Mikrotiterplattenfermentation mit einer herkömmlichen, gasdurchlässigen Klebefolie deutlich reduziert. Die Kultivierungszeiten in der Mikrotiterplatte entsprachen mit 40 h außerdem der Kultivierungszeit im 9 L-Bioreaktor. Somit stellen Mikrotiterplattenkultivierungen mit dem neuen maßgeschneiderten Deckel eine Plattform für Hochdurchsatzstudien an der Essigfermentation dar, die vergleichbare Ergebnisse zur Kultivierung im 9 L-Bioreaktor liefert.

1 Introduction

1.1 Vinegar production by acetic acid bacteria

Since antiquity, vinegar has been very important in food preparation, not only as preservative for vegetables, fish and meat but likewise as an ingredient in mustard, ketchup, mayonnaise, sauces and dressings [1-3]. In Germany, vinegar is defined as a product which in 100 mL contains a minimum of 5 g and a maximum of 15.5 g water-free acetic acid. Vinegar is either produced by acetous fermentation of liquids containing alcohol, by dilution of acetic acid with water (vinegar from acetic acid) or by blending vinegar made by fermentation with acetic acid or vinegar from acetic acid [4]. The biological production of vinegar is by definition a two-step process: The first step is the anaerobic fermentation of sugars such as glucose, fructose and sucrose to ethanol and carbon dioxide through yeast cultures. The second step is the stoichiometric conversion of ethanol with oxygen to acetic acid and water by acetic acid bacteria. This aerobic fermentation is generally understood as vinegar fermentation. Depending on the raw material vinegar can be classified into various types. For instance, wine vinegar, cider vinegar or rice vinegar are made from grape wine, apple wine or rice wine, respectively. Spirit vinegar, which is the subject of this thesis, is made from rectified ethanol (spirit) of biological origin. Vinegar is either produced via submerged fermentation, solid state fermentation or by various other traditional methods [5]. Submerged fermentation was first described by Hromatka and Ebner in 1949 [6] and is today industrially predominant.

Acetic acid bacteria belong to the family of Acetobacteraceae. The most important genera of this family are *Acetobacter* and *Gluconobacter*. Acetic acid bacteria are Gram-negative and polymorphous. The morphology varies from ellipsoidal to rod shaped or straight to slightly curved forms. They occur as single cells, in pairs or in chains. There are non-motile and motile forms with polar or peritrichous flagella. Acetic acid bacteria are outstanding because of their ability to oxidize ethanol to acetic acid at low pH [7].

In vinegar production acetic acid bacteria are obligatory aerobic and a sufficient oxygen supply is essential for submerged fermentation. Accordingly, the first studies on the submerged fermentation to form vinegar extensively focused on that issue [6, 8-11]. As ethanol and acetic acid are relatively volatile, aeration of the bioreactor with excess air flow is not a feasible option. Instead, an even dispersion of very small air bubbles is preferred for oxygen supply [9]. Already in the first studies [6, 9] on submerged production of vinegar in 3.5 L-bubble columns it was shown that the oxygen transfer rate is an essential limiting factor. At larger air bubbles in these bubble columns and, therefore, low oxygen transfer rates low acetic acid formation rates were found. Thus, nowadays the bioreactors for vinegar

production in industry are equipped with special turbines which generate very fine air bubbles and homogenously disperse the air and liquid in the reactor [12, 13]. Thereby, sufficient oxygen supply is guaranteed at very low aeration rates, and evaporation of the volatile substrate ethanol and product acetic acid is minimized. Industrial aeration rates are as low as 2 vvh (volumes air / volumes culture medium / hour) to 5 vvh. Today, the smallest laboratory-scale for submerged vinegar fermentation under industrial conditions is in the magnitude of liters. For instance, the 9 L “Frings-Acetator” [14] is a typical bioreactor for vinegar fermentation in laboratory-scale.

Several studies dealt with the interruption of aeration during vinegar fermentation. The degree of damage of the bacteria depended on the time point of interruption of aeration [10]. Thus, the interruption of aeration for 30 seconds caused only 17 % reduction in acetic acid formation rate for a wine vinegar culture in the early phase where ethanol concentration was still high (65 g/L) and acetic acid concentration (11.5 g/L) as well as acetic acid formation rate (0.8 g/L/h) were low. In contrast, the interruption of aeration for 30 seconds caused a substantial reduction of 94 % in acetic acid formation rate for a wine vinegar culture in the late phase where ethanol concentration was already low (9 g/L) and acetic acid concentration (45.5 g/L) as well as acetic acid formation rate (8.7 g/L/h) were high. In comparison, diluted wine vinegar cultures were less susceptible: interruptions of aeration of even more than a minute did not adversely affect the bacteria. Similarly, it was found that interrupting aeration in spirit vinegar fermentation with higher concentrations of ethanol and acetic acid impaired the bacteria to a greater extent [11]. This proved that not the oxygen depletion per se affected the bacteria, but rather the oxygen depletion in presence of certain concentrations of ethanol and acetic acid. Moreover, Mesa et al. [15] proposed a model for the viability reduction of *Acetobacter aceti* UCA1 as a result of oxygen deficiency at particular time points marked by specific ethanol and acetic acid concentrations. Using an *Acetobacter aceti* W-419 culture, Muraoka et al. [16] demonstrated that undissociated acetic acid rather than the dissociated form is responsible for damaging bacterial cells during oxygen deficiency.

Generally, industrial submerged fermentations are initiated with inoculation vinegar – microbiologically undefined residues of other fermentations yielding vinegar [13]. The process can be conducted in an unsterile system, since the high ethanol and acetic acid concentrations in vinegar fermentation act auto-selective for acetic acid bacteria. Hence, bacterial cultures for vinegar production are not pure cultures but mixtures of different acetic acid bacteria. For instance, Entani et al. [17] isolated 14 *Acetobacter polyoxogenes* strains from various kinds of vinegar broth collected from some vinegar breweries in Japan. Kittelmann et al. [18] isolated 23 *Acetobacter* strains from five different vinegar production

sites in Germany and France. Sievers et al. [19] found at least 24 *Acetobacter* strains at vinegar production sites in Germany and Switzerland. Further, Sokollek et al. [20] investigated 10 different bacteria strains isolated from different wine and spirit vinegars with respect to their characteristics of growth and metabolism.

Acetic acid bacteria may change their characteristics during long storage. Sokollek et al. [20] remarked that the isolate *Acetobacter* sp. LTH 4342 showed reduced productivity and tolerance to acetic acid and ethanol in high concentrations compared to the original bacterial culture in the industrial bioreactor after three months of growth on agar plates. Moreover, a reproducible start of vinegar fermentations was not guaranteed with *Acetobacter* isolates as they exhibited lag phases of growth of two to five days [20]. The change of the phenotypic characteristics of acetic acid bacteria can be linked to strong genetic variations [21, 22]. Already in 1968, Asai [23] reviewed mutations of acetic acid bacteria based on phenotypic observations. Among others, phenotypic changes included loss of cellulose formation [24, 25] or switches in ketogenic activities [26, 27]. However, the most undesired genetic mutation with respect to vinegar production was the loss of their ethanol-oxidizing ability and their resistance to acetic acid [25, 27, 28]. Since the 1990s, insertion sequence (IS) elements have been linked to frequent mutations in acetic acid bacteria. IS elements were found in various species of the genera *Acetobacter* [28, 29], *Gluconobacter* [30, 31], *Gluconacetobacter* or *Granulibacter* [32] of the Acetobateraceae family. For example, IS*1380* [29] and IS*1452* [31] from *Acetobacter pasteurianus* as well as IS*12528* [30] from *Gluconobacter suboxydans* were associated with the loss of or reduced ethanol-oxidizing ability. Furthermore, Prust et al. [33] and Azuma et al. [34] identified a plenty of insertion sequences and transposase genes when they analyzed the genomes of *Gluconobacter oxydans* 621H and *Acetobacter pasteurianus* NBRC 3283, respectively. A broad overview on the IS elements in acetic acid bacteria can be obtained from the IS data base (http://www-is.biotoul.fr/) [35]. Besides IS elements, high frequency of plasmid rearrangements might cause mutations in acetic acid bacteria [36, 37]. Thus, about 60 % of non-reverting cellulose-negative mutants of *Acetobacter xylinum* ATCC 10245 had identifiable changes in their plasmid DNA content compared to the wild type. Only recently, Gullo et al. [38] reported on the difficulty to preserve *Acetobacter* species. Long-term preservation methods with a number of only 17.4 generations confirmed to be suitable for preservation of *Acetobacter pasteurianus* strain AB0220 over a period of nine years. In contrast, short-term preservation methods with a much higher number of 540.54 generations resulted in phenotypic differences due to genetic damage and mutations.

1.2 Repeated batch processes

Considering the aforementioned problems involving oxygen dependency as well as isolation and maintenance of acetic acid bacteria, it is not surprising that vinegar is produced industrially in repeated batch, repeated fed-batch or cascaded repeated fed-batch fermentations. At the end of a given fermentation period only a part of the vinegar is harvested and the residual culture, remaining in the reactor under aeration, is replenished with fresh medium. Thus, the residual culture broth of the preceding batch serves as inoculum of the subsequent batch [12-14]. This avoids the death of the bacteria in ordinary inoculation cascades or changes of the bacteria with regard to strain maintenance under mild cultivation conditions.

Vinegar production is one of the most important examples of repeated batch fermentation on industrial scale. The main advantage of repeated batch processes is their increased productivity compared to usual batch processes because of shorter cycle times. Downtimes due to reactor cleaning, medium preparation and sterilization can be avoided. Moreover, in repeated batch fermentations the respective lag phase of the cells is usually much shorter or even absent. Furthermore, the cells can slowly adapt to adverse environmental conditions and, therefore, show higher turnover rates than that of batch cultures. Repeated batch processes may be superior to continuous cultivation, for instance, in biological systems which suffer from a severe product inhibition such as acetic acid inhibition in vinegar fermentation.

There is currently increasing interest in repeated batch fermentation, since several recent studies on repeated batch fermentation have shown improved productivity. For instance, citric acid [39-41], D-lactic acid [42] or ethanol [43] were obtained with higher productivities in repeated batch than in batch cultivation with various organisms and substrates. Even more complex molecules such as the polysaccharides bacterial cellulose [44], and heteropolysaccharide-7 [45], the polyester poly(β-hydroxybutyrate) [46], the drug cordycepin(3'-doxyadenosine) [47] or the food additive cyanine [48] were investigated in repeated batch fermentation. Also biomass of the nitrogen fixing bacteria *Azotobacter chroococcum* as biofertilizer [49] could be efficiently produced by repeated batch fermentation.

1.3 Small scale cultivation methods

Nowadays, small-scale bioreactors are typically used to grow cells in liquid culture in many bioprocess applications ranging from biocatalyst and medium screening to bioprocess

optimization [50-55]. Small-scale cultivation allows saving of media, space, workload and, thus, costs. Moreover, such small-scale cultivations in parallel and automated experimental setups facilitate higher throughput [52, 53]. Small-scale bioreactors can be categorized as shaken, stirred or gas-sparged systems according to their agitation method [50]. The predominant small-scale bioreactor type is represented by shaken vessels comprising shake flasks, test tubes and microtiter plates [52]. Shake flasks are outstanding and widely used in both academia and industry, because they are an inexpensive and effective way of reproducibly performing many types of industrially-relevant cell cultivations including bacteria, yeast, fungi, animal, insect and also plant cells [50-54, 56]. Unlike controlled bioreactors, shake flasks used to be a kind of ‘black box’, because suitable online monitoring techniques to obtain information about the fermentation process were hitherto not available. This disadvantage, however, has been overcome with the invention of the so-called RAMOS device [57, 58] and other techniques. RAMOS means Respiration Activity MOnitoring System and enables the determination of oxygen transfer rate, carbon dioxide transfer rate and respiration quotient during shake flask cultivations. The oxygen transfer rate at the gas liquid interface can be regarded as the oxygen uptake rate of the bacteria as the storage capacity for oxygen in fermentation media is negligibly small. In contrast to large-scale fermentations that are widely conducted in fed-batch or in some cases even continuous mode, small-scale cultivation used to be limited to batch mode. No techniques were available to feed small amounts of substrate in small scale. This disadvantage, however, was addressed in the past decades. Several authors [50, 53-55] comprehensively reviewed the current state-of-the-art of high-throughput systems for fermentations ranging from shake flasks to fully equipped microfermenters.

There are two entirely different approaches to control fed-batch fermentation and pH in small-scale bioreactors. One way is to add the necessary substrate, acid or base via micropumps, valves or automated liquid handling devices into the small-scale bioreactors. The other options are dialysis or controlled-release systems. With respect to feeding by the use of instruments first attempts date back to 1953. Dale et al. [59] worked with a shaker and incremental feeding unit consisting of 50 mL syringes in a motor-driven actuating cam assembly. Later, Weuster-Botz et al. [60] developed a system where the feed, acid or base was supplied to shake flasks by a high-precision syringe pump, liquid distribution system and one 2/2-way miniature valve for each parallel shake flask. Moreover, Ruottinen et al. [61] constructed a wireless control and feeding device which could be placed onto a shaker. In their experiments, the feed solutions were simply driven by gravity through microcomputer-triggered miniature valves, silicon tubes and steel needles into the shake flasks. Alternatively, constant flow could also be generated in this assembly by applying an air overpressure container or micropump. Furthermore, van Leeuwen et al. [62] designed a

special micropump based on the Hagen-Poiseuille law for parallel fed-batch fermentations in microtiter plates. Also Buchenauer and Funke et al. [63-66] accomplished fed-batch fermentations or pH-control in microtiter plates using microfluidics with pneumatically actuated microvalves. Besides shaken systems, other miniature bioreactor systems such as stirred systems [67-70], bubble columns [71, 72], or gas-inducing impeller milliliter-scale bioreactors [73, 74] were used for fed-batch or pH-controlled fermentation with the same instrumentation as described for shake flasks or with automated liquid-handling systems. With regard to feeding by dialysis Gerhard and Gallup [75] constructed a dual chambered shake flask, whereby the two chambers were separated from each other with a semipermeable membrane. Whereas the bottom reservoir was completely filled with concentrated nutrient solution, the top chamber was filled with a less concentrated solution or even water for fermentation. Nutrients then diffused from the bottom reservoir into the top fermentation broth, while inhibitory products diffused back to the bottom reservoir. The same diffusion principle was utilized in a diffusion capsule which could be dropped in shake flasks [76, 77] or in a membrane-based diffusion tip which follows the rotation of the bulk liquid as reported recently by Bähr et al. [78]. With regard to controlled-release systems there are two types for fermentation. In the first case the substrate or pH-adjusting agent is embedded in and gradually released from a solid matrix such as agar [79] or silicone elastomers [80, 81]. In the second case the substrate, e.g. glucose, is enzymatically cleaved from a polymer such as starch. Here, the polymer can be either incorporated into solid agar [82] or it is fully dissolved in the fermentation medium [83]. Controlled-release systems have been implemented in shake flasks as well as in microtiter plates.

Apart from fed-batch or pH-controlled cultivations also continuous fermentations have been realized in small-scale. For instance, Walther et al. [84] constructed a magnetically stirred and membrane aerated miniaturized 3 mL-bioreactor for cultivating yeast cells in space laboratories. Zhang et al. [70] described a disposable 150 µL-chip bioreactor for batch, fed-batch and continuous culture. Nutrients, pH-adjusting agents or fermentation broth were supplied or drained through micro-channels. Mixing took place with a tiny ring-shaped magnetic stir bar and optical techniques were applied to measure pH, dissolved oxygen tension and biomass yield. In contrast, Akgün et al. [85, 86] developed a Continuous Operated Shaken BIOreactor System (COSBIOS). The improved system consisted of six cylindrical quartz glass reactors each having a distinct outlet at the reactor wall and distinct inlets for feed and air in the reactor lid. Due to centrifugal forces in shaken operation, the fermentation broth is driven against the reactor wall and overflows when the liquid height reaches the outlet. Hence, feeding fresh substrate via a multichannel pump with differently sized pump tubes enables parallel continuous operation at different dilution rates with liquid volumes in the magnitude of 10 mL to 200 mL.

Concerning microtiter plates as miniaturized bioreactors, substantial progress has been made with the invention of the so called BioLector [87-90], a microtiter plate fermentation system with scattered light and fluorescence optic measurement techniques. Furthermore, different well geometries for microtiter plates have been studied to assure high oxygen transfer capacities and sufficient oxygen supply for microorganisms during cultivation [91]. The 6-petal flower shape with an edge diameter of 5 mm proved to be best and is marketed as Flowerplate by m2p-labs GmbH (Baesweiler, Germany).

With respect to microtiter plates, evaporation losses of fermentation medium are a critical issue. Evaporation can be reduced with suitable seal membranes that preferably minimize the evaporation of water vapor while having no relevant impact on gas exchange [92]. These seal membranes are typically made from polymer materials such as copolymers of ethylene and vinyl acetate as well as polyethylene, silicone or rayon [92]. Zimmermann et al. [93] classified various seal membranes, including also wound dressings, into two groups. In the first group the oxygen transfer is high, but water vapor retention is relatively low. On the contrary, in the second group, water retention capability is comparably high but oxygen transfer is low. All the wound dressings they examined fall into the second group except for one. This wound dressing, Tendra Mefilm, exhibits both good oxygen permeability and water retention capability.

In addition to different seal foils, Arain et al. [94] also examined oxygen diffusion through a layer of paraffin oil or paraffin wax as well as the plate material. Paraffin oil is commonly used to prevent evaporation of samples in microtiter plate wells and can reduce gas exchange with the ambient air. Oxygen flux through paraffin oil into the sample was considerably increased as soon as the microtiter plate was shaken. Whereas different paraffin wax layers showed lower oxygen permeability than cellulose acetate foils, these paraffin wax layers showed higher oxygen permeability than polyester foils. Furthermore, aluminum foils were impermeable to oxygen [94].

Seal membranes may impair to some extent quantitative work, since droplets may cover parts of the membrane, especially when vigorous shaking is involved. Due to such droplet formation, the conditions in the various wells may differ from each other [54, 95]. Well-to-well heterogeneity also occurs in microtiter plates covered by conventional hard plastic lids. These lids allow rapid gas exchange around their perimeters but a lesser rate of gas exchange toward the center of the microtiter plate [96].

Another approach to reduce evaporation losses and cross-contamination between adjacent wells is to use a sandwich lid for 96 well plates [95, 97] commercialized by Enzyscreen B.V. (ER Haarlem, The Netherlands). This lid is composed of a perforated spongy silicone base

layer, a perforated top plate and a thin 2 mm cotton wool layer between the base layer and the top plate. Each of the 96 holes in the base layer and top plate is positioned over the center of each well and has a diameter of 1.5 mm and 6 mm, respectively. The top plate is made either of rigid polypropylene or stainless steel. The microtiter plate and the lid are then tightly clamped together onto the shaking platform. In cultivation experiments with the bacterium *Pseudomonas putida,* evaporation losses were less than 2 % per well and day for filling volumes of 500 µL to 1000 µL. Typically evaporation is also minimized by placing the microtiter plate in humidified chambers [92].

1.4 Objectives and Overview

Hitherto, there were no suitable small-scale cultivation methods to replace tedious studies for media and process optimization in vinegar industry. Therefore, the first aim of this thesis is to establish a method for reproducible and parallel small-scale cultivation of obligatory aerobic acetic acid bacteria at industrially relevant high ethanol and acetic acid concentrations. Hereby, the focus was on ensuring constant oxygen transfer during the inoculation steps. For that purpose, batch cultivation experiments in shake flasks should be conducted in the RAMOS device. Main cultures inoculated according to a traditional procedure have to be compared to main cultures inoculated following an aerated inoculation scheme (chapters 3.6.2 and 4.1). A shut off experiment in the mobile bubble column should demonstrate the effect of oxygen depletion during inoculation in more detail (chapters 3.7 and 4.1.4).

So far, repeated batch fermentation has not been addressed in any high-throughput system. It is, therefore, the second aim of this thesis to design a shaken culture system for parallel repeated batch vinegar fermentations. The Shaken Repeated Batch System (ShaRBS) and the envisaged flushing operation mode is first theoretically investigated (chapter 2.2) and then empirically evaluated (chapters 3.3, 3.4, 3.6.3 and 4.2.1 to 4.2.3). To improve the ShaRBS device an oxygen analysis should be developed. This oxygen analysis is again theoretically presented (chapter 2.3) and practically implemented (chapters 3.5 and 4.2.4 to 4.2.6).

After vinegar fermentation has become possible in milliliter shake flask scale, the third aim of this thesis is to present a new method to scale-down vinegar fermentation to the microliter scale for high-throughput cultivation using microtiter plates. A new custom-made lid is introduced specifically for vinegar fermentation to minimize evaporation losses of ethanol and acetic acid while allowing sufficient oxygen transfer. The theory on oxygen supply in the microtiter plate with the custom-made lid and the estimation of appropriate shaking conditions based on a reference fermentation in a 9 L-bioreactor are handled (chapter 2.4).

The reference fermentation in the 9 L-bioreactor is then shown in chapter 4.3.2 (chapter 3.6.1). Finally, vinegar fermentation in a microtiter plate with the custom-made lid is empirically evaluated (chapters 4.3.3 to 4.3.5).

2 Theory

2.1 Introduction of the proposed shaken repeated batch culture system

In this thesis the repeated batch operation should be established in a small-scale system. It is desirable to keep the construction as simple as possible to save costs and to avoid equipment failure. Especially, as the system should allow for parallel operation, the equipment of each reactor should be limited to the absolutely necessary parts. In figure 1 the operation principal of a repeated batch process in a conventional bioreactor is compared to the envisaged flushing repeated batch process in a ShaRBS. In a conventional bioreactor part of the reactor content is drained off from the bioreactor at the end of a batch when the substrate is (nearly) depleted. Afterwards, the remaining culture broth is replenished with fresh substrate. Subsequently the next batch is started. The proposed approach in ShaRBS is to replace the draining and filling phase in a conventional bioreactor by just one flushing phase at the end of the batch when the substrate is (nearly) depleted. At a constant filling volume the reactor is flushed with fresh substrate solution to form the next batch. Whereas in the conventional bioreactor two pumps per bioreactor are necessary for draining and filling the bioreactor, only one pump per reactor is necessary for the flushing repeated batch in ShaRBS. This approach is, of course, only meaningful for screening purposes, but not for industrial production. During flushing the product is mixed with fresh medium resulting in the fact that part of the substrate is wasted. For screening purposes, however, this higher substrate consumption is acceptable as only small amounts are used. The main issue is that the fermentation conditions, i.e. the concentrations of biomass, substrate and product, in the screening ShaRBS and conventional production system are literally the same. The idea is to use special shaken overflow vessels, which had been originally designed for continuous culture in COSBIOS [86]. These cylindrical vessels are characterized by a precisely fabricated overflow. Thus, in shaking operation the culture fluid in the vessel is subjected to centrifugal forces and is driven against the vessel wall forming a rotational paraboloid. The culture fluid eventually is spilling over if the upper tip of the rotating liquid reaches the overflow tube. Therefore, vessel fluid is leaving the bioreactor, if new fluid is supplied. At

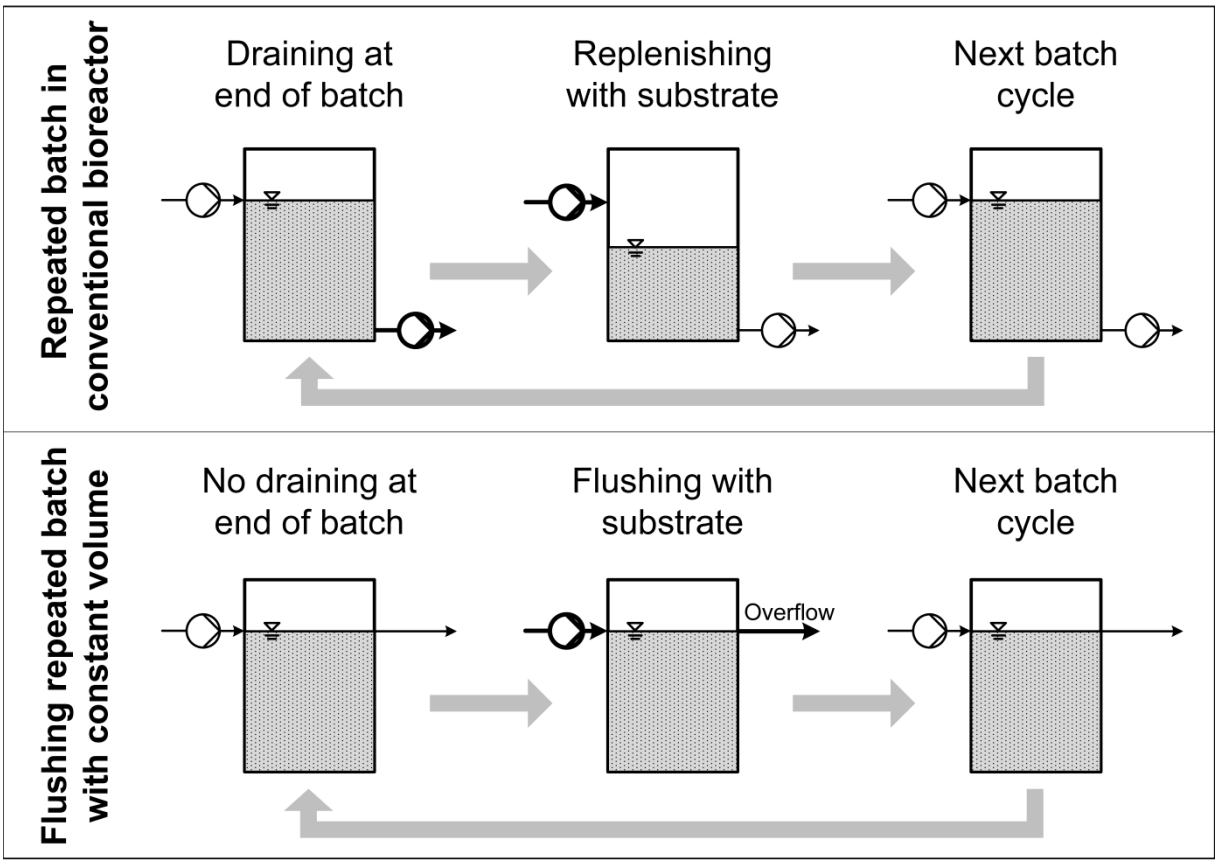


Figure 1: Scheme of repeated batch in conventional bioreactor and ShaRBS. In a conventional bioreactor part of the reactor content is drained off from the bioreactor at the end of a batch using a draining pump. Afterwards, the remaining culture broth is replenished with fresh substrate to form the next batch using a feeding pump. In ShaRBS the draining and filling phase in the conventional bioreactor at the end of the batch is replaced by one flushing phase. At a constant liquid filling volume the reactor is flushed with a substrate solution to form the next batch. Thus, only one pump per reactor is necessary for the ShaRBS.

steady state, a constant liquid filling volume is achieved. This operating principle is consequently applied for the flushing repeated batch operation. When the substrate is (nearly) depleted at the end of a batch, fresh substrate solution is pumped into the reactor while at the same time the fermentation broth automatically leaves the reactor through the overflow (figure 5).

2.2 Theoretical comparison of repeated batch in conventional bioreactor and the proposed flushing repeated batch in ShaRBS

To demonstrate that both approaches, i.e. the conventional repeated batch and the flushing repeated batch fermentation, are comparable to each other, the changes in the respective concentrations of the substrate ethanol, the product acetic acid as well as of biomass in vinegar fermentation were mathematically examined. The models of Romero et al. [98] as

well as Gomez and Cantero [99] were adopted to describe the growth of the acetic acid bacteria as well as the consumption of ethanol and formation of acetic acid, respectively. A recapitulation of these relatively simple well established models can be found in the appendix.

2.2.1 Conventional repeated batch processes

In conventional repeated batch processes, the concentration changes of biomass, ethanol or acetic acid, during the draining phase are only determined by the bacterial activity. During the filling phase, however, there are two additional aspects that lead to concentration changes and must be considered: first, the addition of a specific compound, i.e. ethanol via the ethanol substrate solution, and second, the dilution of any compound (ethanol, acetic acid and biomass) by the volume change. Equation (1) describes the concentration changes by filling the reactor. A detailed derivation of this equation can be found in the appendix.

$$\frac{dc}{dt} = \frac{D \cdot V_{rel,0} \cdot \left(c_f - c_0\right)}{\left(V_{rel,0} + D \cdot (t - t_0)\right)^2} \tag{1}$$

D denotes the dilution rate, $V_{rel,0}$ the relative filling volume at the end of the draining phase when the feed pump is started, c_0 and c_f the concentration of the compound in the residual culture broth and ethanol substrate solution for filling the reactor, respectively, and t and t_0 the time and time when the feed pump is started, respectively. Combining equation (1) with the growth model (equation (III), equation (IV) and equation (V) found in the appendix), the concentration changes of biomass, ethanol and acetic acid during conventional repeated batch vinegar fermentation can be described by equations (2), (3) and (4), respectively. The prerequisite is that there is neither biomass nor acetic acid in the ethanol substrate solution for filling the reactor.

$$\frac{dX}{dt} = \mu \cdot X - \frac{D \cdot V_{rel,0} \cdot X_0}{\left(V_{rel,0} + D \cdot (t - t_0)\right)^2} \tag{2}$$

$$\frac{dE}{dt} = -\frac{1}{Y'_{XE}} \cdot \mu \cdot X + \frac{D \cdot V_{rel,0} \cdot \left(E_f - E_0\right)}{\left(V_{rel,0} + D \cdot (t - t_0)\right)^2} \tag{3}$$

$$\frac{dA}{dt} = \frac{1}{Y_{EA}} \cdot \frac{1}{Y'_{XE}} \cdot \mu \cdot X - \frac{D \cdot V_{rel,0} \cdot A_0}{\left(V_{rel,0} + D \cdot (t - t_0)\right)^2} \tag{4}$$

Here, μ is the growth rate of the acetic acid bacteria, X the biomass concentration, Y'_{XE} the yield coefficient for biomass from ethanol and Y_{EA} the stoichiometric coefficient for the conversion of ethanol into acetic acid. X_0, E_0 and A_0 represent the concentrations of biomass, ethanol and acetic acid, respectively, at the end of the draining phase when the feed pump is started. E_f is the concentration of ethanol in the ethanol substrate solution. Furthermore, defining the draining rate D^* in the manner of the dilution rate as the ratio of the absolute draining rate D_a to the maximum filling volume V_{max} of the reactor (equation (5)) the changes in the relative filling volume of the reactor during draining and filling can be calculated with equation (6) as follows:

$$D^* = \frac{D_a}{V_{max}} \tag{5}$$

$$\frac{dV_{rel}}{dt} = D - D^* \tag{6}$$

2.2.2 Flushing repeated batch fermentation

In the flushing repeated batch fermentations in the ShaRBS, the filling volume is constant in each flushing phase. Thus, by assuming an ideally mixed reactor, the concentration changes of any compound due to flushing the reactor with ethanol substrate solution can be described with:

$$\frac{dc}{dt} = D \cdot \left(c_{fl} - c\right) \tag{7}$$

with c_{fl} the concentration of the specific compound in the ethanol substrate solution for flushing the reactor. Combining equation (7) with the growth model (equation (III), equation (IV) and equation (V) found in the appendix), the concentration changes of biomass, ethanol and acetic acid during repeated batch fermentations in the ShaRBS can be described with equations (8), (9), and (10), respectively. The prerequisite is again that there is neither biomass nor acetic acid in the ethanol substrate solution for flushing the reactor.

$$\frac{dX}{dt} = X \cdot (\mu - D) \tag{8}$$

$$\frac{dE}{dt} = -\frac{1}{Y'_{XE}} \cdot \mu \cdot X + D \cdot \left(E_{fl} - E\right) \tag{9}$$

$$\frac{dA}{dt} = \frac{1}{Y_{EA}} \cdot \frac{1}{Y'_{XE}} \cdot \mu \cdot X - D \cdot A \tag{10}$$

In practice, the end of the draining and filling phase of a repeated batch fermentation in a conventional bioreactor is designated by a level sensor and an electronic control. Such a level control is not required for repeated batch fermentations in the ShaRBS, because the fermentation broth level is always constant due to the overflow tube. Instead, time control is the easiest way to terminate the flush phase during flushing repeated batch fermentations. Given the basic condition that a flush phase in the ShaRBS should last as long as the draining and filling phase in a conventional bioreactor, the time for the flush phase t_{fl} is described by:

$$t_{fl} = \frac{1 - V_{rel,0}}{D} + \frac{1 - V_{rel,0}}{D^*} \tag{11}$$

Integrating equation (7) over the time of a flush phase leads to equations (12) and (13).

$$\int_{c_0}^{c_{t_{fl}}} \frac{dc}{c_{fl} - c} = D \cdot \int_0^{t_{fl}} dt \tag{12}$$

$$\frac{c_{fl} - c_0}{c_{fl} - c_{t_{fl}}} = e^{D \cdot t_{fl}} \tag{13}$$

Here, c_0 and $c_{t_{fl}}$ are the concentrations in the ShaRBS reactor at the beginning of the flush phase (end of a given batch) and at the end of the flush phase (start of the next batch), respectively. To reach a specific acetic acid concentration in the vinegar broth at the end of the flush phase the dilution rate is given by rearranging equation (13) to:

$$D = \frac{ln \frac{A_0}{A_{t_{fl}}}}{t_{fl}} \tag{14}$$

In turn, the dilution rate then determines the concentration of ethanol in the ethanol substrate solution for flushing E_{fl} by rearranging equation (13) to:

$$E_{fl} = \frac{E_{t_{fl}} \cdot e^{D \cdot t_{fl}} - E_0}{e^{D \cdot t_{fl}} - 1} \tag{15}$$

E_0 and A_0 as well as $E_{t_{fl}}$ and $A_{t_{fl}}$ denote the concentrations of ethanol and acetic acid in the ShaRBS reactor at the beginning of the flush phase (end of a given batch) as well as at the

end of the flush phase (start of the next batch), respectively. As ethanol and acetic acid are stoichiometrically (1:1) coupled in vinegar fermentation, the concentration of ethanol in the ethanol substrate solution for flushing will intrinsically be the same as in the ethanol substrate solution for filling the conventional bioreactor. The models for the repeated batch in conventional bioreactor and the flushing repeated batch in ShaRBS, were implemented in a ModelMaker (Version 3.0.4, Cherwell Scientific Ltd.) program and were solved using the Runge-Kutta method. The draining or flush phase in the conventional bioreactor or the ShaRBS, respectively, was triggered whenever the ethanol concentration fell below the specified threshold of 4 g/L.

2.3 Development of an oxygen analysis for the ShaRBS

2.3.1 Oxygen partial pressure in the headspace of ShaRBS during vinegar fermentation

The oxygen partial pressure in the headspace of the ShaRBS reactor is of interest because of two main reasons: First, the oxygen transfer rate is useful to determine information on bacterial activity. Second, it is intended to use semiconductor gas sensors to monitor the ethanol concentration during vinegar fermentation in ShaRBS whereby the electrical resistance of the sensor depends on absorbed oxygen on the semiconductor surface [100-102]. Figure 2 depicts the balance area for oxygen in a ShaRBS reactor explained in the following in detail. The reduction in the oxygen partial pressure in the headspace of the ShaRBS reactor can be estimated depending on the following four simplifying assumptions. First, oxygen is solely consumed in order to oxidize ethanol to acetic acid; hence, the oxygen fraction used for other metabolic activities is assumed to be negligible. Second, the bacteria do not emit any carbon dioxide, and the amounts of evaporating ethanol, acetic acid and water are negligible. Thus, volumetric changes in the exhaust gas stream compared to the supply air are ascribed only to the amount of oxygen passing over into the fermentation broth. Third, the gas phase is ideally mixed, and fourth, the gas phase follows the ideal gas law. Consequently, the material balance of oxygen in the gas phase of the ShaRBS can be described by the following equation:

$$\frac{dn_{O_2,out}}{dt} = \dot{V}_{in} \cdot c_{O_2,in} - \dot{V}_{out} \cdot c_{O_2,out} - V_l \cdot OTR_{g/l} \tag{16}$$

with $n_{O_2,out}$ denoting the amount of oxygen in the gas phase, $\dot{V}_{in}$ the volumetric aeration stream entering the reactor, $c_{O_2,in}$ the molar oxygen concentration of the aeration stream, V_l

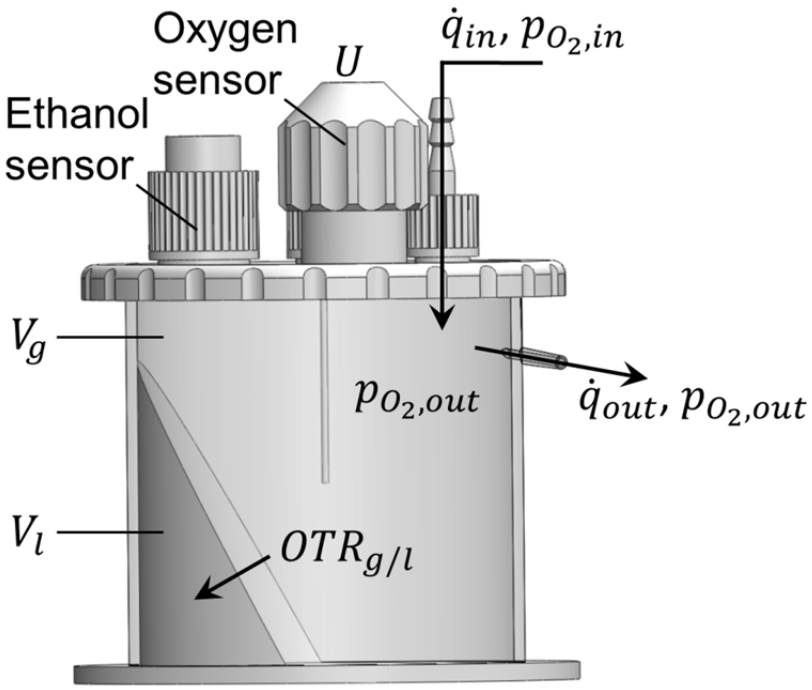


Figure 2: Oxygen balance in a ShaRBS reactor. The ShaRBS reactor is aerated at a certain volume specific aeration rate $\dot{q}_{in}$ with humidified air having the oxygen partial pressure $p_{O_2,in}$. Due to bacterial activity, oxygen passes from the gas phase with the volume V_g to the liquid phase with the volume V_l. The oxygen transfer rate is denoted as $OTR_{g/l}$. As the gas phase is idealy mixed in the ShaRBS reactor, the oxygen partial pressure $p_{O_2,out}$ is the same as in the exhaust. The volume specific exhaust rate is denoted as $\dot{q}_{out}$. The voltage U of the electrochemical oxygen sensor is proportional to the oxgen partial pressure in the gas phase.

the volume of the fermentation liquid in the reactor, $OTR_{g/l}$ the oxygen transfer rate from the gas to the liquid phase, $\dot{V}_{out}$ the volumetric exhaust gas stream leaving the reactor, and $c_{O_2,out}$ the molar oxygen concentration of the reactor headspace and exhaust gas stream. By applying the ideal gas law, equation (16) can be converted to the following equation:

$$\frac{V_g}{R \cdot T} \cdot \frac{dp_{O_2,out}}{dt} = \frac{\dot{V}_{in} \cdot p_{O_2,in} - \dot{V}_{out} \cdot p_{O_2,out}}{R \cdot T} - V_l \cdot OTR_{g/l} \tag{17}$$

The terms V_g, R, T, $p_{O_2,in}$, and $p_{O_2,out}$ represent the volume of the gas phase, the ideal gas constant, the absolute temperature, the oxygen partial pressure of the aeration stream and the oxygen partial pressure of the reactor headspace and exhaust gas stream, respectively. By using the volume specific aeration rate $\dot{q}_{in}$ (equation (18)) as well as the volume specific exhaust rate $\dot{q}_{out}$ (equation (19)), equation (17) results in equation (20) as follows:

$$\dot{q}_{in} = \frac{\dot{V}_{in}}{V_l} \tag{18}$$

$$\dot{q}_{out} = \frac{\dot{V}_{out}}{V_l} \tag{19}$$

$$\frac{dp_{O_2,out}}{dt} = \left(\dot{q}_{in} \cdot p_{O_2,in} - \dot{q}_{out} \cdot p_{O_2,out} - OTR_{g/l} \cdot R \cdot T\right) \cdot \frac{V_l}{V_g} \tag{20}$$

As the acetic acid bacteria have an extremely low growth rate and grow predominantly on the small glucose amounts contained in the added nutrients, it can be assumed that they solely consume oxygen to oxidize ethanol to acetic acid. Thus, the oxygen transfer rate (equation (21)) can be obtained from the ethanol consumption rate $\frac{dE}{dt}$ (equation (IV) in the appendix) and the molecular weight of ethanol M_E, which is 46.07 g/mol.

$$OTR_{g/l} = -\frac{1}{M_E} \cdot \frac{dE}{dt} = \frac{1}{M_E} \cdot \frac{1}{Y'_{XE}} \cdot \mu \cdot X \tag{21}$$

By using the aforementioned assumptions, the exhaust gas stream can be described as:

$$\dot{V}_{out} = \dot{V}_{in} - \frac{OTR_{g/l} \cdot R \cdot T}{p_{abs}} \cdot V_l \tag{22}$$

with p_{abs} the absolute pressure. By applying equation (18) and equation (19), the volume specific exhaust gas stream is obtained from equation (22):

$$\dot{q}_{out} = \dot{q}_{in} - \frac{OTR_{g/l} \cdot R \cdot T}{p_{abs}} \tag{23}$$

2.3.2 Online calibration of oxygen sensor on ShaRBS

The balance for oxygen in the headspace of the ShaRBS reactors is not only helpful to model the gas composition in the headspace but also to determine the oxygen partial pressure and oxygen transfer rate during fermentation with the help of an oxygen sensor. Rearranging equation (20), the oxygen transfer rate can be determined during fermentation as:

$$OTR_{g/l} = \frac{\dot{q}_{in} \cdot p_{O_2,in} - \dot{q}_{out} \cdot p_{O_2,out}}{R \cdot T} - \frac{V_g}{R \cdot T \cdot V_l} \cdot \frac{dp_{O_2,out}}{dt} \tag{24}$$

Since the incoming air is humidified in wash bottles, the oxygen partial pressure of the incoming air needs to be corrected for the additional water vapor in comparison to dry air:

$$p_{O_2,in} = p_{O_2,air} \cdot \left(p_{abs} - p_{H_2O}\right) \tag{25}$$

with $p_{O_2,air}$ the oxygen partial pressure of dry air and p_{H_2O} the partial pressure of water in water saturated air. The partial pressure of water in saturated air is calculated according to equation (26), which was obtained by approximating the data for water vapor pressure from Beitz and Küttner [103, 104].

$$p_{H_2O} = \frac{0.059 \cdot (T - 273.15)^2 - 1.042 \cdot (T - 273.15) + 20.631}{1000} \tag{26}$$

Inserting equation (23) into equation (24), the oxygen transfer rate can be calculated as:

$$OTR_{g/l} = \frac{\dot{q}_{in} \cdot \left(p_{O_2,in} - p_{O_2,out}\right) - \frac{V_g}{V_l} \cdot \frac{dp_{O_2,out}}{dt}}{R \cdot T \cdot \left(1 - \frac{p_{O_2,out}}{p_{abs}}\right)} \tag{27}$$

The headspace of the ShaRBS is assumed to be ideally mixed, thus, the oxygen partial pressure in the headspace and exhaust stream is the same. The oxygen partial pressure in the headspace is measured with an electrochemical sensor that needs to be calibrated. A linear dependency can be expected between the oxygen sensor voltage and the oxygen partial pressure in the headspace of the ShaRBS reactor:

$$p_{O_2,out} = CF \cdot U + b \tag{28}$$

with CF the calibration factor, U the oxygen sensor voltage and b the intercept. With equation (28) equation (27) is modified as follows:

$$OTR_{g/l} = \frac{\dot{q}_{in} \cdot \left(p_{O_2,in} - (CF \cdot U + b)\right) - \frac{V_g}{V_l} \cdot \frac{d(CF \cdot U + b)}{dt}}{R \cdot T \cdot \left(1 - \frac{CF \cdot U + b}{p_{abs}}\right)} \tag{29}$$

The intercept b for a particular oxygen sensor can be determined once before the experiment. Furthermore, it can be taken for granted that the intercept does not change with time, i.e. $\frac{db}{dt} = 0$. Referring to the method of Hansen et al. [105] the calibration factor can then be determined at a time point of gas flow change. As long as the bacteria are not in an oxygen limitation a sudden change of the oxygen transfer rate due to gas flow change can be excluded. Thus, the oxygen transfer rate at the time point of flow change can be described by applying equation (29) on the conditions before and after gas flow change:

$$\frac{\dot{q}_{in,1} \cdot \left(p_{O_2,in} - (CF \cdot U_1 + b)\right) - \frac{V_g}{V_l} \cdot CF \cdot \frac{dU_1}{dt}}{R \cdot T \cdot \left(1 - \frac{CF \cdot U_1 + b}{p_{abs}}\right)}$$

$$= \frac{\dot{q}_{in,2} \cdot \left(p_{O_2,in} - (CF \cdot U_2 + b)\right) - \frac{V_g}{V_l} \cdot CF \cdot \frac{dU_2}{dt}}{R \cdot T \cdot \left(1 - \frac{CF \cdot U_2 + b}{p_{abs}}\right)} \quad (30)$$

The indices 1 and 2 mark the conditions before and after gas flow change, respectively. With $U_1 = U_2$ at the time point of gas flow change, the calibration factor for the oxygen sensor is obtained by rearranging equation (30) to equation (31):

$$CF = \frac{\left(p_{O_2,in} - b\right) \cdot \left(\dot{q}_{in,1} - \dot{q}_{in,2}\right)}{\left(\dot{q}_{in,1} - \dot{q}_{in,2}\right) \cdot U_1 + \frac{V_g}{V_l} \cdot \left(\frac{dU_1}{dt} - \frac{dU_2}{dt}\right)} \quad (31)$$

The sensor voltage U_1 can be obtained directly from the sensor reading at the time point of gas flow change. The changes of the sensor voltage $\frac{dU_1}{dt}$ and $\frac{dU_2}{dt}$ are obtained by fitting and then differentiating the sensor data in the near range before and after gas flow change, respectively.

2.4 Design of custom-made lid for vinegar fermentation in microtiter plates

2.4.1 Oxygen balance in microtiter plate with custom-made lid

The envisaged custom-made lid has one borehole per well through that gas exchange with the ambient air takes place during fermentation. Figure 3 depicts the oxygen supply in a microtiter plate well with such a lid. Oxygen that is consumed by the bacteria in the medium is replenished from the headspace of the well. Oxygen from the ambient air, in turn, diffuses through the borehole into the headspace under the microtiter plate lid. Analogous to the diffusion through a cotton plug in shake flasks [106], the oxygen transfer rate OTR_{lid} through a borehole in the microtiter plate lid is estimated as follows:

$$OTR_{lid} = k_{lid,O_2} \cdot \frac{p_{O_2,air} - p_{O_2,g}}{V_l \cdot p_{abs}} \quad (32)$$

The terms p_{abs}, $p_{O_2,air}$ and $p_{O_2,g}$ denote the absolute pressure, oxygen partial pressure of the ambient air and oxygen partial pressure in the gas phase of the microtiter plate well,

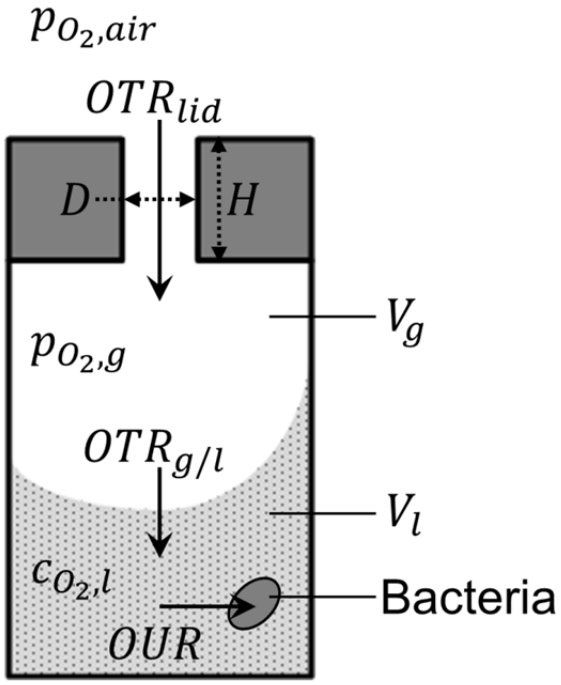


Figure 3: Oxygen supply in microtiter plate well during fermentation. Microorganisms take up dissolved oxygen for metabolism. The depleting dissolved oxygen in the medium is replenished with oxygen from the gas phase in the well headspace passing the gas-liquid interface. Driven by the arising concentration gradient, oxygen diffuses through a borehole in the microtiter plate lid from the ambient air to the well headspace. $c_{O_2,l}$ oxygen concentration of the medium at the gas-liquid interface, D diameter of the borehole in the microtiter plate lid, H height of the microtiter plate lid, $OTR_{g/l}$ oxygen transfer rate at the gas-liquid interface, OTR_{lid} oxygen transfer rate through the borehole in the microtiter plate lid, OUR oxygen uptake rate of the bacteria, $p_{O_2,air}$ oxygen partial pressure of air, $p_{O_2,g}$ oxygen partial pressure in gas phase of microtiter plate well, V_g gas volume of the well headspace, V_l filling volume of the well

respectively. The term V_l is the filling volume of the well. The mass transfer coefficient of oxygen k_{lid,O_2} can be approximated considering Fick's diffusion law [106, 107]:

$$k_{lid,O_2} = \frac{D_{e,O_2} \cdot A}{V_m \cdot H} = \frac{D_{e,O_2} \cdot p_{abs} \cdot \pi \cdot D^2}{4 \cdot R \cdot T \cdot H} \tag{33}$$

where H, D and A are the height, diameter and cross-sectional area of the borehole in the lid, respectively. The term V_m is the molar gas volume that can be calculated according to the ideal gas law with the universal gas constant R, absolute temperature T and pressure p_{abs}:

$$V_m = \frac{R \cdot T}{p_{abs}} \tag{34}$$

The effective diffusion coefficient of oxygen D_{e,O_2} is assumed to be the diffusion coefficient of oxygen in air $D_{O_{2,air}}$:

$$D_{e,O_2} = D_{O_{2,air}} \tag{35}$$

Referring to the literature [106, 108-113] and outlined in the appendix (chapter 7.3), the diffusion coefficient of oxygen in air can be calculated based on the composition of a multicomponent gas mixture with the binary diffusion coefficients of the components of this gas mixture. Thus, the oxygen mass transfer through a borehole in the microtiter plate lid can be calculated. Taking into account the oxygen transfer rate $OTR_{g/l}$ at the gas-liquid interface, the change in the oxygen partial pressure in the headspace of the microtiter plate can be described as follows:

$$\frac{dp_{O_2,g}}{dt} = \left(OTR_{lid} - OTR_{g/l}\right) \cdot R \cdot T \cdot \frac{V_l}{V_g} \tag{36}$$

where V_g is the gas volume in the headspace of the microtiter plate well. This headspace gas volume is easily determined by subtracting the liquid volume from the total well volume V_{well}:

$$V_g = V_{well} - V_l = A_{well} \cdot H_{well} - V_l \tag{37}$$

with A_{well} and H_{well} being the cross-sectional area and the height of the microtiter plate well, respectively. The oxygen transfer rate $OTR_{g/l}$ at the gas-liquid interface can generally be described as follows:

$$OTR_{g/l} = k_L a \cdot \left(c_{O_2,g} - c_{O_2,l}\right) = k_L a \cdot \left(S_{O_2} \cdot p_{O_2,g} - c_{O_2,l}\right) \tag{38}$$

whereby $k_L a$ is the volumetric mass transfer coefficient, $c_{O_2,g}$ the oxygen concentration of the gas at the gas-liquid interface, $c_{O_2,l}$ the oxygen concentration of the bulk liquid and S_{O_2} is the oxygen solubility of the fermentation medium. The $k_L a$-value for shaken microtiter plates can be approximated via empirical correlations. Equation (8) was obtained by fitting the $k_L a$-values for the Flowerplate at a fixed shaking diameter of 3 mm from Funke et al. [91] with respect to the shaking frequency n in rpm and filling volume V_l in µL:

$$k_L a = 8.53 \cdot 10^{-5} \cdot n^{2.70} \cdot V_l^{-0.46} \tag{39}$$

In practice, the dissolved oxygen tension as percent of air saturation is used instead of the dissolved oxygen concentration. Dissolved oxygen concentration and dissolved oxygen tension can be converted into each other as follows:

$$DOT = \frac{c_{O_2,l} \cdot 100}{p_{O_2,air} \cdot S_{O_2}} \tag{40}$$

For vinegar fermentation, the oxygen solubility in the medium is calculated according to Wilhelm et al. [114] and Rischbieter et al. [115] as 0.00123 mol/L/bar. The dissolved oxygen concentration during fermentation is affected by the oxygen consumed by the microorganisms and oxygen passing from the gas to the liquid phase. Thus, the change in the oxygen concentration in the fermentation broth can be calculated according to the following equation:

$$\frac{dc_{O_2,l}}{dt} = OTR_{g/l} - OUR \tag{41}$$

where OUR is the oxygen uptake rate of the microorganisms in the microtiter plate. Providing that the microorganisms in the microtiter plate behave like those in the 9 L-bioreactor, then the oxygen transfer rate at the gas-liquid interface in the 9 L-bioreactor $OTR_{bioreactor}$ is a good approximation for the activity of the microorganisms in the microtiter plate:

$$OUR \cong OTR_{bioreactor} \tag{42}$$

It is valid to regard the oxygen transfer rate at the gas-liquid interface as the oxygen uptake rate of the bacteria, because the storage capacity for oxygen in fermentation media is negligibly small.

2.4.2 Oxygen balance of bioreactor for vinegar fermentation

In order to adapt the oxygen conditions in the microtiter plate to the conditions in the 9 L-bioreactor, certain characteristics of the bioreactor for vinegar fermentation need to be known. The 9 L-bioreactor has probes for dissolved oxygen tension and ethanol. Moreover, the measurement of the ethanol concentration and its consumption permits the calculation of the oxygen transfer rate and oxygen partial pressure in the headspace of the 9 L-bioreactor based on an oxygen balance. The oxygen balance of the 9 L-bioreactor is equal to the oxygen balance of the ShaRBS device (chapter 2.3.1). Hence, the equations (16) to (20),

(22) and (23) are literally the same for the 9 L-bioreactor. Equation (21) to describe the oxygen transfer rate is revised in terms of the molar ethanol consumption rate:

$$OTR_{g/l} = -\frac{dE}{dt} \tag{43}$$

Equations (38) and (40) from the oxygen balance of the microtiter plate (chapter 2.4.1) are likewise valid in the 9 L-bioreactor. Thus, a volumetric mass transfer coefficient of oxygen for the 9 L-bioreactor can be determined if the oxygen transfer rate, the oxygen partial pressure in the headspace of the bioreactor and the dissolved oxygen tension in the bioreactor are known.

2.4.3 Scale-down of vinegar fermentation from 9 L-bioreactor to microtiter plate

The vinegar fermentation can be scaled down from the 9 L-bioreactor to the microtiter plate according to the design scheme shown in figure 4. To characterize the oxygen supply with a constant specific aeration rate (4 vvh) in the 9 L-bioreactor (6 L working volume), the ethanol concentration (E) is measured (figure 4#1) and the ethanol consumption rate ($\frac{dE}{dt}$) (figure 4#2) is determined over time for one batch in a repeated batch fermentation process. As ethanol and oxygen consumption in vinegar fermentation are stoichiometrically coupled to each other, the oxygen transfer rate ($OTR_{g/l}$) can be approximated from the ethanol consumption rate (figure 4#4, equation (43)). With an oxygen balance for the gas phase in the 9 L-bioreactor, the oxygen partial pressure in the headspace of the 9 L-bioreactor ($p_{O_2,out}$) can be calculated (figure 4#5, equations (16) to (20), (22), (23) and (43)). Furthermore, the dissolved oxygen tension (DOT) is measured in the 9 L-bioreactor (figure 4#3), which permits calculation of the oxygen concentration ($c_{O_2,l}$) in the fermentation broth (figure 4#6, equation (40)). According to equation (7), the volumetric mass transfer coefficient ($k_L a$) for oxygen in the 9 L-bioreactor can then be calculated (figure 4#6).

The oxygen supply in microtiter plates depends on five parameters: (I) the shaking diameter, (II) the microtiter plate type, i.e. geometry of the well, (III) the filling volume of the well (V_l), (IV) the shaking frequency (n) and (V) the oxygen diffusion across the lid (OTR_{lid}) (diffusion barrier). To achieve the same conditions for vinegar fermentation in the microtiter plate like in the 9 L-bioreactor, these parameters are consecutively determined. Using the BioLector device (figure 9) for microtiter plate fermentation explained in the Materials and Methods section (chapter 3.6.4), the dissolved oxygen tension (DOT) can be measured via

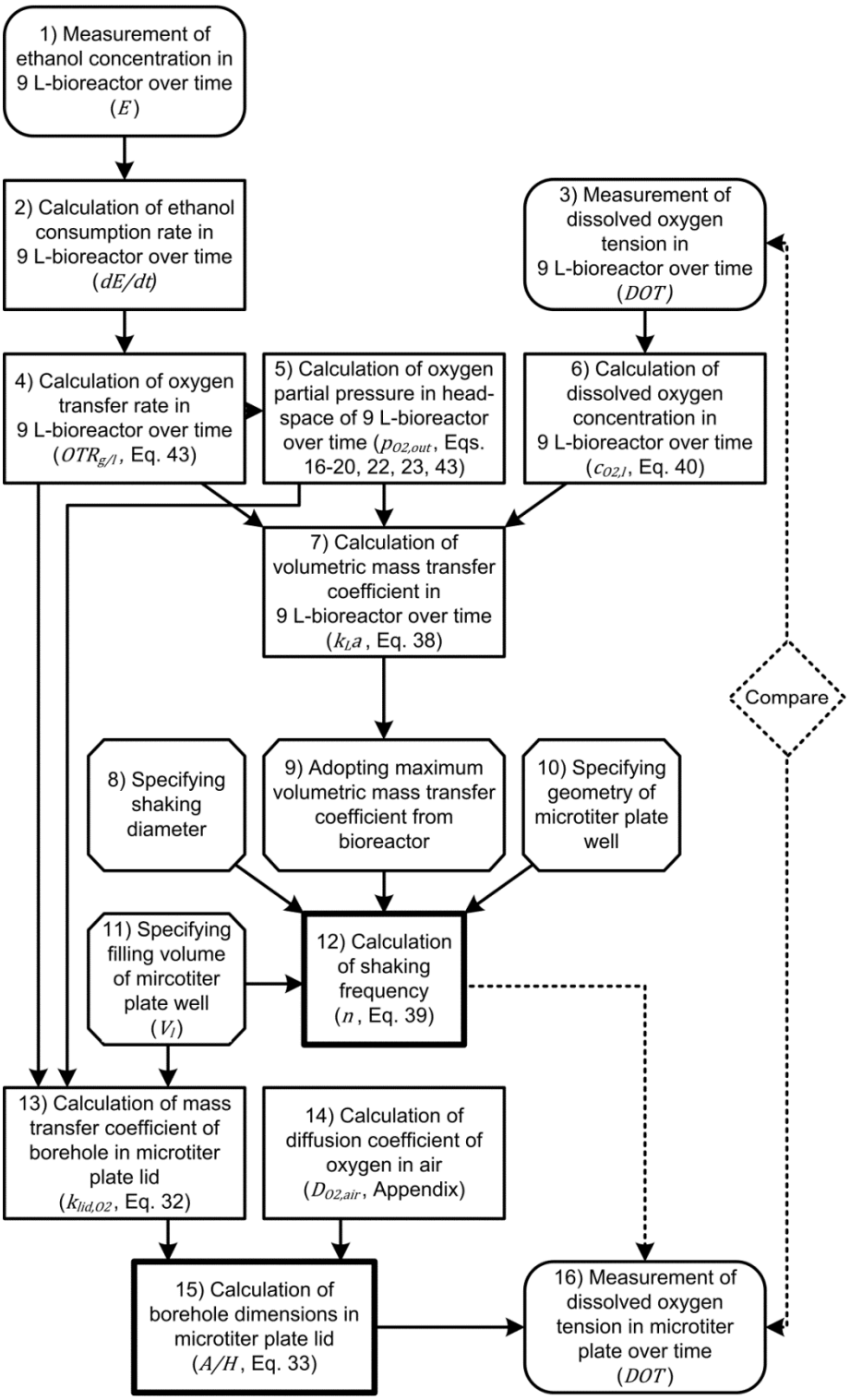


Figure 4: Determination of borehole dimensions in microtiter plate lid for vinegar fermentation. To scale down vinegar fermentation from a conventional 9 L-bioreactor to microtiter plates, the oxygen supply in a conventional 9 L-bioreactor is characterized. Guided by the oxygen supply in the 9 L-bioreactor, the operation conditions for the shaken microtiter plate and the borehole dimensions in the custom made lid are calculated. For a detailed description of the scheme it is referred to the text.

immobilized fluorophores at the well bottom. The shaking diameter of the BioLector is fixed at 3 mm (figure 4#8). To assure a high maximum oxygen transfer capacity, 48-well plates with a flower shaped well geometry, so called Flowerplates [91], are chosen for the cultivation (figure 4#10). The filling volume of the microtiter plate well (V_l) is specified to be 1200 µL (figure 4#11). The maximum volumetric mass transfer coefficient of the 9 L-bioreactor ($k_L a$) is adopted for the microtiter plate (figure 4#9). This most likely avoids an oxygen limitation during cultivation in the microtiter plate. The shaking frequency (n) is then determined by the correlation for the volumetric mass transfer coefficient ($k_L a$, figure 4#12, equation (39)).By applying the oxygen transfer rate of the 9 L-bioreactor ($OTR_{g/l}$, figure 4#4) as reference input for the respiration activity of the bacteria in the microtiter plate, a time-dependent mass transfer coefficient of the borehole in the microtiter plate lid (k_{lid,O_2}) is obtained for the chosen filling volume of the microtiter plate well (V_l, figure 4#11) and oxygen partial pressure in the headspace of the 9 L-bioreactor ($p_{O_2,out}$, figure 4#5) (figure 4#13, equation (32)). Finally, the dimensions (A/H) for the borehole in the microtiter plate lid are obtained from the mass transfer coefficient of the borehole (k_{lid,O_2}) with the diffusion coefficient of oxygen in air ($D_{O_{2,air}}$, figure 4#14) (figure 4#15, equation (33)). During an experiment the resulting dissolved oxygen tension (DOT) in the microtiter plate can be measured (figure 4#16) and compared to the dissolved oxygen tension in the 9 L-bioreactor over time.

3 Materials and Methods

3.1 Chemicals

Chemicals were obtained from Carl Roth (Karlsruhe, Germany), Merck (Darmstadt, Germany), Sigma-Aldrich (Munich, Germany), and VWR (Darmstadt, Germany). The quality was of analytical grade. Ethanol and nutrients for vinegar fermentation were obtained from Kornbrennerei Wilhelmi (Aachen, Germany) and Heinrich Frings (Bonn, Germany), respectively. Inoculation vinegar was obtained from a commercial vinegar producer.

3.2 Devices

Reference is made to special devices within the methods where these devices were used. Special devices made in the electronic and mechanical workshop of the biology group of the RWTH Aachen University were the RAMOS and ShaRBS device as well as the custom-

made lid for vinegar fermentation in microtiter plates. The bubble column for aerated transport of microbial cultures was made in the glass blowing workshop of the inorganic chemistry of the RWTH Aachen University.

3.3 Setup of ShaRBS

Figure 5 shows a schematic diagram and figure 6 a photograph of the ShaRBS for flushing repeated batch fermentation to produce vinegar. The ShaRBS was built up in a temperature-

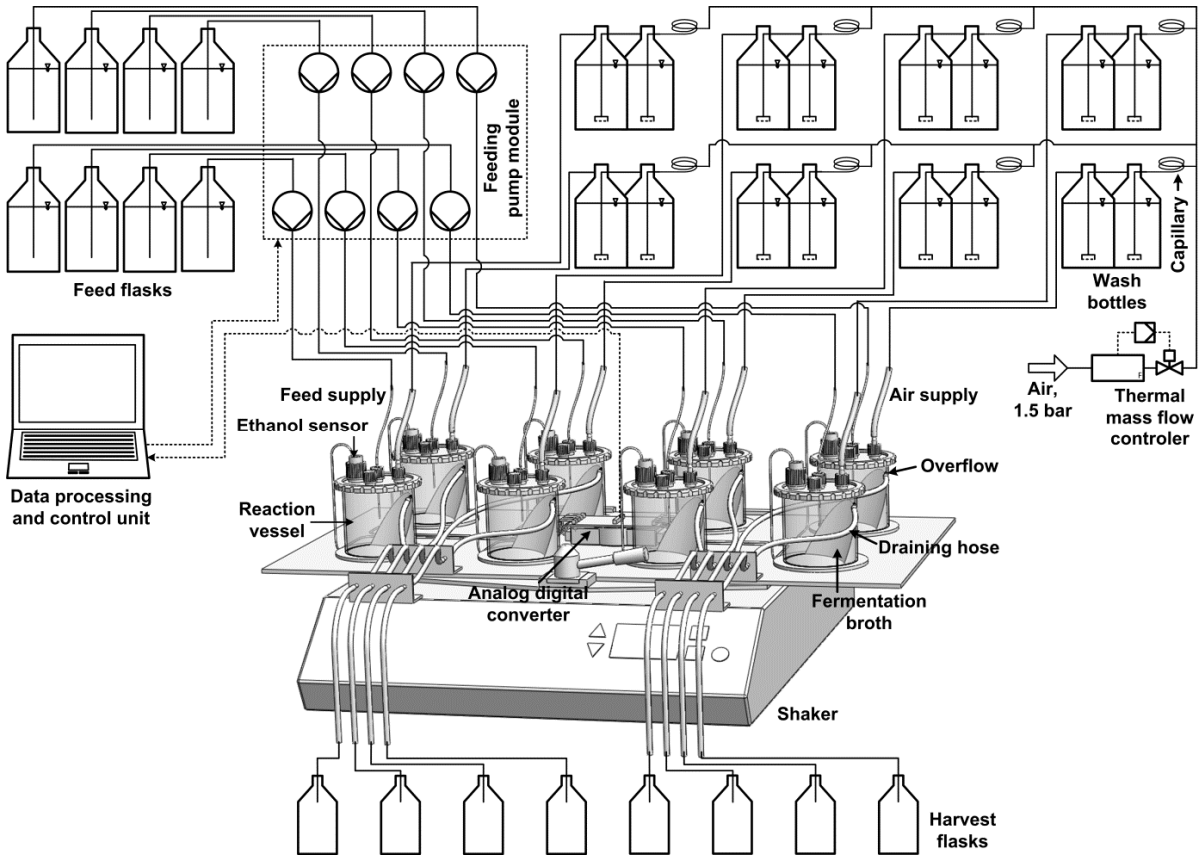


Figure 5: Schematic diagram of the ShaRBS device for parallel vinegar fermentation. Cylindrical reaction vessels with a precise overflow at the vessel wall allow for parallel repeated batch fermentation on one shaker platform (shaking frequency 300 rpm, shaking diameter 5 cm). Due to the centrifugal forces during shaking, the fermentation broth (21.5 mL) is thrown to the reactor wall and spills over, if fresh medium is supplied. To determine the time point for the resupply of substrate, the ethanol concentration in each reactor is measured with semiconductor gas sensors installed on the lid of each reactor. Upon the trigger of too low ethanol concentration (4 g/L) in one reactor, the corresponding pump of an eightfold pump module is switched on via the control unit and fresh ethanol substrate solution is pumped into the reactor from its respective reservoir. The total aeration rate (800 mL/h) is adjusted with a thermal mass flow controler and splitted into eight equal partial flows via capillaries. To reduce evaporation losses in the reactor, the compressed air is humidified by bubbling through water-filled washing bottles. The system is used in a temperature (30 °C) controlled room.

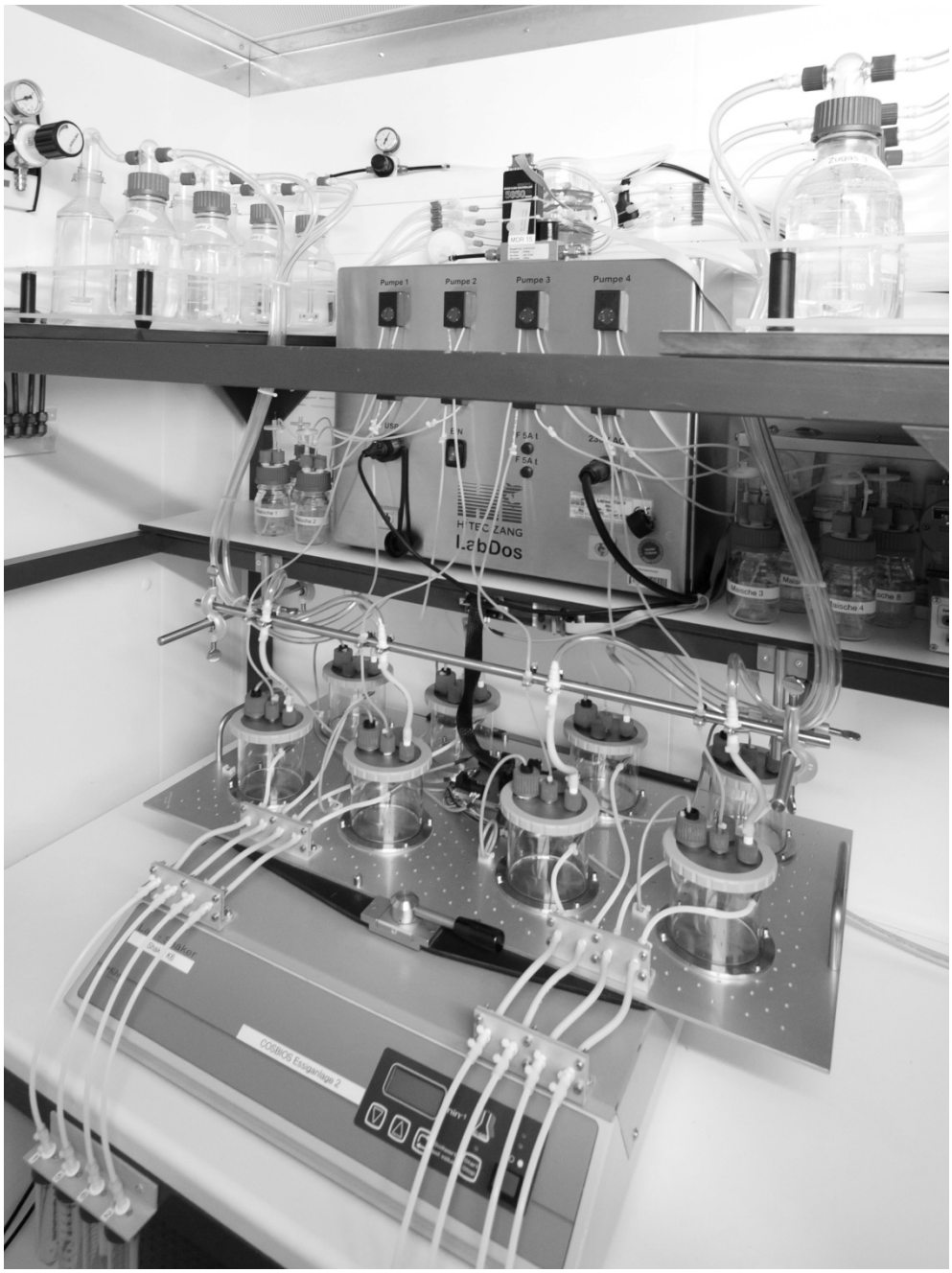


Figure 6: ShaRBS device for parallel vinegar fermentation. Photograph of ShaRBS device described in detail in chapter 3.3 and in legend of figure 5.

controlled room on a lab shaker (LS-X, Kühner, Birsfelden, Switzerland). Eight special overflow vessels known from COSBIOS [86] were used as reaction vessels. To ensure flushing repeated batch fermentation in the ShaRBS, it was essential to determine the time point to start flushing the reactor with ethanol substrate solution. Hence, each reactor was equipped with a semiconductor ethanol sensor (TGS2620, Figaro, Osaka, Japan) on top of the reactor facing to the gas phase. To allow voltage measurement, the sensors were wired to an electrical board and analog digital converter (ADAM 4018, Advantech, Munich, Germany) which, in turn, was connected to the data processing and control unit. To flush

each reactor independently with ethanol substrate solution, individually controllable feed pumps housed in one module (LabDos, HiTec Zang, Herzogenrath, Germany) were connected to each reactor. The total air flow of the ShaRBS was controlled with a thermal mass flow controller (5850 TR, Brooks Instrument, WX Ede, Netherlands) and subdivided into equal partial flows by PEEK-capillaries (length 1.5 m, inner diameter 0.13 mm; CS, Langerwehe, Germany). The aeration rate was adjusted to 5 vvh (volumes air / volumes culture medium / hour) that is a typical aeration rate in conventional bioreactors for vinegar production. To minimize evaporation losses in the reactor, the compressed air was humidified by bubbling through two subsequent washing bottles each filled with 500 mL water. Monitoring and control of the ShaRBS was realized in a LabVIEW (National Instruments, Austin, Texas, U.S.A.) program.

3.4 Characterization of the ethanol sensors of the ShaRBS

To characterize the TGS2620 ethanol sensors mounted on the lid of the ShaRBS reactors, one reactor was consecutively filled with different solutions of varying ethanol concentration, and the voltage signal was recorded. Reduced partial pressures of oxygen in the headspace of the reactor were adjusted by mixing defined air and nitrogen gas streams which were controlled with thermal mass flow controllers (EL-FLOW, Bronkhorst Hi-Tec, AK Ruurlo, Netherlands). Excess gas flow was blown off via a pressure reducing valve in front of the thermal mass flow controller of the ShaRBS device.

3.5 Determination of oxygen partial pressure and oxygen transfer rate in ShaRBS

To measure the oxygen partial pressure in the headspace of the ShaRBS reactors during vinegar fermentation, the reactors were additionally equipped with electrochemical oxygen sensors (SK-25, Figaro, Osaka, Japan) on top of the reactor. The sensors were wired to an analog digital converter (ADAM 4018, Advantech, Munich, Germany) that was connected to the data processing and control unit. To calibrate the oxygen sensors and calculate the oxygen transfer rate during fermentation according to the method presented in the theory section (chapter 2.3.2), the gas flow was automatically increased from 5 vvh to 10 vvh every 4 h for 10 min. To adjust the gas flow automatically, the thermal mass flow controller of the ShaRBS was controlled via an analog output module (ADAM 4021, Advantech, Munich, Germany).

3.6 Fermentation

3.6.1 Preculture fermentation in 9 L-bioreactor

Acetic acid bacteria cultures were maintained in conventional repeated batch mode in 9 L-bioreactors (Pilot-Acetator, Heinrich Frings GmbH & Co KG, Bonn, Germany) at a filling volume of 6 L and at 30 °C. If the ethanol concentration fell below the threshold of 4 g/L, one third of the culture broth was automatically replaced with fresh ethanol substrate solution containing nutrients (Acetozym DS Plus, Heinrich Frings GmbH & Co KG, Bonn, Germany) as specified by the manufacturer. The ethanol concentration was measured online with a probe immersed into the fermentation broth and containing the TGS 822 (Figaro, Osaka, Japan) semiconductor gas sensor. The sensor resistance was approximated with a second-order polynomial function and calibrated against offline samples. The dissolved oxygen tension was determined with an electrochemical dissolved oxygen sensor (AppliSens, Applikon Biotechnology, Schiedam, the Netherlands) connected to an O_2-amplifier type 325 (Ingold, Mettler Toledo GmbH, Gießen, Germany). The measured dissolved oxygen tension was smoothed using a spline function.

3.6.2 Shake flask fermentations in RAMOS

To measure the oxygen transfer rate during shake flask fermentations of acetic acid bacteria for vinegar production, the RAMOS device was used. In principal, the eight measuring flasks of the RAMOS device are 250 mL shake flasks with a modified head. In the upper part of the shake flasks the normal necks are replaced by melted ports for supply and exhaust air, for an oxygen sensor and for inoculation. Ventilation of the flasks is adjusted with a thermal mass flow controller to obtain a headspace gas concentration equal to that of a normal shake flask with a cotton plug [57, 107]. For vinegar fermentation in shake flasks, the aeration rate was reduced to specific aeration rates of 2 vvh (volume gas/volume liquid/hour) to 5 vvh typical for large-scale bioreactors in vinegar production. To study the oxygen mass transfer characteristics in shake flasks during vinegar fermentation, different filling volumes were applied in the shake flasks referring to the method of Maier and Büchs [116]. This resulted in different specific aeration rates, because the total air flow for each shake flask of the RAMOS device was the same. To determine the oxygen transfer rate, the ventilation is periodically and automatically interrupted by closing valves for air inlet and outlet of each shake flask. Then the oxygen transfer rate could be calculated based on the oxygen partial pressure decrease measured with electrochemical oxygen sensors and the change of the total pressure measured with differential pressure sensors [57]. During the experiments the temperature was kept constant at 30 °C either in a temperature controlled room or hood.

For the shake flask fermentations in RAMOS acetic acid bacteria precultures were drawn from the 9 L-bioreactor operated in repeated batch mode. The RAMOS device was inoculated either by traditional pipetting procedure or by using an aerated bubble column as described below. For the traditional inoculation procedure (figure 7, upper part), the acetic acid bacteria preculture was allowed to drain from the bioreactor into a beaker. Some of this drained broth was pipetted into the flasks of the RAMOS device. Afterwards the RAMOS device was installed on the shaker platform and, subsequently, the shaker and data acquisition were started. Hereto, two variations were examined. In one experiment, the preculture was drained off from the 9 L-bioreactor to a time point where there was still a large amount of ethanol present, which could be directly reused for further fermentation in the RAMOS device. In a second experiment the preculture was cultivated almost to depletion of the ethanol substrate. Then the fermentation broth was drained off from the 9 L-bioreactor and fresh ethanol was added to the residue in the beaker to form a new batch for further

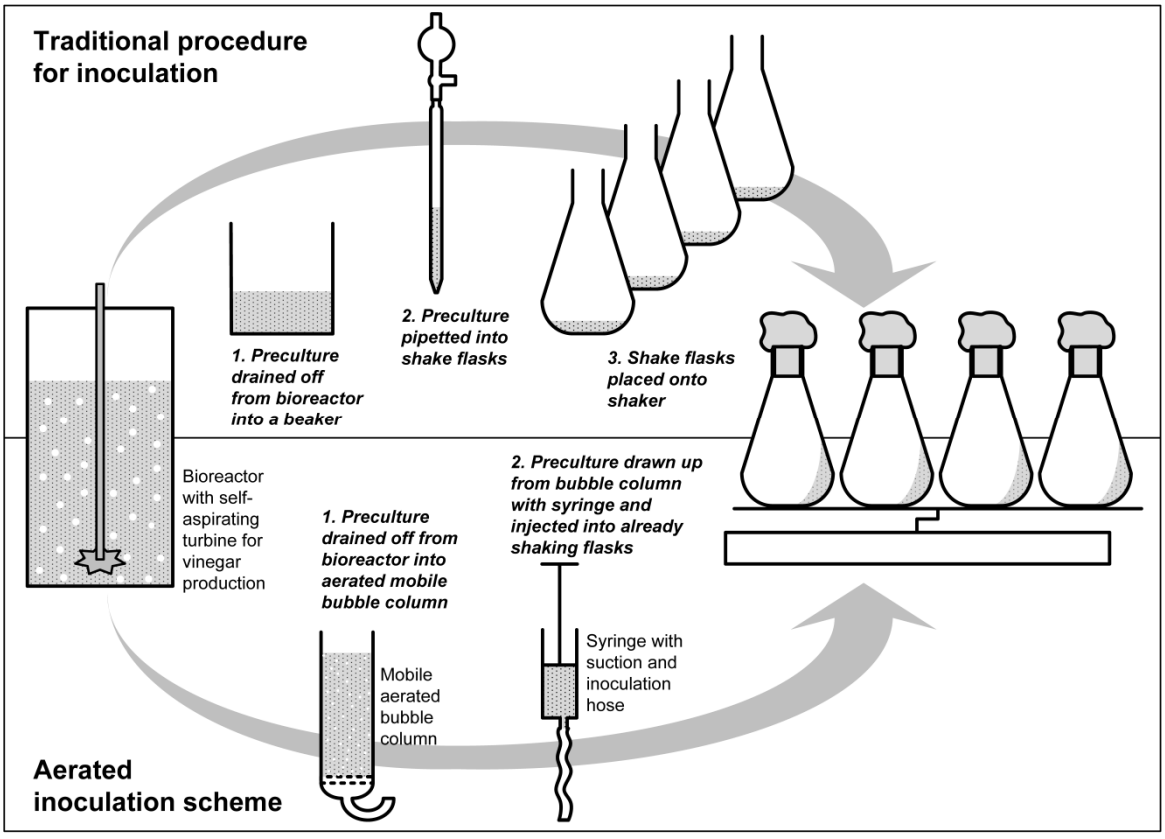


Figure 7: Inoculation schemes for shaken bacterial cultures. In the upper part, the traditional procedure for inoculation is depicted. Main cultures are inoculated from a preculture by pipetting, usually performed in a clean bench. Inoculated flasks are then placed onto a shaker and the shaker is started. In the lower part the procedure for acetic acid bacteria culture for vinegar fermentation is depicted where a constant oxygen transfer is maintained. The culture is drained off from the bioreactor into an aerated bubble column and then transported in the bubble column to the already running shaker. The culture is then rapidly drawn up with a syringe and directly injected into the shaking flasks.

fermentation in the RAMOS device. The traditional inoculation procedure for the RAMOS device lasted 15 minutes.

For the aerated inoculation procedure (figure 7, lower part), the acetic acid bacteria preculture was partially drained off into an aerated bubble column from the 9 L-bioreactor four to five hours after its refilling with fresh ethanol. This bubble column (figure 8) was a truncated 200 mL measurement cylinder with a fritted glass bottom linked to a tube for aeration. It also had a lateral drain valve. Air was supplied from a pressurized air cylinder. The pressure between the gas cylinder and the bubble column was reduced to 1.5 bar via a pressure regulator and the gas flow was adjusted to 1 vvm (volume gas/volume liquid/minute) with a rotameter (Sho-Rate 1350, Brooks Instrument, WX Ede, Netherlands). The pressurized air cylinder and bubble column were installed on a mobile trolley. From the bubble column, volumes of 13 to 32 mL of the acetic acid bacteria preculture were rapidly distributed into the flasks of the already shaking RAMOS device (100 rpm, 5 cm shaking diameter) either with a 20 mL syringe or via a drain hose. Then the RAMOS flasks were

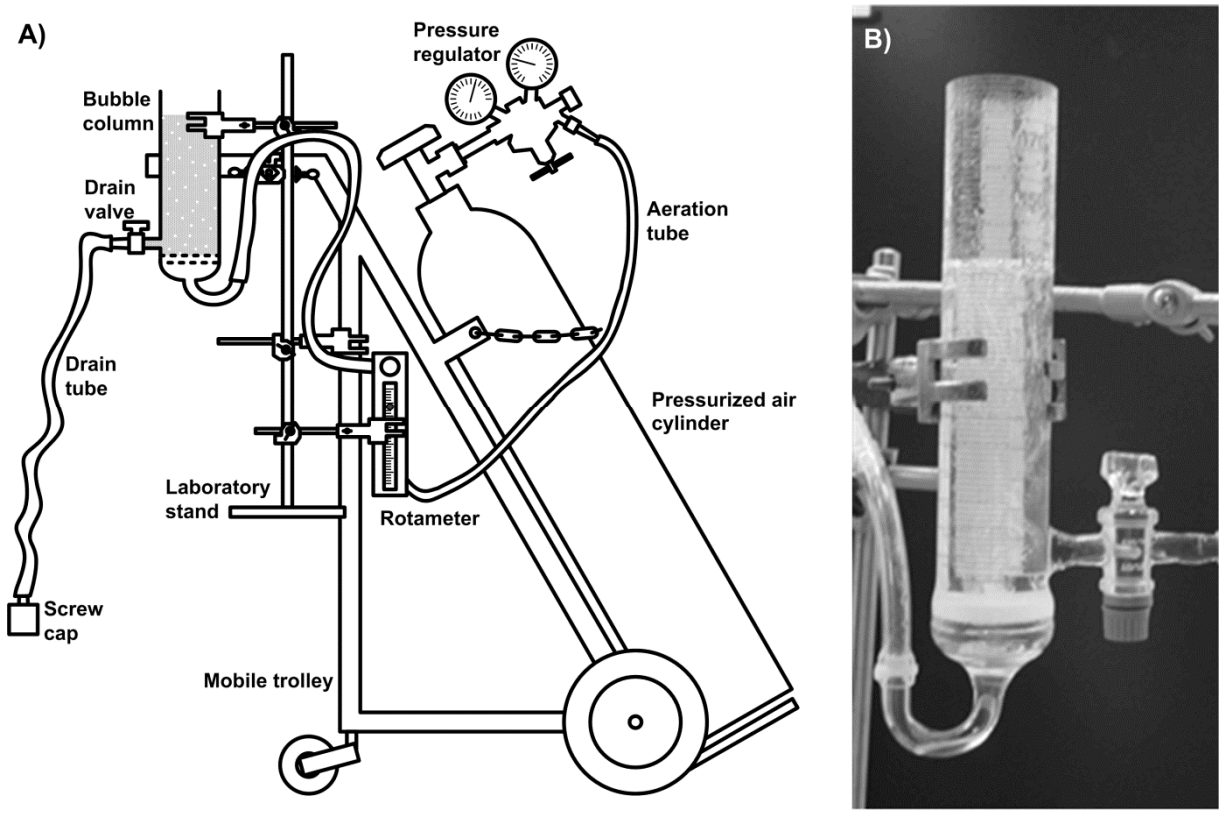


Figure 8: Mobile bubble column for inoculation of shaken acetic acid bacteria cultures for vinegar fermentation. A) Schematic setup of the mobile bubble column: The bubble column was connected via tubes to a pressurized air or oxygen cylinder whereby the flow was adjusted via a rotameter. The bubble column was fixed to a mobile trolley. B) Photograph of the bubble column, which was a truncated 200 mL measurement cylinder with a fritted glass bottom linked to a tube for aeration.

closed with a screw cap, the shaking frequency was increased (300 rpm or 350 rpm) and data acquisition started. The bubble column was either aerated with air or pure oxygen. If the bubble column was aerated with oxygen, oxygen saturation of the 9 L-bioreactor was also boosted with oxygen prior to culture broth discharge. The time for transferring the bacterial culture from the 9 L-bioreactor to the RAMOS device according to the aerated inoculation scheme lasted a quarter of an hour.

3.6.3 ShaRBS fermentations

For the inoculation of the ShaRBS fermentations, acetic acid bacteria precultures were drained from the bioreactor described above (chapter 3.6.1) into the aerated bubble column (chapter 3.6.2) 4 h after the end of the preceding filling phase. The acetic acid bacteria preculture in the continuously aerated bubble column was transported to the already shaking ShaRBS device (100 rpm, 5 cm shaking diameter) in a temperature (30 °C) regulated room. Then, the preculture was rapidly injected with a syringe into the ShaRBS reactors. Afterwards, the shaking frequency was increased to 300 rpm leading to a liquid filling volume of 21.5 mL. These shaking conditions guaranteed a maximum oxygen transfer capacity higher than the oxygen demand of the bacteria, i.e. oxygen limitation is avoided during cultivation. After 26 h, the shaking frequency was increased to 325 rpm to eject part (4.5 mL) of the culture broth. Then the shaking frequency was lowered to 275 rpm, and fresh ethanol (110.5 g/L) substrate solution (10 mL) containing nutrients (Acetozym DS Plus, Heinrich Frings GmbH & Co KG, Bonn, Germany) as specified by the manufacturer was fed into the reactor via the feed pump. At the end of this filling phase (start of the second batch), the shaking frequency was again increased to 300 rpm. Thereby, samples (5.5 mL) of the start of the second batch were obtained. The ethanol concentrations of the ejected fermentation broths at the end of the first batch and overflow samples at the start of the second batch were determined by gas chromatography to calibrate the ethanol sensors of the ShaRBS reactors. After calibration of the ethanol sensors, the eight parallel fermentations were allowed to run independently from each other by starting the following batches via flushing with ethanol substrate solution whenever the ethanol concentration of the respective reactor fell below the threshold concentration of 4 g/L. For comparative fermentation experiments with different ethanol lots, at least five batch cycles with potable, food grade ethanol (96.6 %-vol. Kornbrennerei Wilhelmi, Aachen, Germany; termed lot AC) were conducted before the ethanol in the ethanol substrate solution for the following batches was changed to different ethanol lots, termed lot A, B or C. These non-specified ethanol lots (96.6 %-vol.) were kindly supplied by a regional vinegar producer.

3.6.4 Microtiter plate fermentations

For the fermentations in the microtiter plate, a Flowerplate with optodes to measure dissolved oxygen tension in the BioLector (m2p-labs GmbH, Baesweiler, Germany) was used (figure 9). The Flowerplate is a 48-well baffled microtiter plate for increased oxygen transfer with flower shaped well geometry [91] and is distributed by m2p-labs GmbH (Baesweiler, Germany). To inoculate the Flowerplate, it was essential to ensure constant oxygen supply of the bacteria. Therefore, a special inoculation procedure described below and depicted in figure 10 was designed. Acetic acid bacteria precultures were drained from the 9 L-bioreactor operated in repeated batch mode (chapter 3.6.1) into the aerated bubble column (chapter 3.6.2) 4.5 h after the end of the preceding filling phase. Once in the aerated bubble column, the preculture was transported to the BioLector device and poured into a beaker with a rotating stirrer bar. From the stirred beaker, the acetic acid bacteria preculture was rapidly distributed into the wells of the already shaking Flowerplate in the BioLector with

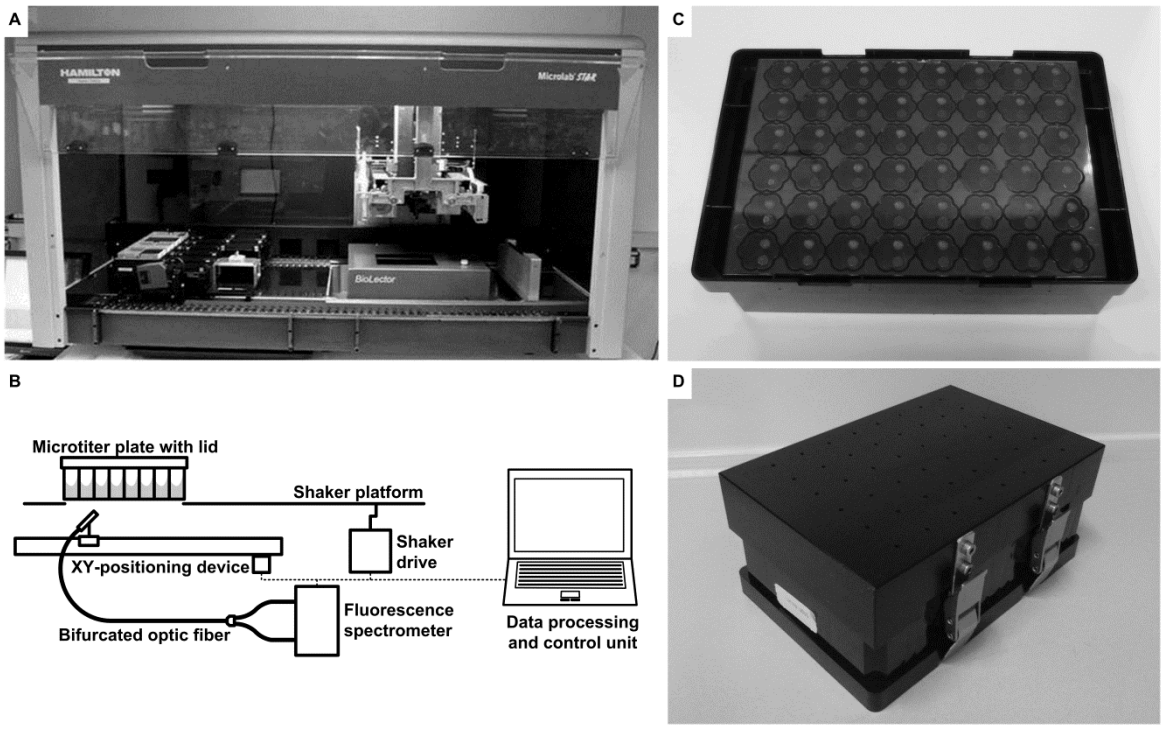


Figure 9: BioLector device for measurement of dissolved oxygen tension in micortiter plates. A) BioLector (m2p-labs) integrated into an automated liquid-handling system (Microlab STAR, Hamilton Robotics), B) Scheme of the measurement setup in BioLector device: The microtiter plate is fixed on the shaker platform above an opening. From the bottom side, the tip of a bifurcated optic fiber is positioned via a XY-positioning device below a certain well for fluorescence measurements. With the help of fluorescent optodes at the bottom of the microtiter plate wells, the dissolved oxygen tension can be measured. C) Bottom view of Flowerplate (m2p-labs) with optodes for measuring dissolved oxygen tension, D) Flowerplate with custom-made lid for vinegar fermentation in microtiter plates

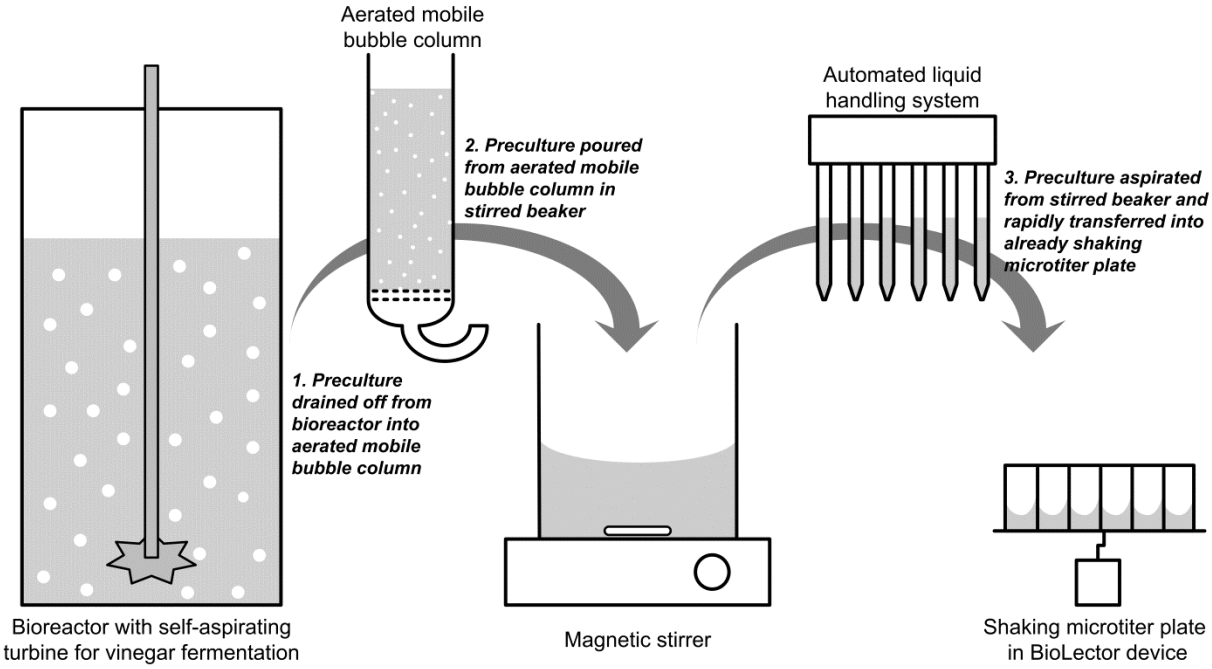


Figure 10: Inoculation scheme for vinegar fermentation in microtiter plates. A virtually non-interrupted oxygen transfer is essential for the inoculation of the acetic acid bacteria in vinegar fermentation. The bacterial preculture is drained off from the 9 L-bioreactor into an aerated bubble column, transported close to the BioLector device and poured into a beaker with an already stirring magnetic bar. Then, the preculture is rapidly pipetted into an already shaking microtiter plate in the BioLector by an automated liquid handling system. Finally, the microtiter plate is manually closed with the lid, and measurement of the dissolved oxygen tension is started.

an automated liquid handling system (Microlab Star, Hamilton Robotics GmbH, Martinsried, Germany). The combination of the BioLector and the liquid handling system is known as “Robo-Lector” [87, 88]. After inoculation the Flowerplate was closed either with a gas-permeable adhesive seal (AB-0718, ABgene – Thermo Scientific, Epsom United Kingdom) or the custom-made lid (figure 9D). The custom-made lid was clamped directly onto a cutted Flowerplate (figure 9C and D), whereby a perforated spongy gasket was sandwiched between Flowerplate and the lid. In the case of the gas-permeable seal, typical shaking conditions were adjusted: shaking frequency of 1000 rpm, shaking diameter of 3 mm and a filling volume of 1000 µL. In case of the fermentation with the custom-made lid these shaking parameters were adjusted according to the designing scheme (figure 4) and explained in the results and discussion section: shaking frequency of 879 rpm, shaking diameter of 3 mm and a filling volume of 1200 µL. The filling volume in the Flowerplate at the end of the culture time was determined via the capacitive liquid level detection function of the liquid handling system. In brief, a weak electrical potential was applied between the pipetting channel and the labware carrier. Using conductive tips and ionic fermentation broth the capacitance of the circuit was measured. From this data the height of the liquid surface was determined by the robotic software and the height position was written to a file. Filling a Flowerplate with

specific volumes of vinegar broth before the measurement allowed for a linear calibration between liquid surface height position and liquid filling volume.

3.7 Shut off experiment in bubble column

For the investigation of cell viability and activity a shut off experiment in the bubble column used for the transfer of the acetic acid bacteria (figure 8) was conducted. In the bubble column the dissolved oxygen tension could be measured with the help of an oxygen sensitive sensor spot (PSt3, Precision Sensing GmbH, Regensburg, Germany). The sensor spot was bonded to the inner wall of the bubble column 3.5 cm above the fritted glass bottom with a silicone glue. The fluorescent dye in the sensor spot was excited and phase angle shift of the fluorescent light was evaluated with a fiber optic transmitter (Fibox 3, Precision Sensing GmbH, Regensburg, Germany). Prior to the experiment the bubble column was filled with vinegar broth from the preceding batch and aerated with nitrogen and air to calibrate the phase angles of 0 % and 100 % air saturation, respectively. For the shut off experiment 150 mL of the bacterial culture were directly drained from the 9 L-bioreactor into the aerated bubble column 6 h after a batch experiment had been started. The culture broth was aerated in the bubble column until the dissolved oxygen tension reached steady state. Then aeration was stopped and the decrease in dissolved oxygen tension was recorded. One minute after the dissolved oxygen tension reached values close to zero aeration was turned on again. After the dissolved oxygen increased and reached steady state the aeration was shut off once more to evaluate a new decrease in dissolved oxygen tension.

3.8 Gas chromatography

Ethanol and acetic acid concentrations were determined by gas chromatography (CP-3800, Varian, Walnut Creek, CA, U.S.A.) using a CP-WAX58(FFAP)-CB (Varian, Walnut Creek, CA, U.S.A.) column and Varian Star 5.51 Software. Sample volumes of 0.2 µL were injected (CP-8400 Autosampler, Walnut Creek, CA, U.S.A.) onto the column at a temperature of 280 °C. The oven temperature was maintained at 40 °C for one minute and then increased from 40 °C to 220 °C at a rate of 60 °C/min. The temperature of 220 °C was maintained for five more minutes. The temperature of the flame ionization detector was 250 °C.

4 Results and Discussion

4.1 Vinegar fermentation in batch mode on shake flask scale

In order to establish a small scale cultivation method for obligatory aerobic acetic acid bacteria in vinegar fermentation experiments focusing on the inoculation procedure of the main culture in shake flasks were conducted. First, the results for the inoculation according to the traditional procedure are shown. Second, improvements that could be made following the aerated inoculation scheme are described. Then, general respiration characteristics of acetic acid bacteria in shake flasks for vinegar fermentation are presented. Finally, the effect of oxygen depletion on cell activity was studied in a bubble column in a shut off experiment.

4.1.1 Shake flask fermentations according to the traditional procedure of inoculation

In the first two experiments, the acetic acid bacteria cultures were inoculated according to a traditional procedure, i.e. a temporarily non-aerated preculture was distributed into the shake flasks of the RAMOS device by pipetting (figure 7, upper part). In the first experiment shown in figure 11, the preculture was taken from the 9 L-bioreactor out of the batch phase at a relatively early time point of 15 h and was cultivated in the main culture at standard shake flask conditions. In the latter experiment shown in figure 12, the preculture was taken from the 9 L-bioreactor almost at the end of the batch phase, mixed with fresh ethanol and nutrients to adjust conditions of a batch start. The cells were cultivated at reduced aeration rates typical for vinegar fermentation in order to avoid evaporative losses of ethanol and acetic acid. All the shake flask cultures showed an increasing respiration activity inferred by the increase of the oxygen transfer rates. Thus, the bacteria were alive and could be cultivated in shake flasks under industrially relevant ethanol and acetic acid concentrations in the range of about 0–32.5 g/L and 80–140 g/L, respectively. Nonetheless, in both experiments the respective respiration curves were not reproducible, neither under standard shake flasks conditions (figure 11) nor at reduced aeration rates typical in the vinegar industry (figure 12). This is obvious as each shake flask culture of one experiment exhibited different initial and maximal respiration rates even though they were derived from the same preculture. Even the curves of the oxygen transfer rates in shake flasks that ran in duplicate were significantly different. The shaking parameters (shaking frequency, shaking diameter, shake flask size and filling volume) during the main cultivation were chosen to guarantee a higher maximal oxygen transfer capacity than necessary for the respiration activity of the bacteria. Thus, there was no oxygen limitation in the beginning of the shaken main

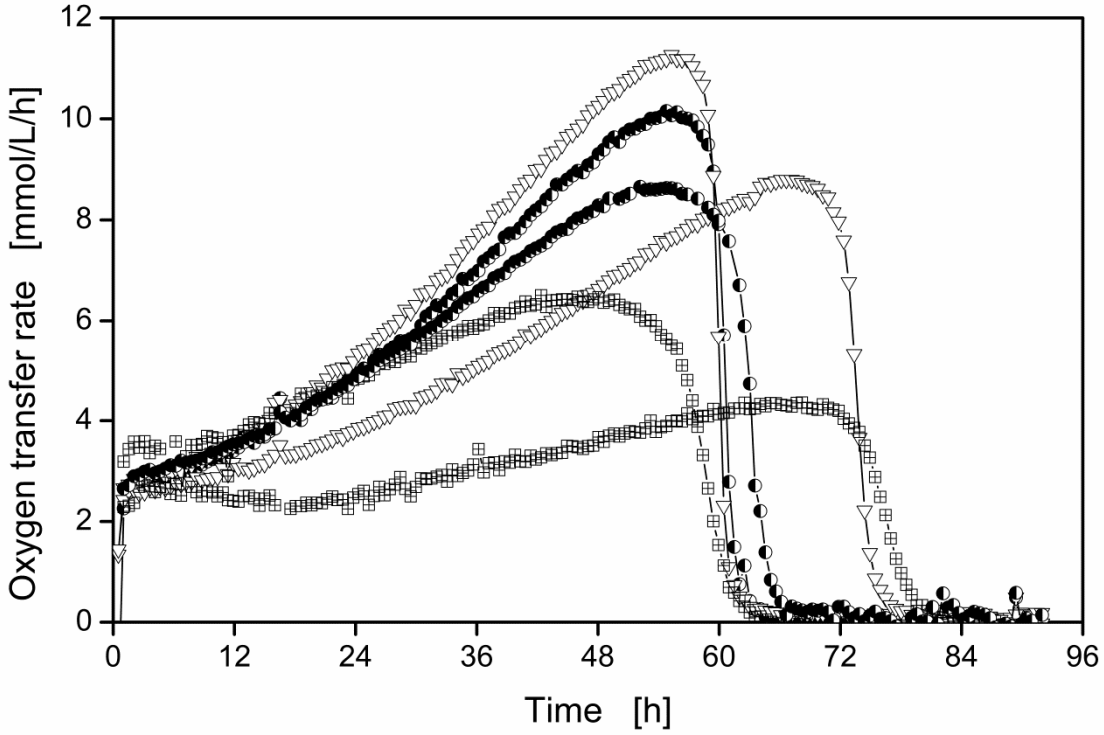


Figure 11: Oxygen transfer rate in shake flasks of acetic acid bacteria inoculated according to a traditional procedure. Vinegar culture was discharged from a 9 L-bioreactor into a beaker. The culture was then distributed into the shake flasks of the RAMOS device by pipetting. Initial ethanol and acetic acid concentration were 22.9 g/L and 92.9 g/L, respectively. Experiments were carried out in duplicates. Shaking frequency was 300 rpm and shaking diameter was 5 cm. —⊞— 10 mL filling volume (V_l) which translates into a specific aeration rate (q) of 60 vvh, —◐— V_l = 15 mL, q = 40 vvh, —▽— V_l = 25 mL, q = 24 vvh

cultivation, which could have been deduced from a plateau of the oxygen transfer curve [57]. Under ordinary shake flask conditions, i.e. aeration rates ranging from 24 vvh to 60 vvh (figure 11), also no oxygen limitation was observed during the whole course of the fermentation. At reduced aeration rates (figure 12), however, a plateau in the oxygen transfer curve indicating oxygen limitation was observed for the cultures with the two smallest aeration rates of 2 vvh and 3 vvh, whereas no oxygen limitation was observed at the higher aeration rates of 4 vvh and 5 vvh. The different level of the maximum oxygen transfer capacity for the different aeration rates could be attributed to the different filling volumes of the shake flasks and the accompanying different mass transfer characteristics. Moreover, the available oxygen in the headspace of the shake flasks decreased with the lower specific aeration rate and, accordingly, the driving oxygen concentration gradient at the gas liquid interface diminished. Hence, the following experiments were mainly conducted at the uppermost aeration rate for vinegar fermentation of 5 vvh to surely avoid oxygen limitation during the course of fermentation.

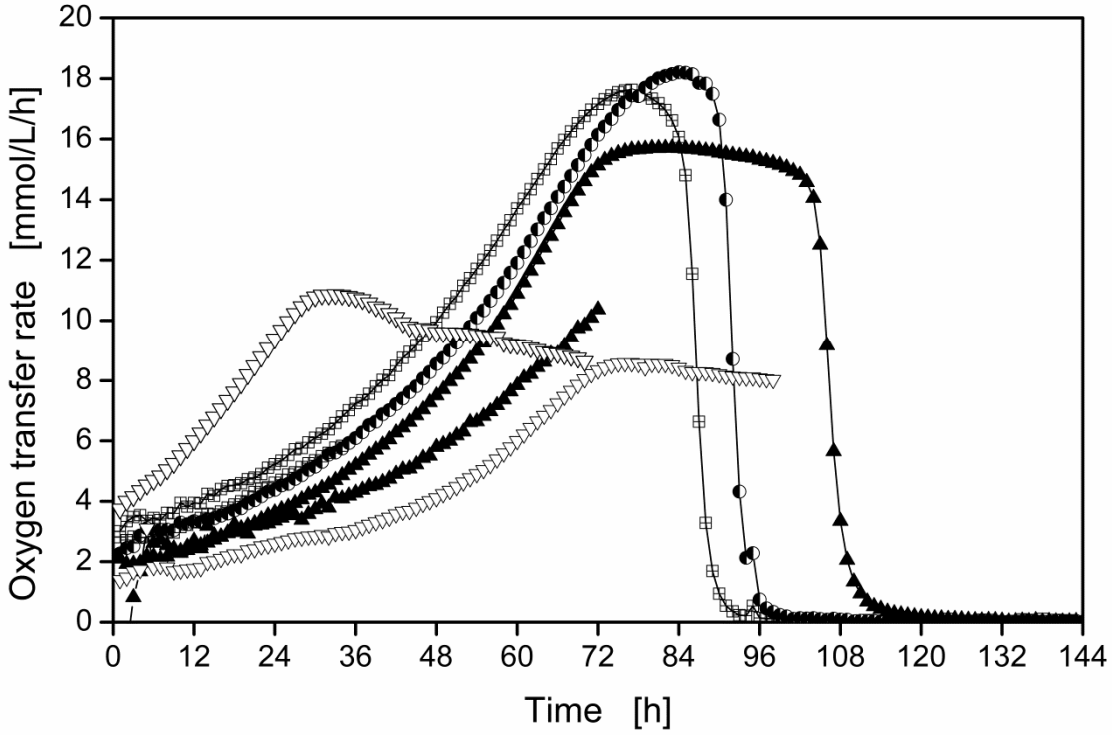


Figure 12: Oxygen transfer rate in shake flasks of acetic acid bacteria with reduced aeration rate typical for commercial vinegar production. The preculture was discharged close to the end of a running batch from a 9 L-bioreactor into a beaker and was adjusted with fresh ethanol for the next batch in the shake flasks. The preculture was then distributed into the shake flasks of the RAMOS device by pipetting. Initial ethanol and acetic acid concentration were 32.4 g/L and 80.3 g/L, respectively. Shaking frequency was 300 rpm and shaking diameter was 5 cm. The specific aeration rate in the shake flasks was lowered to typical aeration rates of vinegar industry. —⊞— 12.7 mL filling volume (V_l) which translates into a specific aeration rate (q) of 5 vvh, —◐— V_l = 15.8 mL, q = 4 vvh, —▲— V_l = 21.1 mL, q = 3 vvh (duplicates), —▽— V_l = 31.7 mL, q = 2 vvh, (duplicates)

4.1.2 Shake flask fermentations according to the aerated inoculation scheme

4.1.2.1 Comparison of traditional procedure of inoculation with the aerated inoculation scheme

As there is no power input assuring mass transfer and thus oxygen supply during inoculation according to the traditional procedure for inoculation, it is likely that the time for preparing the main culture took too long for the acetic acid bacteria to fully survive. Thus, some of the acetic acid bacteria may have suffered from oxygen depletion and died during inoculation, because acetic acid bacteria are highly obligatory aerobic under industrial conditions [6, 8-11, 14-16]. Consequently, the respiration activities of the main cultures were not

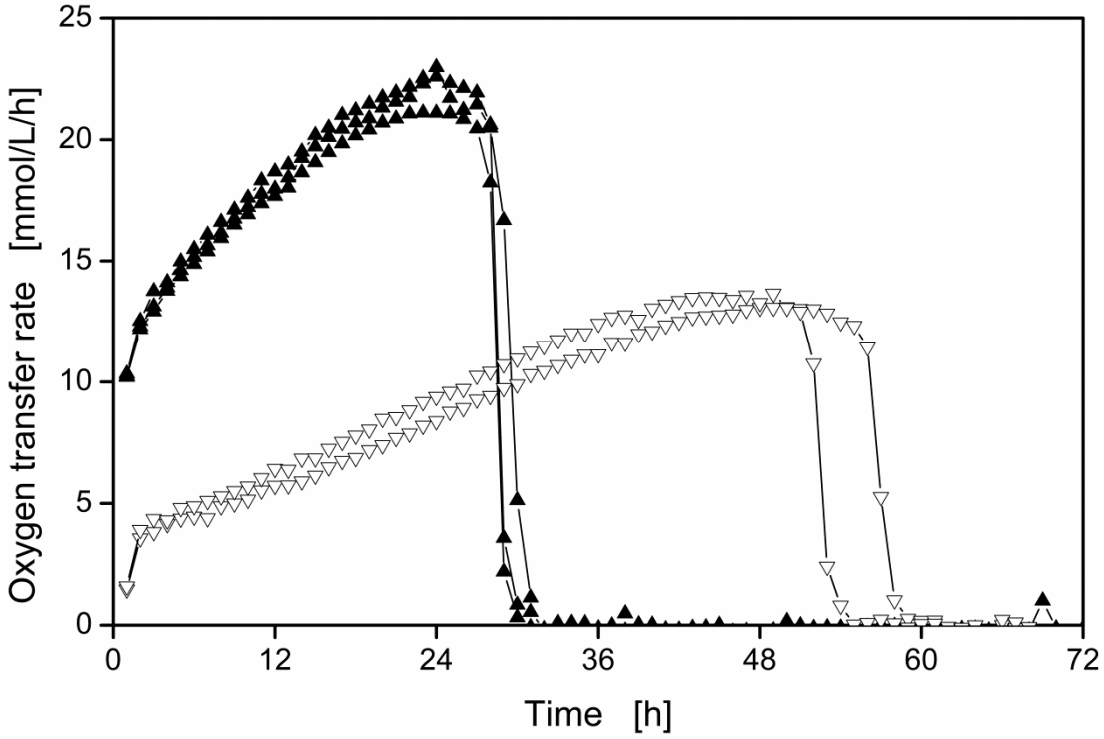


Figure 13: Oxygen transfer rate in shake flasks of acetic acid bacteria inoculated according to a traditional procedure or an aerated inoculation scheme. The preculture from a 9 L-bioreactor was either discharged into a beaker and distributed by pipetting into the shake flasks of the stopped RAMOS device or discharged into the aerated mobile bubble column and then distributed with a syringe into the shake flasks of the already shaking RAMOS device. Initial ethanol and acetic acid concentration were 34.2 g/L and 89.4 g/L, respectively. Shaking frequency was 300 rpm and shaking diameter was 5 cm. In both cases the filling volume was 13 mL which translates into a specific aeration rate of 5 vvh. —▽— main culture inoculated according to a traditional inoculation procedure (duplicates) —▲— main culture inoculated according to an aerated inoculation scheme (triplicates)

reproducible. Therefore, an aerated inoculation scheme was designed in which a permanent oxygen transfer is assured by a mobile bubble column during the transport from the 9 L-bioreactor to the RAMOS device (figure 7, lower part). In figure 13, the traditional procedure for inoculation is compared to the aerated inoculation scheme. First, two of the RAMOS flasks were traditionally inoculated by pipetting and the shaker was started. Subsequently, three other flasks of the RAMOS device were inoculated with the same preculture but according to the aerated inoculation scheme using the bubble column for the transfer from the 9 L-bioreactor. In addition, the preculture was rapidly injected into the already shaking RAMOS device. The cultures inoculated according to the aerated inoculation scheme showed an astonishingly higher initial respiration activity than the traditionally inoculated cultures. This indicates that part of the bacteria in the preculture during the traditional inoculation procedure must have died as a constant oxygen supply was not

guaranteed for that procedure. Therefore, less active bacteria in the beginning of the main cultivation resulted in less respiration activity. These results demonstrate that traditional microbiological procedures are not suitable for the obligatory aerobic acetic acid bacteria in submerged vinegar fermentation. The cultures inoculated according to the aerated inoculation scheme showed a higher respiration activity throughout the whole fermentation and the oxygen transfer rate decreased to zero earlier at about 30 h once all the ethanol substrate was depleted. With the inoculation according to the aerated inoculation scheme, the respiration curves of the acetic acid bacteria cultures coincided with each other, whereas the curves of the traditionally inoculated cultures diverged. Thus, the respective coinciding respiration curves clearly show improved reproducibility for main cultures of obligatory aerobic bacteria inoculated according to an aerated inoculation scheme. The concentrations of ethanol and acetic acid in the main cultures inoculated according to the traditional and aerated inoculation scheme were initially the same. Therefore, also the final acetic acid concentrations were with 138.9 g/L and 136.2 g/L, respectively, practically the same. However, for the main cultures inoculated according to the aerated inoculation scheme these product titers were achieved much faster.

4.1.2.2 Influence of filling volume and aeration rate on oxygen mass transfer characteristic in shake flasks

In general the oxygen transfer rate through the gas liquid interface $OTR_{g/l}$ in bioreactor systems can be described by the following equation:

$$OTR_{g/l} = k_L a \cdot S_{O_2} \cdot p_{abs} \cdot \left(y_{O_2,g} - y_{O_2,l}\right) \tag{44}$$

with $k_L a$ the volumetric mass transfer coefficient, S_{O_2} the oxygen solubility of the fermentation medium, p_{abs} the absolute pressure, $y_{O_2,g}$ and $y_{O_2,l}$ the mole fraction of oxygen in the gas and liquid phase, respectively. The $k_L a$-value in shake flasks is determined by the shaking parameters and can be calculated according to the correlation of Maier and Büchs [116] and Seletzky et al. [117]. For the shaking conditions (5 cm shaking diameter, 300 rpm shaking frequency, 250 mL shake flask) examined in figure 14, the $k_L a$-values were 235 h^{-1}, 197 h^{-1}, 156 h^{-1} and 109 h^{-1} for filling volumes of 13 mL, 16 mL, 21 mL and 32 mL, respectively. Considering the vinegar fermentation medium as a mixture of acetic acid and ethanol, the oxygen solubility can be approximated according to the correlations of Rischbieter et al. [115] and Wilhelm et al. [114] to be 1.25 mmol/L/bar. From the equation (44) above the maximum oxygen transfer capacity can then be predicted, if the oxygen in the liquid is assumed to be

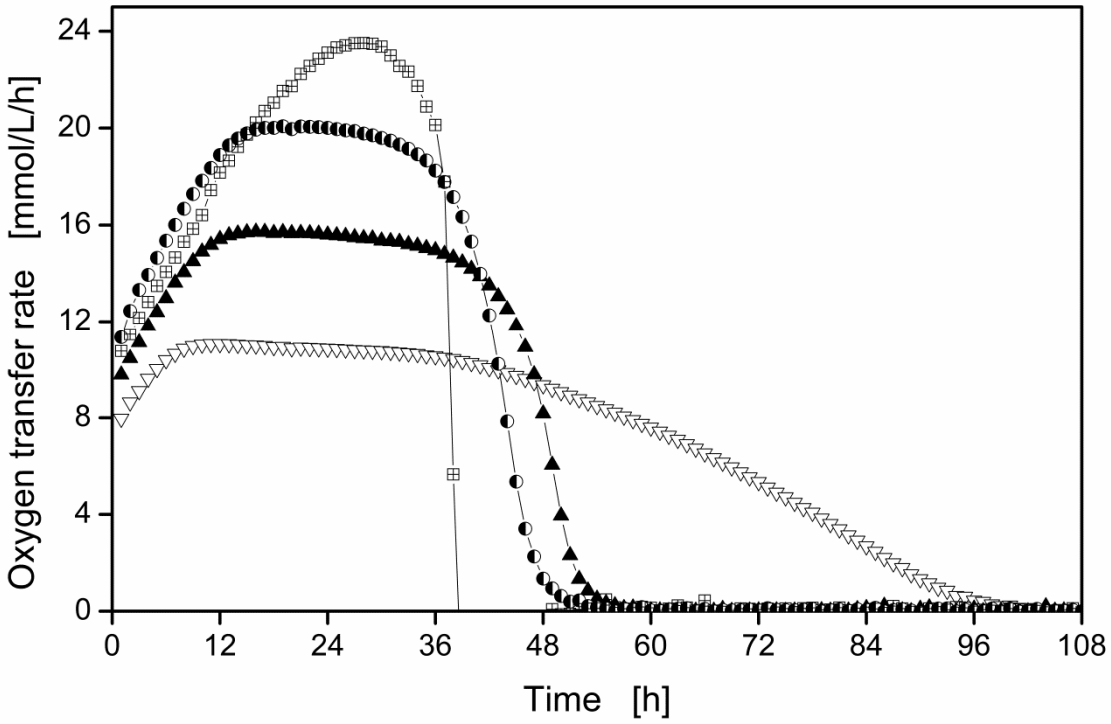


Figure 14: Oxygen transfer rate in shake flasks of acetic acid bacteria inoculated according to an aerated inoculation scheme with different aeration rates. The preculture from the bioreactor was discharged into the aerated mobile bubble column and distributed via the drain hose into the shake flasks of the already shaking RAMOS device. Initial ethanol and acetic acid concentration were 44.8 g/L and 79.0 g/L, respectively. Shaking frequency was 300 rpm and shaking diameter was 5 cm. —⊞— 13 mL filling volume (V_l) which translates into a specific aeration rate (q) of 5 vvh, —◐— V_l = 16 mL, q = 4 vvh, —▲— V_l = 21 mL, q = 3 vvh, —▽— V_l = 32 mL, q = 2 vvh

zero and the oxygen in the gas phase is expected to be equal to air. The maximum oxygen transfer capacities for 13 mL, 16 mL, 21 mL and 32 mL resulted in 62 mmol/L/h, 52 mmol/L/h, 41 mmol/L/h and 29 mmol/L/h, respectively. Figure 14 illustrates the influence of different filling volumes on the oxygen transfer rate in shake flasks of acetic acid bacteria cultures inoculated according to the aerated inoculation scheme. In the beginning of the main cultivation the oxygen transfer rates of the cultures more or less coincided. Later oxygen limitations, indicated by nearly horizontal plateaus in the curve of the oxygen transfer rate [57], occurred at values of about 20 mmol/L/h, 16 mmol/L/h and 11 mmol/L/h for filling volumes of 16 mL, 21 mL and 32 mL, respectively. This proves that the higher the filling volume of the shake flasks, the earlier an oxygen limitation appears [116]. Remarkably, the observed maximum oxygen transfer rates were far below the predicted maximum oxygen transfer capacities. These discrepancies can be explained by the very low aeration rates. These low aeration rates led to a high drop in the oxygen partial pressure in the headspace of the shake flasks compared to air. The actual oxygen partial pressures measured in the

RAMOS device in the headspace of the flasks at the time point of oxygen limitation were 0.095 bar, 0.086 bar and 0.082 bar for the filling volumes of 16 mL, 21 mL and 32 mL, respectively. These oxygen partial pressures were used instead of the oxygen partial pressure of air to recalculate the maximum oxygen transfer capacities according to the equation above. The new values of 23 mmol/L/h, 17 mmol/L/h and 11 mmol/L/h, respectively, agreed very well with the observed maximal oxygen transfer rates.

4.1.2.3 Comparison of aeration with air or pure oxygen during inoculation

In a further experiment (figure 15), the inoculation according to the aerated inoculation scheme was investigated using either air or pure oxygen as the gas in the bubble column. The respiration curves of the cultures supplied with oxygen during inoculation were slightly higher than those of the cultures supplied with air during inoculation. Hence, the fermentations of the cultures supplied with oxygen during inoculation terminated somewhat earlier at about 19 h when all the ethanol was consumed than those of the cultures supplied with air during inoculation. Possibly, the transport with air aeration in the bubble column did not lead to a hundred percent survival of the bacteria. It is likely that few of the bacteria aerated with air during the transport died. It also cannot be excluded, that the shaking period of 1-2 minutes at 100 rpm harmed the bacteria during the inoculation procedure when the other precultures were taken from the bioreactor and transported under oxygen aeration to the RAMOS device. The maximum oxygen transfer capacity at 100 rpm is calculated at 17.4 mmol/L/h. This value infers that there could have been an oxygen limitation during the inoculation process, because this value was just in the magnitude of the initial respiration activity of the bacteria in that experiment (figure 15). Unlike the studies of Hromatka and Ebner [9] who aerated acetic acid bacteria cultures with pure oxygen or oxygen enriched gas mixtures for extended time periods, the aeration with pure oxygen during the transport of the preculture in the bubble column did not adversely affect the bacterial culture. However, the use of pure oxygen as supply gas in the bubble column during the aerated inoculation procedure did not lead to significant improvements compared to the use of air in the bubble column during the aerated inoculation procedure.

Compared to the preceding experiments with main cultures inoculated according to the aerated inoculation scheme (figure 13 and figure 14) all the main cultures in the latter experiment (figure 15) showed a higher initial oxygen transfer rate and the fermentation time was shorter (19 h). This can be explained by the initial ethanol and acetic acid concentrations. In the former experiments the initial ethanol concentrations were higher and

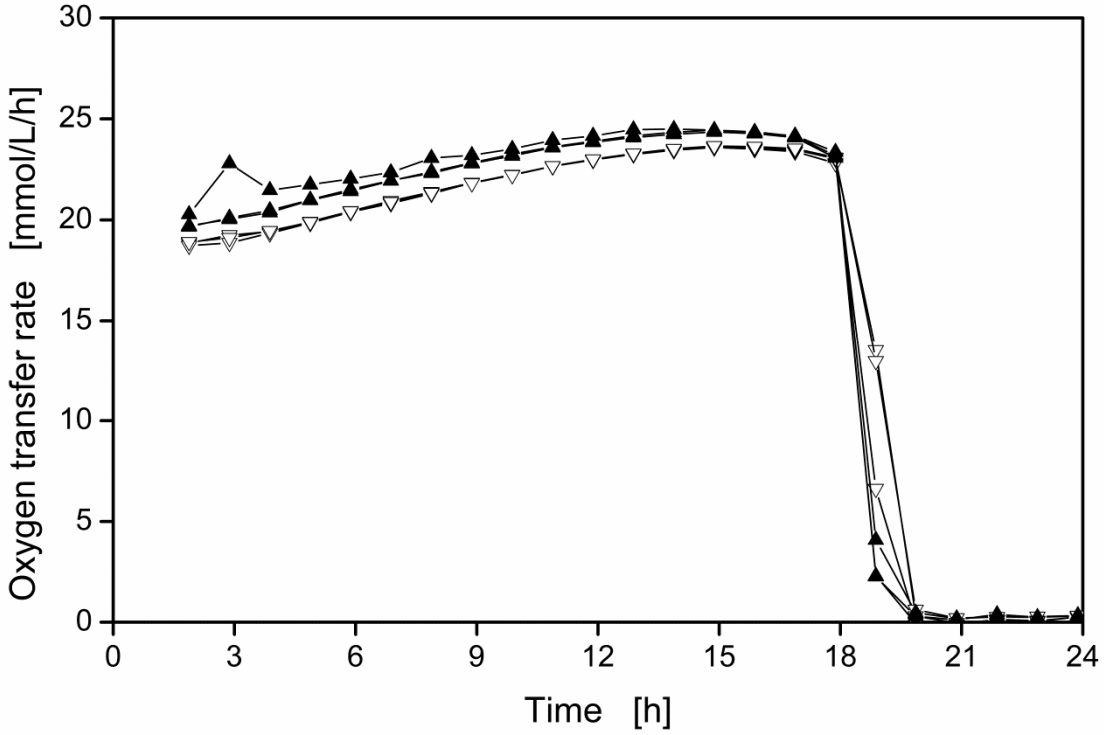


Figure 15: Oxygen transfer rate in shake flasks of acetic acid bacteria inoculated according to an aerated inoculation scheme using either air or pure oxygen as supply gas in the bubble column. The preculture from the 9 L-bioreactor was discharged into the aerated mobile bubble column and distributed with a syringe into the shake flasks of the already shaking RAMOS device. In the first case the bioreactor and bubble column were aerated with air (—▽—). In the second case the bioreactor was saturated with pure oxygen prior to draining and also the bubble column was aerated with pure oxygen (—▲—). Initial ethanol and acetic acid concentration were 29.8 g/L and 88.4 g/L, respectively. Experiments were carried out in triplicates. Shaking frequency was 350 rpm and shaking diameter was 5 cm. In both cases the filling volume was 13 mL which translates into a specific aeration rate of 5 vvh.

acetic acid concentration lower than in the latter experiment. Therefore, the preculture in the latter experiment was in a more progressed state of the fermentation and provided less ethanol substrate for the main cultivation.

4.1.3 Respiration characteristics of acetic acid bacteria in shake flasks for vinegar fermentation

In all of the above fermentations the shape of the curves of the oxygen transfer rates resembled inhibition curves [57]. This observation concurs with earlier studies on kinetic models for vinegar fermentation, where the influence of ethanol and acetic acid had been studied. The substrate ethanol as well as the product acetic acid inhibits bacterial activities

during vinegar fermentation [98, 118-123]. A second increase in the oxygen transfer rate after depletion of the primary carbon source ethanol was also not observed, i.e. there is no diauxic growth on acetate. Such diauxic acetate consumption is known as an undesired phenomenon in vinegar fermentation especially for the genus *Acetobacter* of the acetic acid bacteria [7, 22, 124, 125]. The fact that no diauxic growth of the bacteria took place is likewise in agreement with the studies of Sievers et al. [19] and Saeki et al. [126] who reported that acetate oxidation does not occur at acetic acid concentrations greater than 60 g/L and 45 g/L, respectively. In this study the acetate concentration ranged from about 80 g/L in the beginning to about 130 g/L at the end of the fermentations.

4.1.4 Shut off experiment in bubble column

To study the effect of oxygen depletion during inoculation a shut off experiment in the bubble column with an acetic acid bacteria culture equivalent to the cultures used for inoculation of the shake flask fermentations was conducted. Figure 16 depicts the course of the dissolved oxygen tension in the bubble column during the shut off experiment. In the beginning the dissolved oxygen tension was in steady state and the aeration was shut off at 2.5 min. Within 5 min the dissolved oxygen tension dropped down to 0 % meaning that the bacteria completely consumed the available oxygen. In the range of the steepest decrease between 2.9 min to 3.9 min where the respiration rate was constant the curve of the dissolved oxygen tension was approximated by a straight dashed line. The difference between the measured dissolved oxygen tension and the straight extrapolated line demonstrate that the bacteria already suffered from oxygen limitation below a dissolved oxygen tension of about 30 %. A constant respiration activity can be assumed up to this time because concentration changes of acetic acid and ethanol were negligibly small in the narrow range of time examined here. When the aeration was turned on again the dissolved oxygen tension increased to a level of 92 %. This indicates that part of the bacterial population died during the preceding short time of oxygen depletion. By shutting off the aeration once more at 12.7 min the diminished activity of the bacteria was verified. The slope of the fit during the steepest decrease of the dissolved oxygen tension between 15.9 min and 17.9 min was with -15 %/min only half of that of the former period with -32.8 %/min. In other words, half of the bacteria were impaired during the first shut off of aeration. Taking into account that the dissolved oxygen tension in the 9 L-bioreactor was only 51 % when the culture broth was drained off, oxygen depletion would occur even earlier during a traditional procedure for inoculation than in the shut off experiment. The situation even becomes worse, if the sample from the bioreactor is taken later than 6 h. Then the fermentation is in a more progressed state indicated by less ethanol

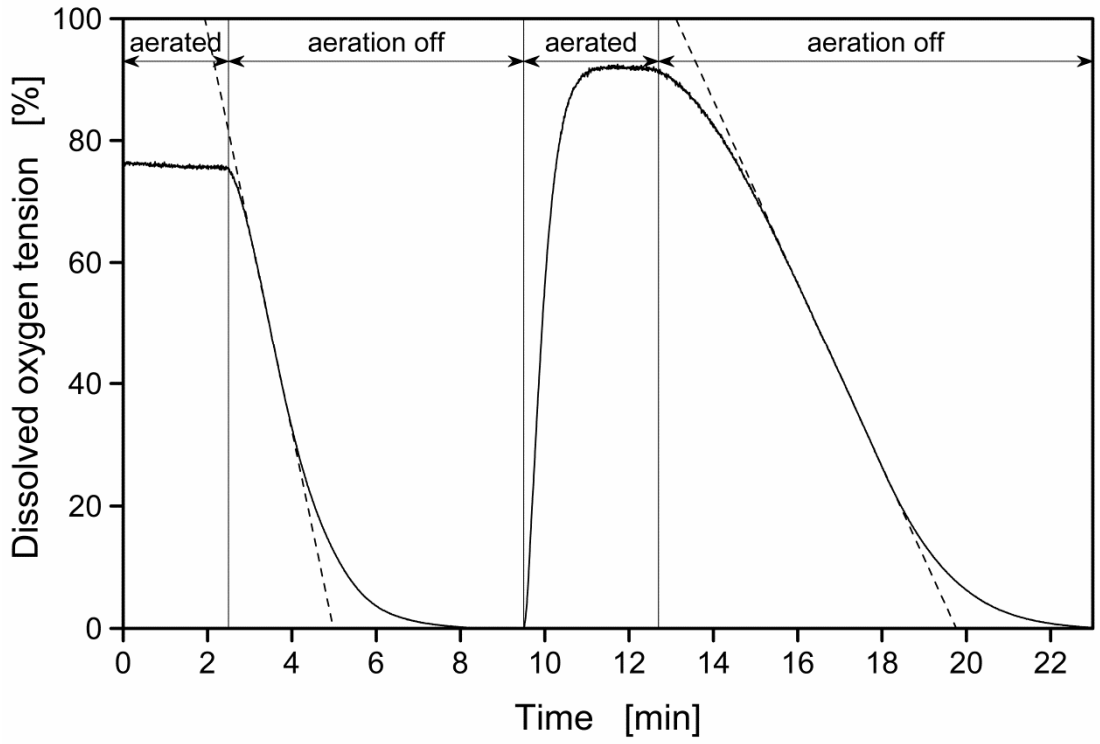


Figure 16: Dissolved oxygen tension in a bubble column during shut off experiment. Acetic acid bacteria culture from a 9 L-bioreactor was discharged into the aerated bubble column and the dissolved oxygen tension in the bubble column (**—**) was measured with a fluorescence optical method. When the dissolved oxygen tension was in steady state, the aeration was shut off at 2.5 min. At 8.5 min the dissolved oxygen tension was zero. After one minute the aeration was turned on again at 9.5 min. After the dissolved oxygen tension reached steady state aeration was shut off once more at 12.7 min. During the non-aerated phases in the periods from 2.9 min to 3.9 min and 15.9 min to 17.9 min the decrease in dissolved oxygen tension was fitted by a straight line (**--**). The acetic acid bacteria culture used for this experiment was withdrawn from a 9 L-bioreactor 6 h after a batch experiment had been started. The ethanol and acetic acid concentrations were 26.3 g/L and 83.1 g/L, respectively.

and more acetic acid in the fermentation broth. Concomitantly, the bacteria exhibit a higher oxygen uptake rate. The curves of the oxygen transfer rates in the shake flasks (figure 11 to figure 15) showed that the oxygen uptake rate of the bacteria increases throughout the course of a vinegar fermentation cycle. All in all, to guarantee reproducible results with acetic acid bacteria in vinegar fermentation in the main culture the dissolved oxygen tension in the preculture should always be kept higher than 30 % air saturation during the inoculation procedure. For the conditions examined here, i.e. a dissolved oxygen tension of 51 % in the preculture and an oxygen consumption rate of the bacteria of -32.8 %/min, any interruption of aeration during the inoculation procedure must not last longer than half a minute. Otherwise, part of the bacterial population suffer from oxygen depletion and will lose viability.

4.2 Vinegar fermentation in repeated batch mode on shake flask scale

4.2.1 Conventional and flushing repeated batch vinegar fermentation

In this study it was intended to develop a small-scale repeated batch system for vinegar fermentation. In contrast to fully equipped bioreactors at laboratory or pilot scale, a small-scale parallel fermentation system ought to be kept as simple as possible. This does not only save costs but it also decreases the probability of equipment failure and increases robustness. An operation mode – the flushing repeated batch method – was designed for repeated batch fermentation where at least the instrumentation for discharge, i.e. pumps or valves and level sensors as well as their control, is not required. By using a shaken system as platform, only one drive is required to agitate and mix the parallel bioreactors. Simulation results for comparing both, the conventional and the flushing repeated batch fermentation, for the production of vinegar in a bioreactor and ShaRBS, respectively, are depicted in figure 17. The initial conditions for the repeated batch fermentation in a conventional bioreactor (time 0 h) were set to typical values in vinegar industry at 39.45 g/L ethanol, 85 g/L acetic acid and 0.45 g/L biomass. In addition, the parameters to control the repeated batch fermentation in the conventional bioreactor were set to typical values in vinegar industry (table 1). Each draining phase was initiated whenever the ethanol concentration fell below 4 g/L. Draining was terminated at a relative filling volume of 0.67 of the maximal filling volume to directly start the filling phase. The draining and filling rate were set at 1.32 h^{-1} and 0.44 h^{-1}, respectively. The ethanol substrate solution contained 106.5 g/L ethanol but neither biomass nor acetic acid. The concentration equilibria of the three components ethanol, acetic acid and biomass in repeated batches in the conventional bioreactor were then reached after 5 batches (17 d, Figure 17). At this point of time (17 d) the equilibrium concentrations of 37.52 g/L for ethanol, 89.41 g/L for acetic acid and 0.492 g/L for biomass at the start of the sixth batch were applied to initiate the model for the repeated batch in the ShaRBS reactor (table 2). According to the sum of times for draining and filling the conventional bioreactor, the flushing phases in the ShaRBS lasted 1 h (equation (11)). With the acetic acid concentration of 132.85 g/L and ethanol concentration of 4.00 g/L at the end of the 5^{th} batch in the conventional bioreactor (17 d), the dilution rate and concentration of the ethanol substrate solution for flushing the ShaRBS reactor were calculated with equation (14) and equation (15) to be 0.396 h^{-1} and 106.5 g/L, respectively. As described in the theoretical part, the concentration of the ethanol substrate solutions for filling the conventional bioreactor and flushing the ShaRBS reactor are the same, because ethanol is converted in equimolar amounts into acetic acid in vinegar fermentation. The simulation results (figure 17 and figure 18) for conventional and flushing repeated batch fermentation of an acetic acid bacteria

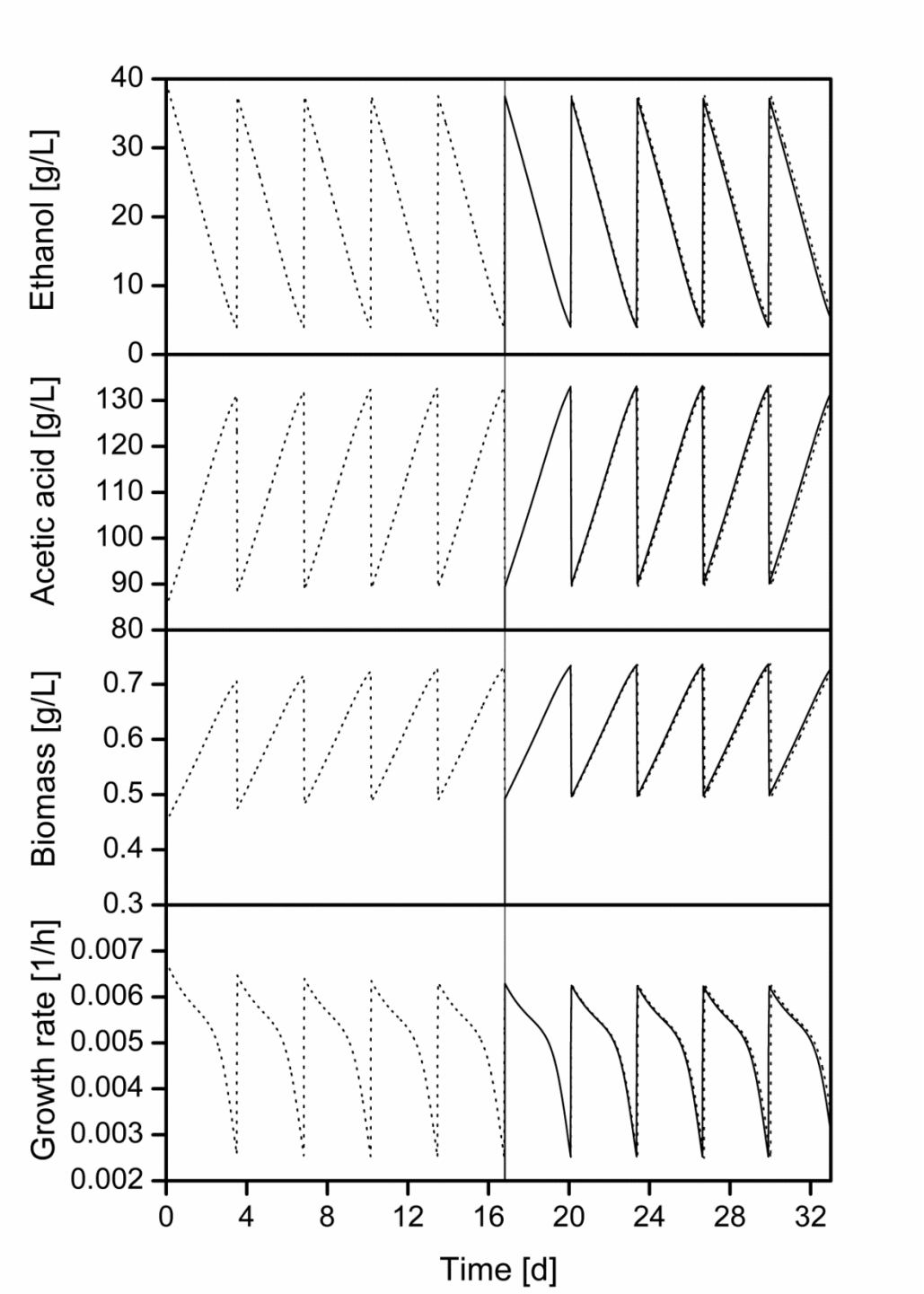


Figure 17: Simulated repeated batch fermentations for the production of vinegar in conventional bioreactor and ShaRBS. Simulation was started for the repeated batch in the conventional bioreactor with the initial conditions as stated in the text. After five batches when equilibrium was reached (17 d), the simulation for the repeated batch fermentation in the ShaRBS device was initiated using the values of the equilibrium as initial values (37.52 g/L ethanol, 89.41 g/L acetic acid and 0.492 g/L biomass). Dilution rate for flushing as well as ethanol concentration of the ethanol substrate solution were calculated according to equations (14) and (15) from the concentrations of the conventional bioreactor at the end of the 5th and start of the 6th batch. Detailed values for the parameters in the growth model and the parameters to control the repeated batch in the conventional bioreactor as well as in the ShaRBS can be found in table 3 (appendix), 1 and 2, respectively. ····· conventional bioreactor, ━ ShaRBS

Table 1: Initial conditions, parameters and results for modeled repeated batch vinegar fermentation in conventional bioreactor

Description	Equation symbol	Value	
Initial ethanol concentration	$E(0)$	39.45	g/L
Initial acetic acid concentration	$A(0)$	85	g/L
Initial biomass concentration	$X(0)$	0.45	g/L
Draining rate	D^*	1.32	h^{-1}
Filling rate	F	0.44	h^{-1}
Relative residual filling volume after draining	$V_{rel,0}$	0.67	
Duration of draining		0.25	h
Duration of filling		0.75	h
Ethanol concentration of ethanol substrate solution	E_f	106.5	g/L
Final ethanol concentration in equilibrium (threshold)		4	g/L
Final acetic acid concentration in equilibrium		132.85	g/L
Final biomass concentration in equilibrium		0.73	g/L
Initial ethanol concentration in equilibrium		37.52	g/L
Initial acetic acid concentration in equilibrium		89.41	g/L
Initial biomass concentration in equilibrium		0.492	g/L

Table 2: Initial conditions, parameters and results for modeled repeated batch vinegar fermentation in ShaRBS

Description	Equation symbol	Value	
Initial ethanol concentration (in equilibrium)	$E_{t_{fl}}$	37.52	g/L
Initial acetic acid concentration (in equilibrium)	$A_{t_{fl}}$	89.41	g/L
Initial biomass concentration (in equilibrium)		0.492	g/L
Duration of flush phase	t_{fl}	1	h
Dilution rate in flush phase	D	0.396	h^{-1}
Ethanol concentration of ethanol substrate solution	E_{fl}	106.5	g/L
Final ethanol concentration in equilibrium (threshold)	E_0	4	g/L
Final acetic acid concentration in equilibrium	A_0	132.85	g/L
Final biomass concentration in equilibrium		0.73	g/L

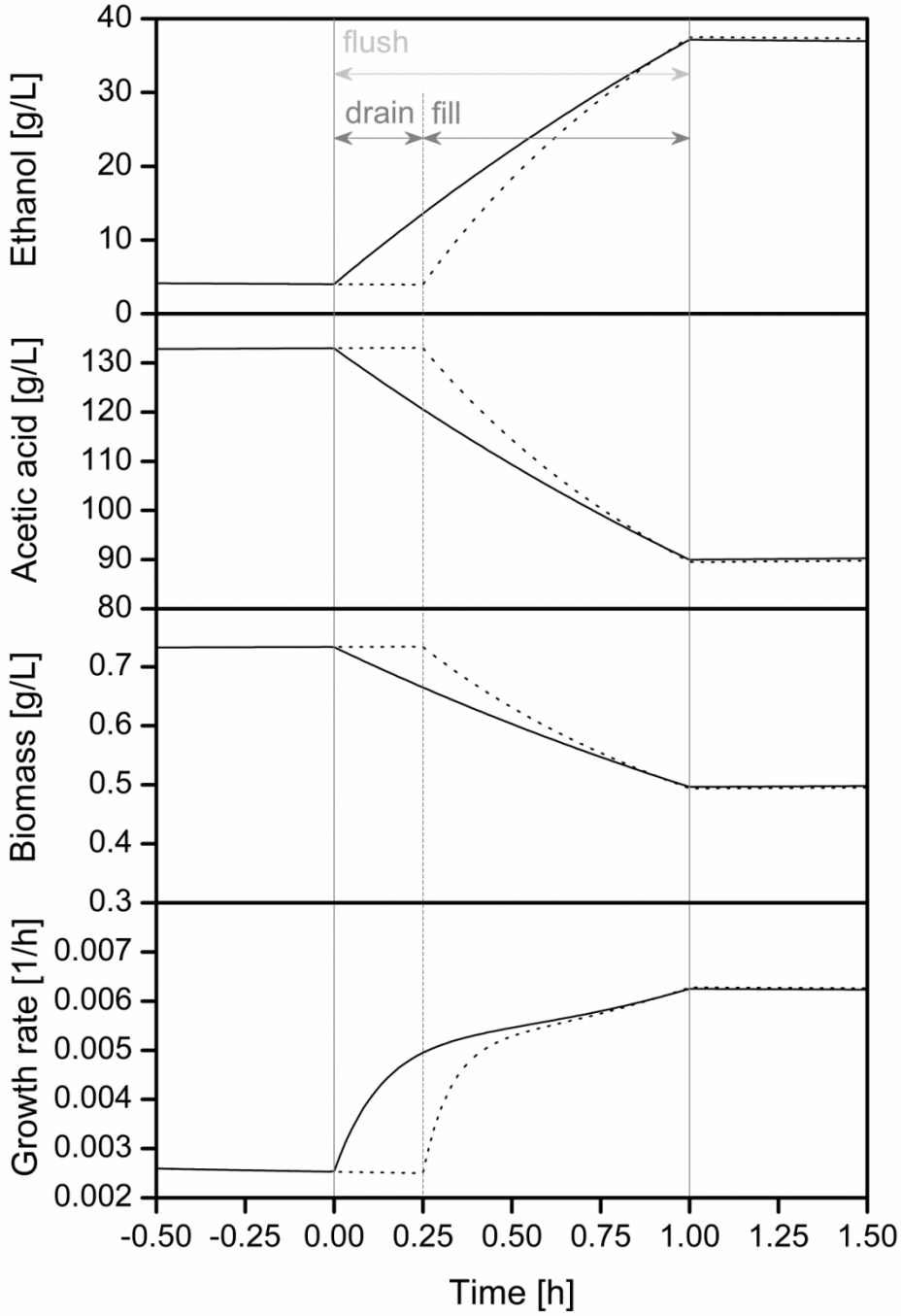


Figure 18: Draining and filling phase in conventional bioreactor compared to flush phase in ShaRBS in repeated batch vinegar fermentation. Enlarged view of Figure 17 during the sixth draining and filling phase in the conventional bioreactor and the first flush phase in the ShaRBS. The residual relative filling volume was 0.67 at the end of draining of the conventional bioreactor. The draining and filling phase lasted 0.25 h at a draining rate of 1.32 h^{-1} and 0.75 h at a filling rate of 0.44 h^{-1}, respectively. According to equation (11), the flush phase in the ShaRBS likewise lasted 1 h. Detailed values for the parameters in the growth model and the parameters to control the repeated batch in the conventional bioreactor as well as in the ShaRBS can be found in table 3 (appendix), 1 and 2, respectively. ····· conventional bioreactor, ━ ShaRBS

culture for vinegar production show that both procedures agree very well with one another. Figure 18 shows that flushing the ShaRBS reactor under the above specified conditions leads to the same initial conditions for the next batch (1 h) as in the conventional bioreactor. The differences in the courses of the ethanol, acetic acid and biomass concentration during the draining and filling phase in the conventional bioreactor and the flushing phase in the ShaRBS (figure 18) do not considerably affect the bacterial growth and progress of the fermentation afterwards. The simulation results show only infinitesimal delays between the fermentation courses of the conventional and flushing repeated batch fermentations (20 d – 33 d, figure 17).

4.2.2 Ethanol sensor characteristics in ShaRBS for vinegar fermentation

To control vinegar fermentation in the ShaRBS, semiconductor gas sensors were chosen. They are relatively inexpensive and are known from ethanol probes in conventional bioreactors, e.g. the Frings Alcosens probe [127, 128], or in a custom-made dipping probe for online control of methanol in shake-flask cultures of *Pichia pastoris* [129]. The electrical resistance of the sensors depends on the oxygen adsorbed on the semiconductor surface [100-102]. Thus, the commercial probe uses an oxygen-rich carrier gas to admit the volatile ethanol to the sensor and to compensate for oxygen partial pressure changes in the surrounding. In this current study, however, no carrier gas was used for reasons of system simplicity. Since the ShaRBS reactors were initially not equipped with oxygen sensors, which would allow for compensation of the oxygen partial pressure effect on the measurement signal, the oxygen partial pressure in the ShaRBS reactor was at first calculated for the aforementioned simulation example (figure 17). As figure 19 illustrates, the oxygen partial pressure drops down to about 0.17 bar during the first hours of the first batch, remains constant at that level during that batch and slightly increases to 0.18 bar to the end of the batch. In the subsequent batches, the curve of the oxygen partial pressure in the headspace then leveled off at 0.17 bar to 0.18 bar. This level might even be lower in reality, because the model data was obtained from literature where batch fermentation data was acquired. Therefore, the activity of the acetic acid bacteria in repeated batch vinegar fermentation would very likely be higher. The absolute level of the partial pressure is not as interesting as the fact that the oxygen partial pressure like the concentrations of ethanol, acetic acid and biomass levels off in an equilibrium with fluctuations in the order of ±0.01 bar during repeated batch fermentation. In this narrow range, the effect of oxygen on the sensor signal is relatively small and could be neglected. This oxygen partial pressure equilibrium is attained

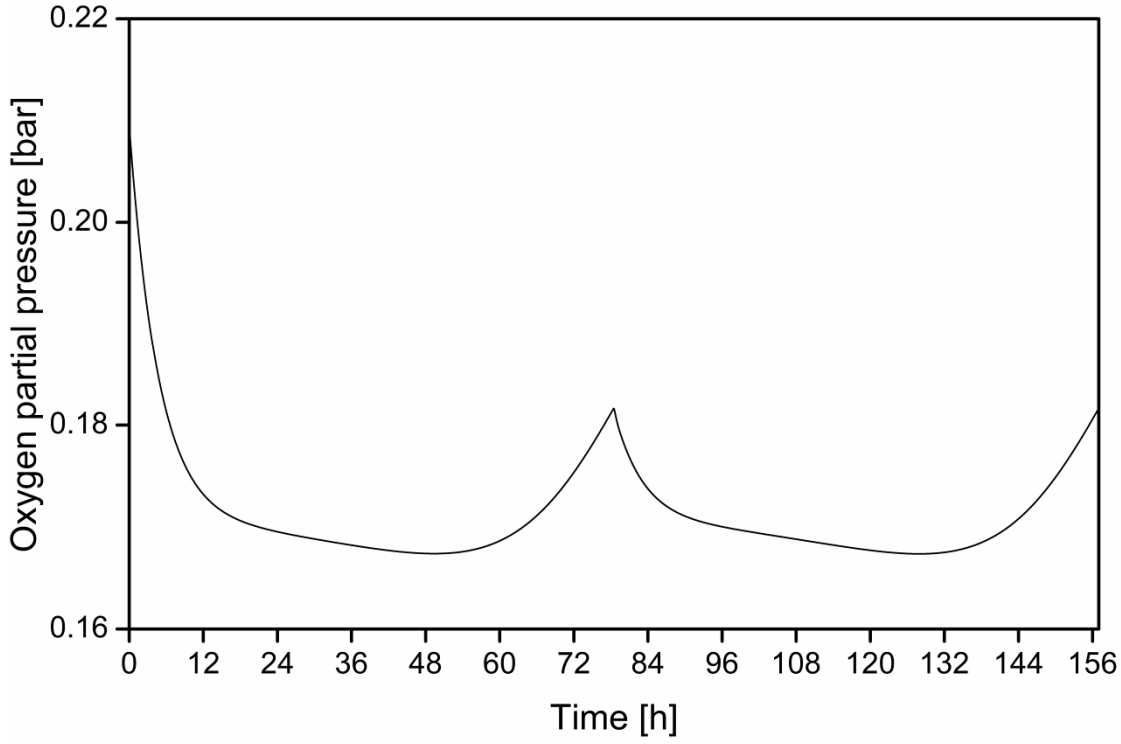


Figure 19: Simulated oxygen partial pressure in the headspace of a ShaRBS reactor during vinegar fermentation. Oxygen partial pressure in the headspace of the ShaRBS reactor during vinegar fermentation was estimated based on the ethanol oxidation. The course of the oxygen partial pressure of the repeated batch fermentation in ShaRBS is illustrated for the first two batches of the ShaRBS from figure 17.

at the end of the first batch and start of the second batch in the ShaRBS reactor. Thus, a calibration formula (equation (45)) for the ethanol sensors during fermentation was applied disregarding the oxygen partial pressure influence. In preliminary experiments (data not shown) it could be ascertained that the logarithm of the sensor voltage is proportional to the logarithm of the ethanol concentration in the solution:

$$\log E = a \cdot \log U + b \tag{45}$$

By applying the ethanol concentrations E_1 and E_2 of two samples as well as the corresponding sensor voltages U_1 and U_2, the slope a and intercept b of the calibration line can be calculated. During the following fermentations (figure 20), these two samples were obtained at the end of the first batch and start of the second batch as described in the methods part. In figure 20, the ethanol concentrations of the samples used to calibrate the voltage signals of the respective sensors are marked as squares.

4.2.3 Flushing repeated batch fermentation for vinegar fermentation in ShaRBS

Figure 20 illustrates the flushing repeated batch vinegar fermentations in three different reactors of the ShaRBS. During the first ten hours of the first batch the sensor voltage of the ethanol sensors slightly increased, and thereafter slowly decreased up to 17 h when it finally steeply decreased. Since the logarithm of the sensor voltage was also proportional to the logarithm of the oxygen partial pressure (data shown in chapter 4.2.4), the sensor voltage increased during the first ten hours with decreasing oxygen partial pressure in the ShaRBS headspace. This effect of the oxygen partial pressure on the voltage signal is not considered in the simplified non-oxygen compensated sensor reading. Consequently, it is reasonable to calibrate the ethanol sensors based on offline samples from time points when the oxygen partial pressures have more or less reached steady state values with only small variations. The voltage signals from the three sensors are quite different. However, due to the calibration procedure it could be shown that the ethanol concentrations over time in all three reactors are quite similar. Utilizing the online ethanol concentration to initiate the flushing phases when the ethanol concentration fell below 4 g/L, the flushing repeated batch fermentation in ShaRBS was proven to be stable. The time point to flush the reactors with fresh ethanol substrate solution is especially critical. If this point is missed and ethanol is exhausted, the acetic acid bacteria would die immediately [14]. This could be successfully avoided with the control based on the calibrated ethanol sensors.

In previous studies of repeated batch fermentations other than vinegar production, medium exchange was often scheduled in a time-dependent manner, disregarding the state of the individual microbial culture, and sometimes even lacking an online control [40-44, 48]. In such cases, it is not certain if the best time point for the medium exchange is met. If the exchange took place too late, the productivity would be underestimated and microbial activity might already have begun to decline. Zhang et al. [48] demonstrated this problem for the anthocyanin production by strawberry cells. If the medium exchange takes place too early, maximum productivity or product concentration may not be achieved. Logically, the optimal time point for medium exchange varies with the culture conditions, e.g. composition of fermentation medium, pH and temperature, or with the microbial strain used. Thus, there is the urgent need for an online control, if many different conditions are to be compared in screening projects. The online detection of the substrate ethanol in vinegar fermentation in the headspace of the ShaRBS is a suitable technique to monitor and to control the fermentation. Replacement of the ethanol sensor or addition of more sensors to the system for other fermentations is easily conceivable.

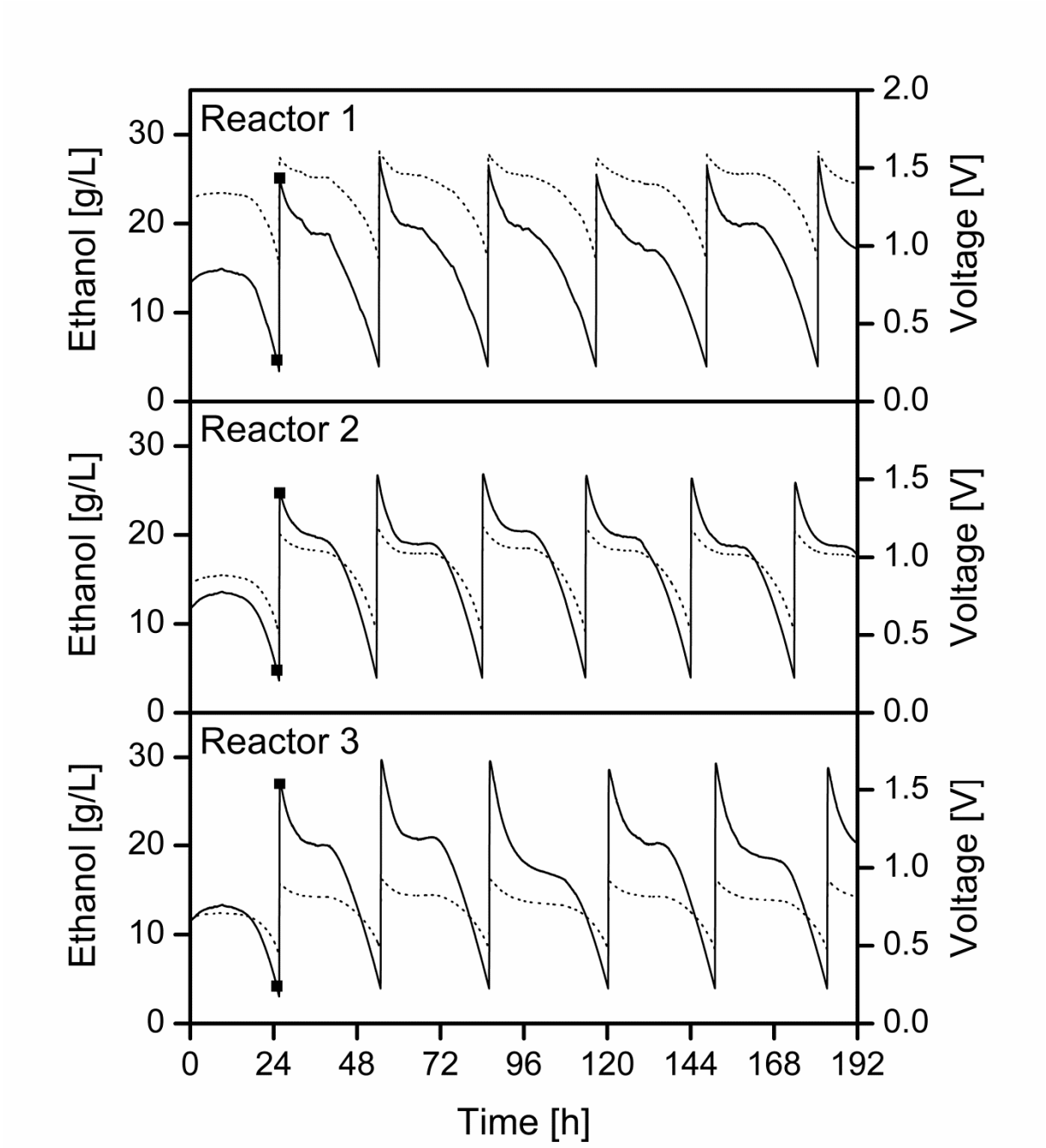


Figure 20: Parallel repeated batch fermentations in ShaRBS. The ShaRBS reactors were inoculated from laboratory-scale bioreactor as described in the methods part. After 25 h at the end of the first batch, 4.5 mL of the fermentation broth (21.5 mL) were ejected by raising the shaking frequency from 300 rpm to 325 rpm. Then, at reduced shaking frequency of 275 rpm, reactors were refilled with 10 mL ethanol substrate solution to form the new batch. After refilling the reactors, the shaking frequency was again raised to 300 rpm. Thus, samples of 5.5 mL of the start of the second batch were obtained. Ethanol concentrations of the overspilled fermentation broths were determined by gas chromatography and used to calibrate the ethanol sensors. In the subsequent batches, the ethanol substrate solutions were flushed in at constant shaking frequency of 300 rpm whenever the ethanol concentration fell below the threshold concentration of 4 g/L. ····· ethanol sensor voltage, ─ calibrated ethanol sensor signal, ■ ethanol concentration of samples to calibrate the ethanol sensor

Repeated batch fermentations in screening procedures would allow the cells to adapt to stresses induced by e.g. alcohols, acids, high osmotic pressure or any other adverse chemical agents. This might lead to the selection of better producing strains. Anastassiadis and Rehm [39] and Madhavan et al. [43] already observed better productivities after repeated batch cycles attributed to adaptation in citric acid and ethanol production, respectively. In this current study, the phenomenon of selection or adaptation could be demonstrated with different ethanol lots in vinegar fermentation: Figure 21 presents the influence of three different ethanol lots on the course of fermentation. After the ethanol of lot AC was used for five batches, the reactors were flushed for the subsequent batches with new ethanol of lot A, B and C, respectively. With the altered ethanol lots, in all three cases (figure 21) the first fermentation phase was prolonged until the ethanol was nearly consumed. However, with repeated use of the altered ethanol lots, the length of subsequent fermentation phases decreased considerably and the performance of the initial bacterial culture recurred. As the bacterial culture for vinegar fermentation is a mixed culture, it is not certain whether prevailing preadapted strains had been selected or whether the existing dominant bacteria had adapted to the new substrate lot. Taking the adaptability of the producing microbial strains to changing environmental parameters into account may be very important for a production manager who has to decide whether to turn off and restart a production plant or to wait until the culture has regenerated. In particular, when the plant start-up takes a long time, it would save operational costs to wait for the microbial community to adapt. This further exemplifies that repeated batch studies on small scale are important for process robustness and stability especially if a bioprocess is subjected to changing environmental parameters such as changing ethanol lots.

Acetic acid bacteria are genetically instable due to mutations caused by insertion sequence elements or transposons [22, 33, 34]. They are very difficult to isolate and change their characteristics during long storage [20, 38]. Therefore, the proposed repeated batch system might be helpful for long-term physiological studies on acetic acid bacteria in vinegar fermentation. For instance, the harvest at the end of a batch can be readily used for PCR and sequence analysis or for other biochemical assays. Furthermore, sampling of the reactors would be possible by simply raising the shaking frequency so that culture broth spills over. Besides mutation, plasmid segregational instability compromises genetic stability, i.e. plasmids might dilute out from daughter cells in subsequent generations [130]. In several cases repeated batch fermentations lost their stability. For example, a decrease in bacterial cellulose yield was reported after the fourth batch with *Acetobacter xylinum* subsp. *sucrofermentas* [44]. In hyaluronic acid production, a non-producing *Streptococcus zooepidemicus* mutant was found after the third batch [131]. Looking beyond the scope of

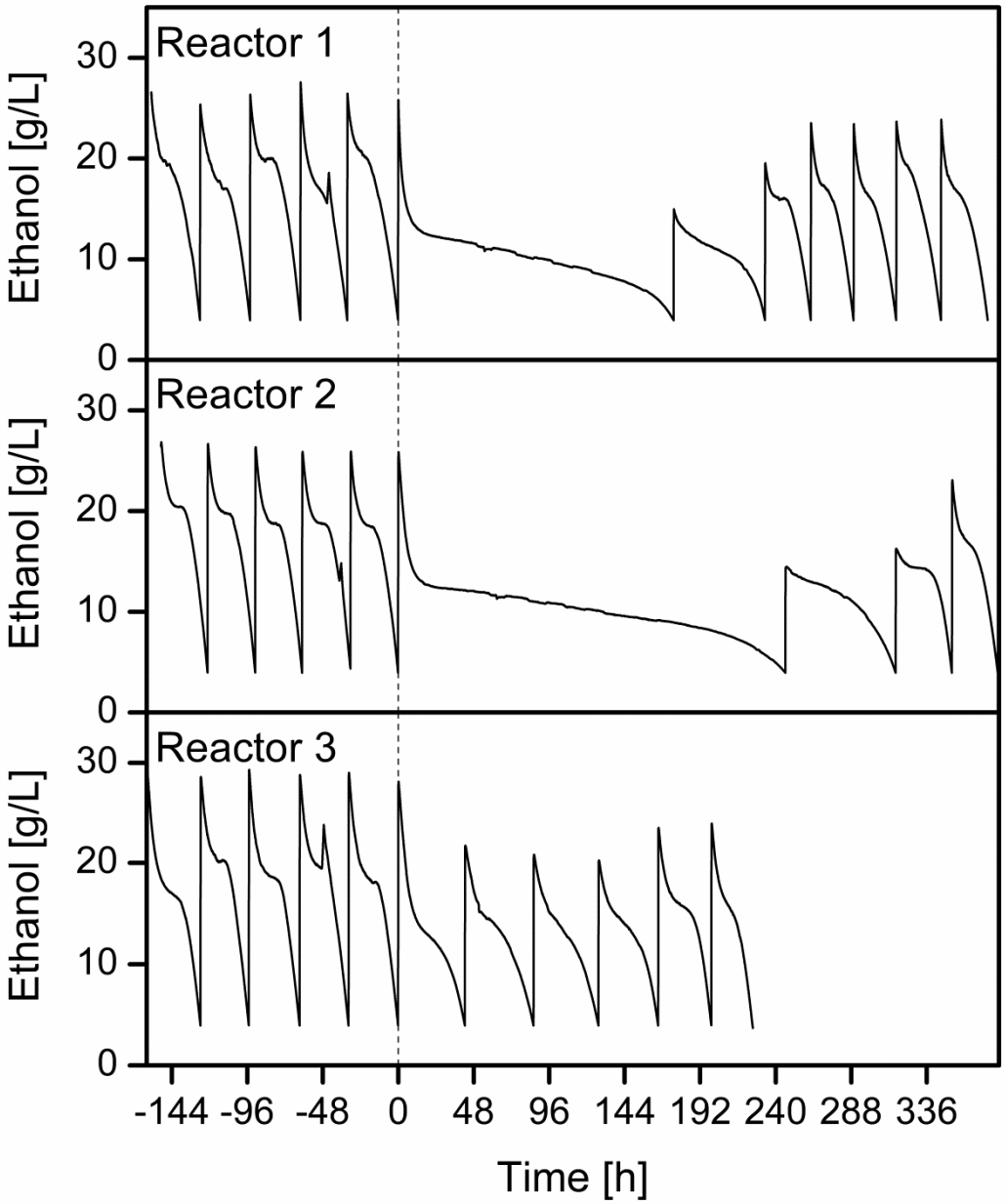


Figure 21: Repeated batch vinegar fermentation in the ShaRBS with change of ethanol lots in the ethanol substrate solution. Parallel flushing repeated batch vinegar fermentations were established in three reactors of the ShaRBS with a liquid volume of 21.5 mL at a shaking frequency of 300 rpm. Whenever the ethanol concentration fell below the threshold concentration of 4 g/L fresh ethanol substrate solution with ethanol of lot AC was flushed into the reactors. At time zero, new ethanol substrate solutions with ethanol of lot A, B and C instead of ethanol of lot AC were flushed into the ShaRBS reactors 1, 2 and 3, respectively, to initiate the next batches.

vinegar fermentation, repeated batch cultivations in screening programs would be valuable, since the best producing (recombinant) strain in one batch might not be the best producing strain in succeeding batches due to genetic and process-stability reasons.

4.2.4 Oxygen dependency of the ethanol sensors and co-monitoring of oxygen partial pressure in headspace during fermentation in ShaRBS

As already mentioned, the dependency of the ethanol sensor signal on different ethanol concentrations and oxygen partial pressures in the headspace of the ShaRBS reactor was studied. Figure 22 demonstrates that the logarithm of the sensor voltage is proportional to the logarithm of the ethanol concentration in the solution as well as the logarithm of the oxygen partial pressure. Hence, the sensor voltage U depicts a plane described by equation (46), which can be rearranged to the exponential expression in equation (47) as follows:

$$\log U = \mathrm{A} + \mathrm{B} \cdot \log p_{O2,out} + \mathrm{C} \cdot \log E \tag{46}$$

$$U = 10^{A} \cdot {p_{O2,out}}^{B} \cdot E^{C} \tag{47}$$

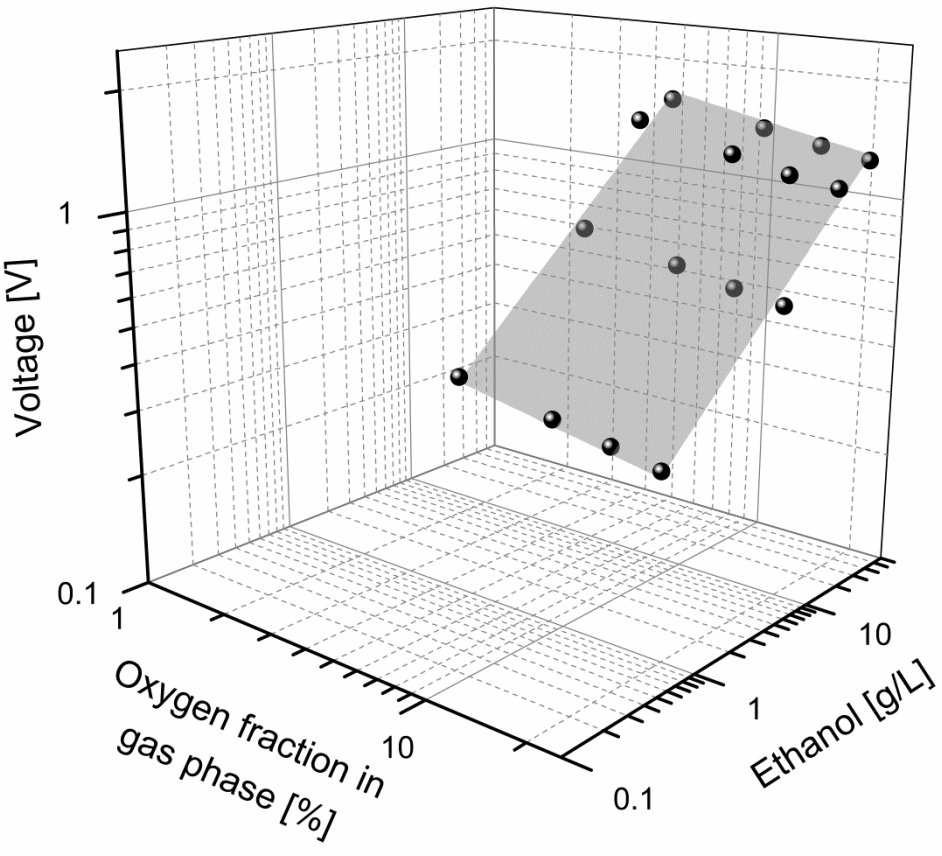


Figure 22: Ethanol sensor voltage as a function of ethanol concentration and oxygen partial pressure. Different solutions containing 0.8 g/L, 8 g/L, 24 g/L and 48 g/L ethanol were filled in the ShaRBS reactor. Different oxygen partial pressures with 5 %, 10 %, 15 % and 21 % were realized by mixing air and nitrogen. The sensor voltage was determined when the voltage signal remained constant.

For the used sensor, the surface can be described by the exponents -0.261, -0.164 and 0.351 for A, B and C, respectively, with a R^2-value of 0.964. Figure 22 depicts this as a grey plane.

Figure 23 demonstrates the start of repeated batch vinegar fermentation in a ShaRBS reactor with simultaneous measurement of the oxygen partial pressure in the headspace. The oxygen partial pressure dropped down from 0.20 bar to 0.06 bar during the first 13 hours. For the following batches the oxygen partial pressure oscillated between 0.09 bar

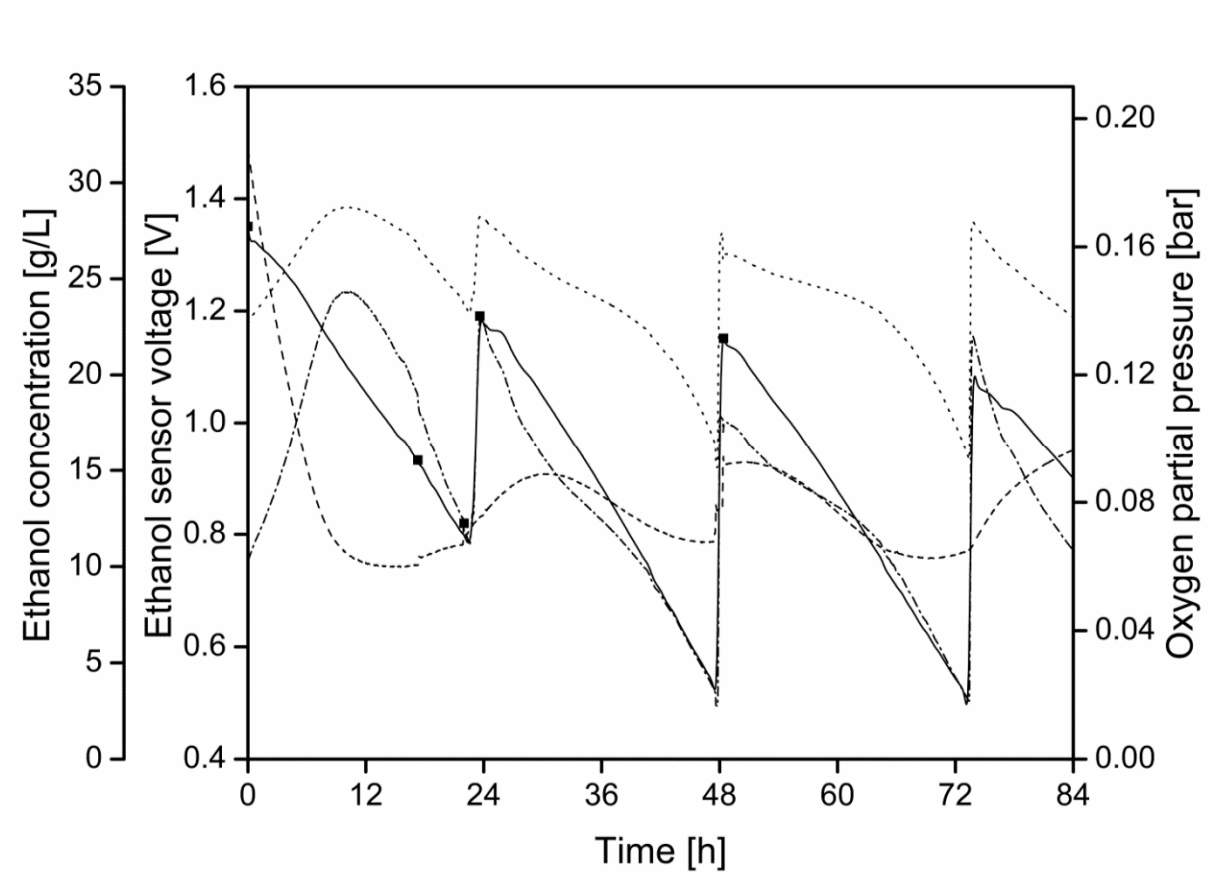


Figure 23: Compensation of oxygen partial pressure dependency of ethanol sensor signal in repeated batch fermentation in ShaRBS. The ShaRBS reactors were inoculated at 275 rpm from laboratory-scale bioreactor as described in the methods part. After 17.3 h 7 mL of the fermentation broth (27 mL) were ejected by raising the shaking frequency to 300 rpm. After 22 h at the end of the first batch, once again 7 mL of the fermentation broth were ejected by raising the shaking frequency to 325 rpm. Then, at reduced shaking frequency of 275 rpm, reactors were refilled with 7 mL ethanol substrate solution to form the new batch. After refilling the reactors, the shaking frequency was shortly raised to 310 rpm and then fermentation was conducted at 300 rpm. Thus, a sample of 3.5 mL was obtained at the start of the second batch. Ethanol concentrations of the overspilled fermentation broths were determined by gas chromatography. In the subsequent batches, whenever the ethanol concentration fell below the threshold concentration of 4 g/L the ethanol substrate solutions were flushed in at a constant shaking frequency of 300 rpm. ▬ oxygen partial pressure, ····· ethanol sensor voltage, ▪▪▪ non-oxygen compensated calibrated ethanol sensor signal, ▬ oxygen compensated calibrated ethanol sensor signal, ■ ethanol concentration of samples

and 0.06 bar for each batch cycle, respectively. The ethanol sensor signal increased during the first 13 h although from a biological point of view ethanol was continuously converted by the bacteria to acetic acid. This discrepancy can be explained by the oxygen dependency of the ethanol sensor. The decrease of the oxygen partial pressure is coupled with the simultaneous increase of the ethanol sensor voltage. When the ethanol concentration is calculated without considering the oxygen partial pressure compensation (equation (45)) the abovementioned course of the ethanol sensor voltage is incorrectly reconstructed. Whereas, when the ethanol concentration is calculated with the oxygen partial pressure compensation (equation (47)) the course of the ethanol concentration is correctly depicted for the entire fermentation. Even though there is a discrepancy for non- and oxygen partial pressure compensated calculated ethanol concentrations, the concentrations converge to the same value at the end of each batch cycle. That is the reason why also the non-oxygen partial pressure compensated measurement is sufficient to control vinegar fermentation. Hereby, it is important that the time point for fresh substrate supply at the end of the batch is not missed. Still, the oxygen partial pressure compensated measurement of the ethanol concentration is preferable as the influence of oxygen on the ethanol sensor is taken into account and the online monitored ethanol concentration becomes more accurate; especially during the first batch of repeated batch fermentation.

4.2.5 Online calibration of oxygen sensor on ShaRBS

Since the oxygen partial pressure is important for the correct determination of the ethanol concentration and, thus, for the control of vinegar fermentation in ShaRBS, a reliable measurement of the oxygen partial pressure should be guaranteed. However, it is well-known that electrochemical oxygen sensors show a general drift and need to be calibrated on a regular basis. Therefore, a calibration procedure similar to the method of Hansen et al. [105] was designed (chapter 2.3.2). Since the ShaRBS reactor is an open system, a stop phase of the gas flow as in RAMOS experiments could not be realized. Nevertheless, it is possible to calculate the calibration factor for the oxygen sensor at any time point of gas flow change (equation (31)). Figure 24 exemplarily depicts the measured oxygen sensor voltage during a batch cycle for vinegar fermentation in ShaRBS with gas flow change. At the time points of increased gas flow (252.6 h, 256.8 h, 260.9 h, 265.1 h and 269.3 h), the oxygen partial pressure in the headspace and, thus, the oxygen sensor signal were rising. When the flow was lowered again, the oxygen partial pressure in the headspace and, in turn, the oxygen sensor signal slowly decreased due to the bacterial activity. The magnification (figure 24) around the flow changes at 260.9 h depicts the procedure for calibration of the oxygen

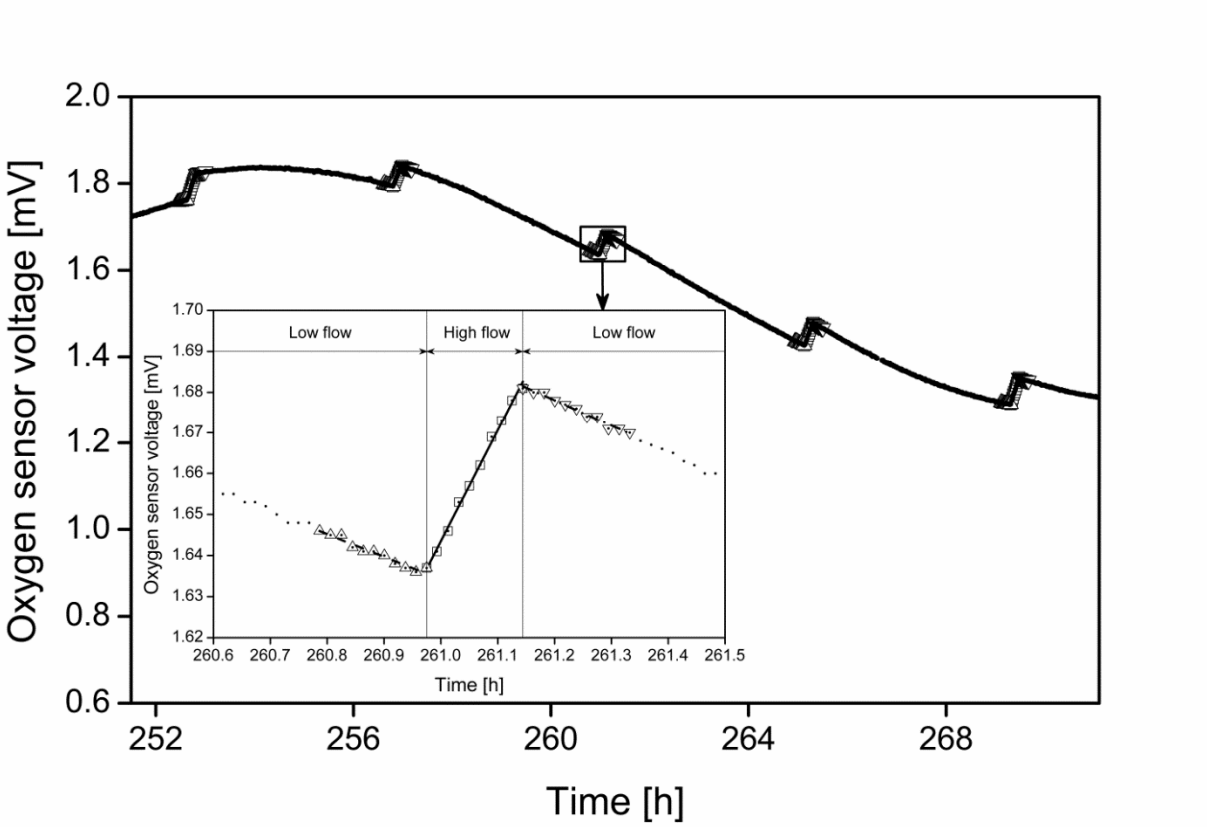


Figure 24: Oxygen sensor calibration on ShaRBS during repeated batch fermentation. To calibrate the oxygen sensor during repeated batch fermentation on ShaRBS according to the method of gas flow change proposed in the theory section (chapter 2.3.2), the gas flow was regularly increased. To be able to differentiate the sensor signal, the oxygen sensor voltage was linearly fitted in the high flow phase as well as in the low flow phases 10 min before and after the high flow phases. The oxygen sensor signal for one batch cycle out of a repeated batch vinegar fermentation is depicted. The magnification shows the calibration procedure for one gas flow change. • oxygen sensor voltage, △ measuring points of oxygen sensor used for a calibration fit in the low flow phase before the high flow phase, □ measuring points of oxygen sensor used for a calibration fit in the high flow phase, ▽ measuring points of oxygen sensor used for a calibration fit in the low flow phase after the high flow phase, **--** calibration fit in the low flow phase before the high flow phase, **—** calibration fit in the high flow phase and **-·-** calibration fit in the low flow phase after the high flow phase

sensor at the two time points of gas flow change. The measuring points in the low flow phase 10 min before the high flow phase, the measuring points in the high flow phase and the measuring points in the low flow phase 10 min after the high flow phase were linearly fitted. The slopes of these fits represent the changes of the oxygen sensor voltage that were needed to calculate the calibration factor of the oxygen sensor at the two time points of gas flow change according to equation (31). The R^2-values of these fits are a criterion for the goodness of these fits. In figure 25 the R^2-values were plotted over the time of repeated batch cultivation. Many more R^2-values in the low flow phase before the high flow phase were less than 0.5 compared to the R^2-values of the fits in the high flow phase and those in

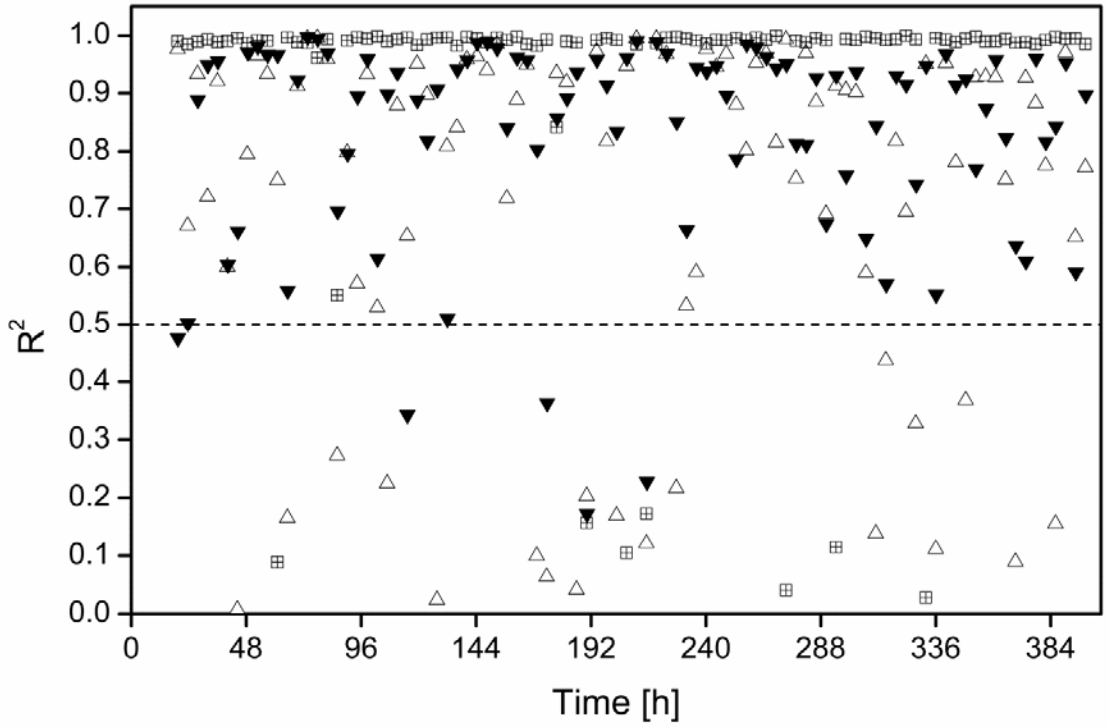


Figure 25: R^2-values of linear fits for the determination of the calibration factor of the oxygen sensor on ShaRBS during fermentation. The oxygen sensor was calibrated online during repeated batch fermentation by the method of gas flow change (chapter 2.3.2). At the two points of gas flow change, i.e. when the gas flow was increased and set back, the sensor signal was fitted linearly in low and high flow phase for a time span of 10 min. These fits allowed for differentiation of the sensor signal. △ R^2 of calibration fit in low flow phase before high flow phase, ⊞ R^2 of calibration fit in high flow phase and ▼ R^2 of calibration fit in low flow phase after high flow phase

the low flow phase after the high flow phase. That means that the fits of the low flow phase before the high flow phase were not as good as the others. Thus, if linear fits are chosen to differentiate the oxygen sensor voltage, the evaluation of the calibration factor at the time point when the gas flow is lowered is preferred to the evaluation of the calibration factor at the time point when the gas flow is increased. However, the calibration factors determined at both time points of gas flow change correlated very well with each other (figure 26). This correlation fit revealed that the calibration factors determined at the gas flow change from low to high flow are tendentially a little higher than the calibration factors determined at the corresponding gas flow change from high to low flow. The slope of the correlation fit was 0.98, i.e. the calibration factors determined at the gas flow change from high to low flow were about 2 % smaller than those determined at the gas flow change from low to high flow. For the following calculations the calibration factors determined at the gas flow change from high to low flow were used, because of better R^2-values of the corresponding low flow fits. Only

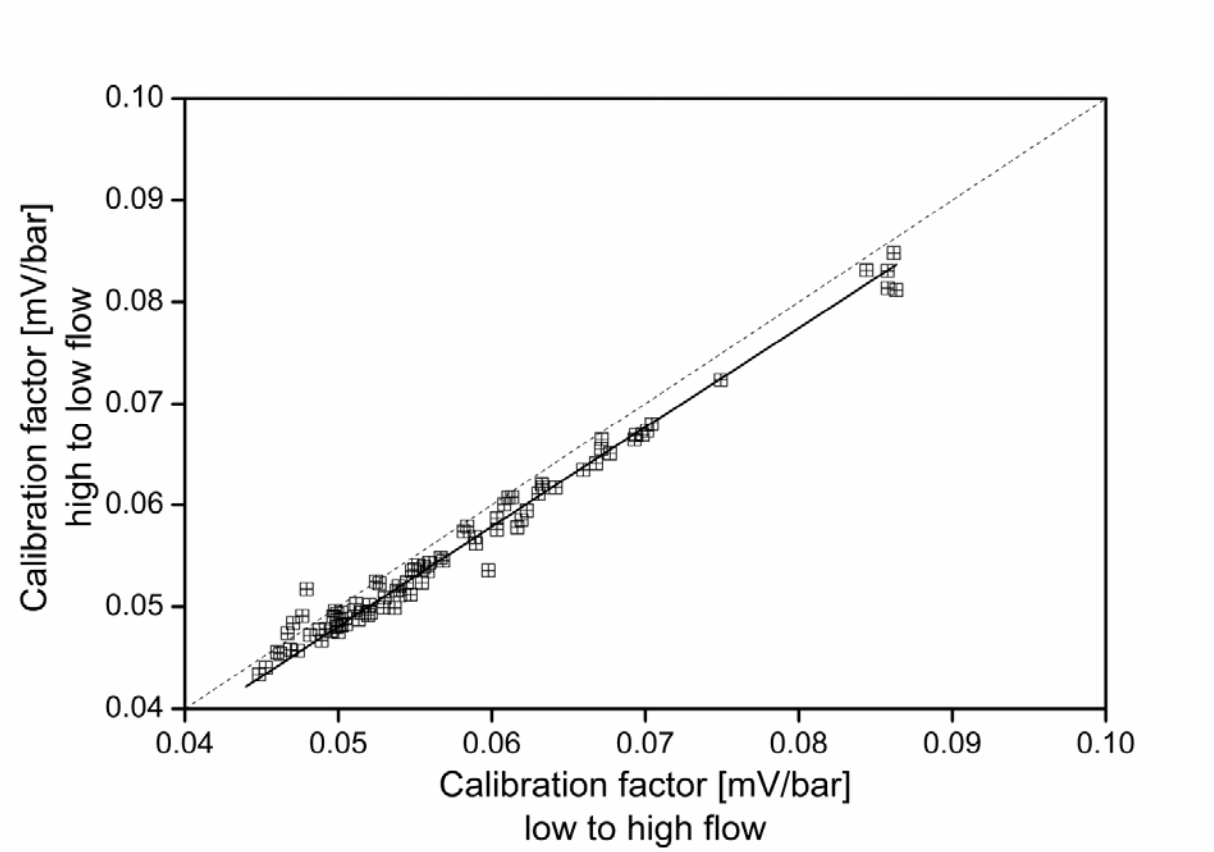


Figure 26: Correlation of calibration factors of oxygen sensor on ShaRBS during fermentation determined at time points of flow change from low to high and high to low flow. The oxygen sensor was calibrated online during repeated batch fermentation by the method of gas flow change (chapter 2.3.2). Calibration factors determined at the corresponding two points of gas flow change, i.e. when the gas flow was increased and set back, were correlated with one another. ⊞ calibration factors determined at the time point of flow change from high to low flow phase vs. calibration factors determined at the corresponding time point of flow change from low to high flow phase, ━ correlation fit of calibration factors determined at the corresponding two time points of flow change, ╍ angle bisector

those calibration factors were selected for which the R^2-values of both fits were larger than 0.5. Figure 27 shows these calibration factors for a repeated batch fermentation. The calibration factors increased with time substantiating the need to calibrate the oxygen sensor online during fermentation. Even the calibration factors that were not considered for further calculations because of their low R^2-values (19.5 h, 115.3 h and 173.6 h) were in line with the other calibration factors. The low R^2-values resulted from a bit unsteady sensor signals (figure 28). The trend was though approximated quite well with linear fits resulting in good calibration factors. During fermentation at around 72 h, 93 h, 118 h, 215.5 h and 239.5 h the oxygen sensor was put on a second ShaRBS reactor of the same device without a running cultivation. In this reactor the oxygen partial pressure was equal to that of water saturated air at the fermentation temperature of 30 °C, i.e. the oxygen partial pressure amounted 0.20 bar

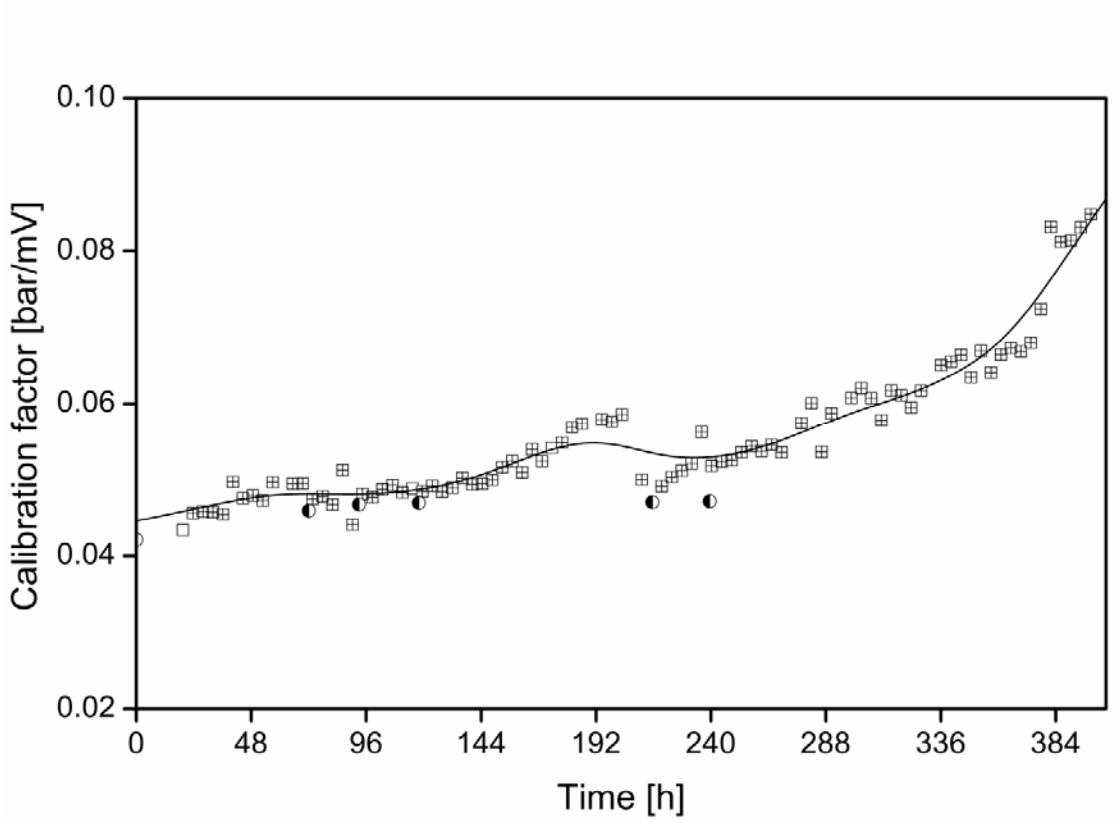


Figure 27: Calibration factor of oxygen sensor on ShaRBS during fermentation. The oxygen sensor was calibrated online during repeated batch fermentation by the method of gas flow change (chapter 2.3.2). During the fermentation the oxygen sensor was put on a second ShaRBS reactor without a fermentation but with defined gas composition in the headspace to control the sensor calibration. The calibration factors were described by a smoothing spline to obtain a continuous function of the calibration factor for further analysis. For that, only those calibration factors were considered that had R^2-values larger than 0.5 for both calibration fits. ⊞ calibration factors determined at the time point of gas flow change from high to low flow and used for a continuous smoothing spline function, ━ smoothing spline (regularization parameter of $5 \cdot 10^{-5}$) of calibration factors, □ outliers of calibration factors (R^2<0.5) determined at the time point of gas flow change from high to low flow, ◐ calibration factors determined by putting the oxygen sensor on a second ShaRBS reactor with defined gas composition in headspace

(equations (25) and (26)). Therefore, the calibration factors for the oxygen sensor could be determined with this defined oxygen partial pressure of the second reactor and the sensor voltage at the corresponding time points. These calibration factors were a little lower than the ones determined online. This confirmed that the calibration factors determined at the time point when the gas flow was changed from high to low flow should be preferred to the ones determined at the change from low to high flow, because the latter ones were even higher (figure 26). Using a smoothing spline function the calibration factor could be expressed as a function of time (figure 27). The regularization parameter of $5 \cdot 10^{-5}$ for the smoothing spline showed a good approximation of the calibration points. Consequently, the oxygen partial

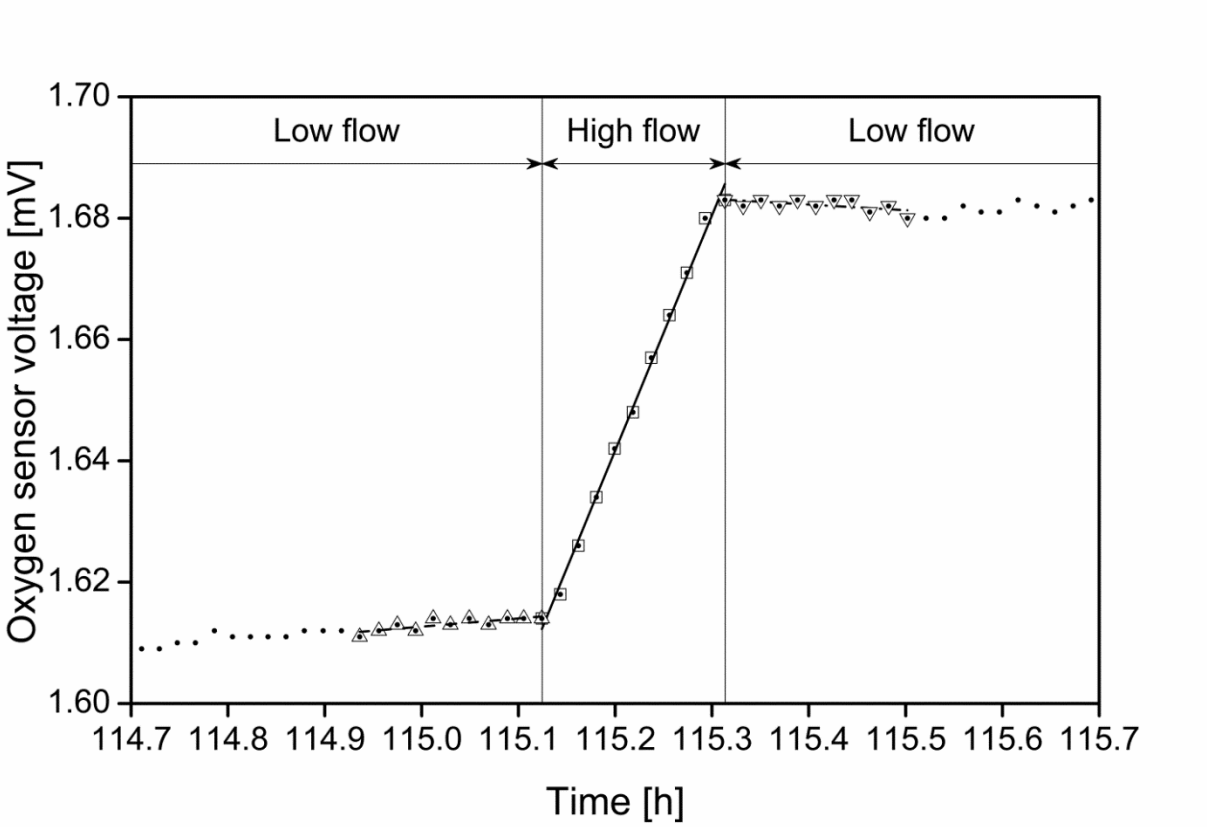


Figure 28: Determination of calibration factor with low R^2-value for the oxygen sensor on ShaRBS during repeated batch fermentation. To calibrate the oxygen sensor during repeated batch fermentation on ShaRBS according to the method of gas flow change proposed in the theory section (chapter 2.3.2), the gas flow was regularly increased. To be able to differentiate the sensor signal, the oxygen sensor voltage was linearly fitted in the high flow phase as well as in the low flow phases 10 min before and after the high flow phase. The sensor signal in the second low flow phase was unsteady leading to a low R^2-value for the linear fit • oxygen sensor voltage, △ measuring points of oxygen sensor used for a calibration fit in the low flow phase before the high flow phase, □ measuring points of oxygen sensor used for calibration fit in the high flow phase, ▽ measuring points of oxygen sensor used for a calibration fit in the low flow phase after the high flow phase, **- -** calibration fit in the low flow phase before the high flow phase (R^2=0.654), **—** calibration fit in the high flow phase (R^2=0.996) and **-·-** calibration fit in the low flow phase after the high flow phase (R^2=0.343)

pressure in the headspace of the ShaRBS for vinegar fermentation was calculated with the continuous calibration factor and the oxygen sensor signal (figure 29). During the flush phases marked by the running feed pump the oxygen sensor signal had often outliers to high partial pressures. These outliers might be due to increased pressure resulting from fermentation liquid not flowing off properly and plugging the shared effluent and exhaust of the ShaRBS reactor for a short while. As the ShaRBS reactor was not equipped with a pressure sensor, the increase of the absolute pressure was not registered. The mass flow controller did not show any unusual behavior that could have been linked to an absolute pressure increase. Since the oxygen partial pressure was considered in the calculation of the

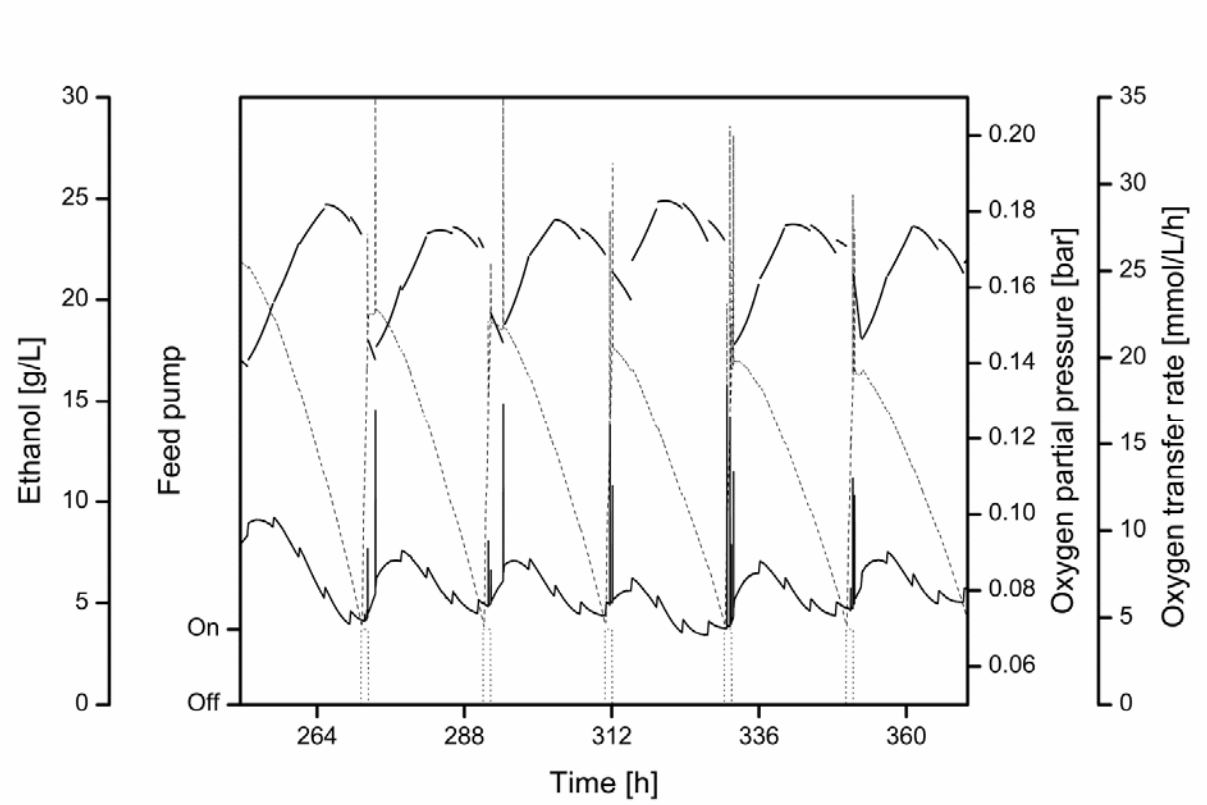


Figure 29: Repeated batch vinegar fermentation in ShaRBS with oxygen analytic during fermentation I. The oxygen sensor was calibrated online during repeated batch fermentation by the method of gas flow change (chapter 2.3.2). The continuous calibration factor obtained by the smoothing spline (Figure 27) was used to calculate the oxygen partial pressure (—) in the headspace of the ShaRBS reactor during repeated batch fermentation. With the oxygen partial pressure the oxygen transfer rate (•) was calculated in the low flow phases. -- ethanol content, ····· running of feed pump

ethanol concentration these outliers were also found in the ethanol concentration. However, when these outliers were removed a reasonable diagram was obtained (figure 30). In the beginning of a new batch cycle marked by the stop of the feed pump and high ethanol concentration, the oxygen partial pressure increased from about 0.07 bar to about 0.09 bar. This can be explained by the reduced bacterial population due to wash out of some bacteria during the flush phase to form the new batch. Therefore, the oxygen is enriched in the headspace by the supplied air. With increasing bacterial activity the oxygen partial pressure in the headspace decreased until the end of a batch cycle. Whenever the gas flow was increased due to the calibration procedure of the oxygen sensor, the oxygen partial pressure of course increased. The oxygen partial pressure in the headspace was with values around 0.07 bar to 0.09 bar quite low. Hence, oxygen partial pressure compensation of the ethanol sensor signal is favorable to determine correct ethanol concentrations in ShaRBS with semiconductor gas sensors. The oxygen partial pressure in the air is much higher and, thus,

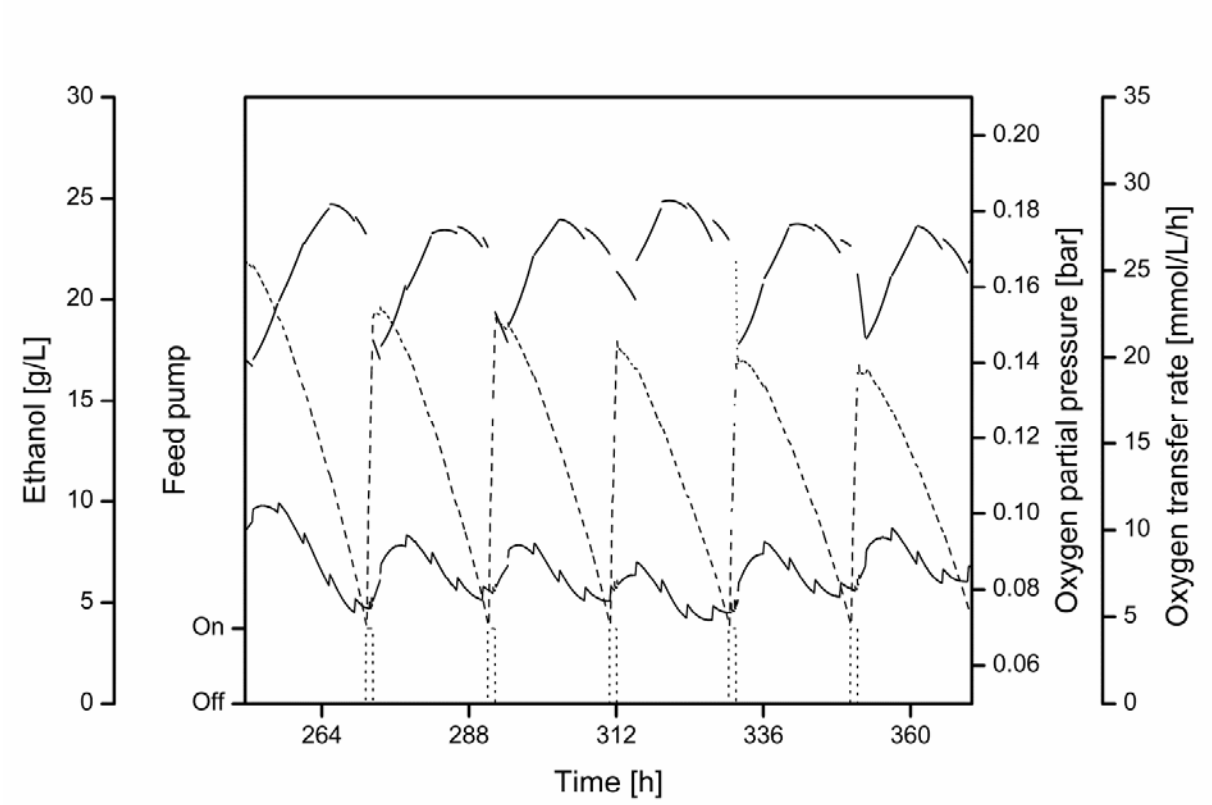


Figure 30: Repeated batch vinegar fermentation in ShaRBS with oxygen analytic during fermentation II. This figure is the same as figure 29, but with outliers removed. The oxygen sensor was calibrated online during repeated batch fermentation by the method of gas flow change (chapter 2.3.2). The continuous calibration factor obtained by the smoothing spline (figure 27) was used to calculate the oxygen partial pressure (—) in the headspace of the ShaRBS reactor during repeated batch fermentation. With the oxygen partial pressure the oxygen transfer rate (•) was calculated in the low flow phases. -- ethanol content, ····· running of feed pump

calibration of the ethanol sensors before the experiment fails unless the oxygen partial pressure is reduced for the calibration e.g. by mixing nitrogen to the air. Furthermore, the oxygen partial pressure was much lower than predicted by the simulation (figure 19). This is explainable as the model parameters relied on batch fermentations with a different bacterial culture and fermentation system. The model kinetic was slower than the repeated batch fermentation considered here (figure 30). Hence, in the model the time of one batch (ca. 78 h) was as well considerably longer than in the conducted repeated batch fermentation (ca. 20 h).

4.2.6 Determination of oxygen transfer rate in SharRBS

The oxygen transfer rate was calculated from the oxygen partial pressure (equation (27)) during the low flow phases (figure 29 and figure 30). For that purpose, the oxygen partial

pressure was approximated with polynomials of second order during the low flow phases. These polynomials allowed a good approximation of the measured data, correction of outliers and differentiation of the oxygen partial pressure. The course of the oxygen transfer rate was in agreement with that of the batch fermentation in RAMOS cultivations (chapter 4.1.2). Maximum oxygen transfer rates of about 28 mmol/L/h were obtained during fermentation in ShaRBS. This value was in the same order of magnitude as that obtained in the RAMOS cultivations (ca. 25 mmol/L/h) while it was a little higher than in the 9 L-bioreactor culture (18.5 mmol/L/h, chapter 4.3.2), where the oxygen transfer rate was deduced from the ethanol signal. As different fermentations in different systems were compared to each other, minor differences of oxygen transfer rate values were accepted. Additionally, the acetic acid bacteria in vinegar fermentation are subjected to natural variation, because of long-term adaptation of the mixed bacterial culture to the adverse culture conditions and the genetic predisposition of the bacteria for mutation. For that reason variations of growth in different cultures cannot be excluded.

4.3 Scale-down of vinegar fermentation into microtiter plates

4.3.1 Vinegar fermentation in Flowerplate under typical shaking conditions

Figure 31 shows the course of the dissolved oxygen tension for vinegar fermentation in a Flowerplate with typical shaking conditions and a conventional gas-permeable adhesive seal. The dissolved oxygen tension of about 80 % was relatively high during the whole fermentation and considerably higher compared to the fermentation conditions in the9 L-bioreactor (figure 33C). Once the ethanol substrate had been depleted, fermentation ceased and the dissolved oxygen tension increased accordingly to 100 % air saturation at 20 h to 22 h. Therewith, the fermentation time was much shorter than in the 9 L-bioreactor. The shortened fermentation time can be attributed to the evaporation losses of ethanol. Figure 32 shows that especially ethanol did evaporate through the gas-permeable seal. Compared to the inoculated culture, roughly half of the ethanol but nearly no acetic acid evaporated in the filtered culture broth by the end of fermentation. In the cases of the parallel bacterial cultures in well 1 and 2, the acetic acid concentration was in both cases with 1.9 mol/L considerably higher than that of the inoculation sample, but clearly below the theoretical maximum of 2.1 mol/L. The theoretical maximum corresponds to the total molar concentration of the inoculation sample, whereby the total molar concentration is the sum of the molar ethanol and molar acetic acid concentration. The total molar concentration is useful, because ethanol is stoichiometrically converted one-to-one into acetic acid in vinegar

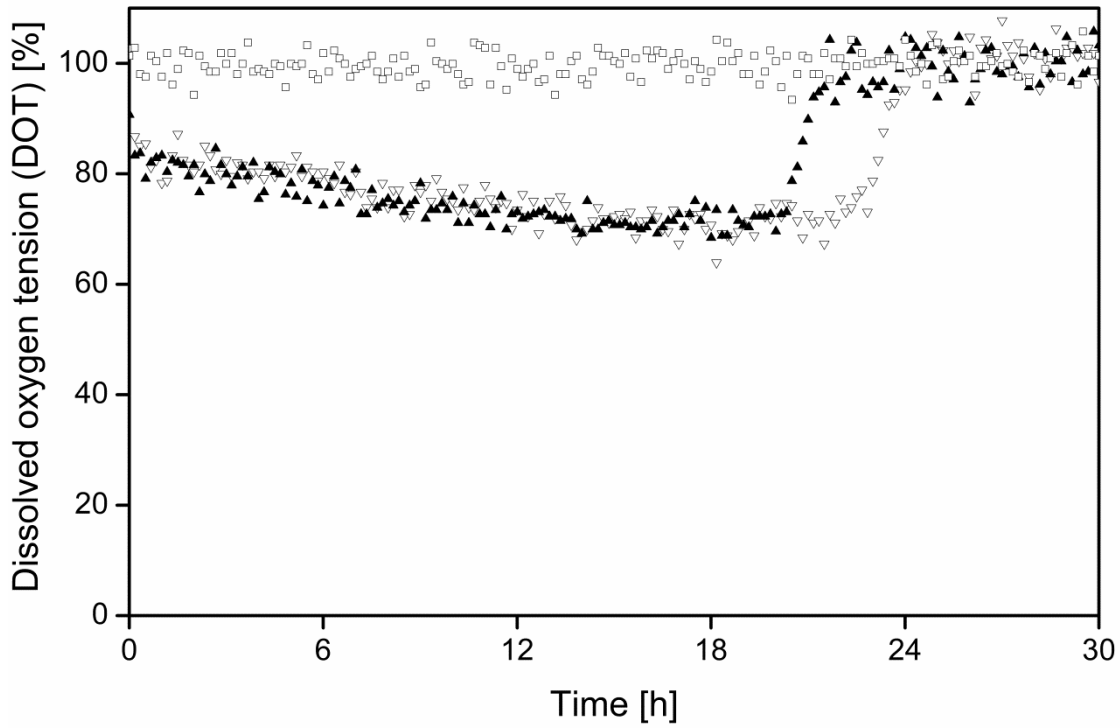


Figure 31: Dissolved oxygen tension in vinegar fermentation using a Flowerplate with a conventional gas-permeable seal. Parallel fermentations with typical experimental parameters were conducted in the BioLector device (shaking diameter 3 mm and shaking frequency 1000 rpm) at 30 °C and 100 % relative humidity using the Flowerplate (filling volume 1000 µL) with a gas-permeable seal. The dissolved oxygen tension was measured with a fluorescence optical method. The curves for two different wells are depicted. ▽ and ▲ acetic acid bacteria culture from well 1 and well 2, respectively, □ filtered culture broth (100 % reference for dissolved oxygen tension)

fermentation and the fermentations were initiated from a running repeated batch fermentation. Therefore, the product acetic acid was already present in the fermentation broth at the beginning of the new batch. The results from the Flowerplate applying typical shaking conditions were unsatisfactory. Typical shaking conditions for the Flowerplate with a conventional gas-permeable adhesive seal did not prove to be suitable for vinegar fermentation. Therefore, in the following, vinegar fermentation was scaled down from the 9 L-bioreactor to the microliter scale according to the design scheme proposed in figure 4.

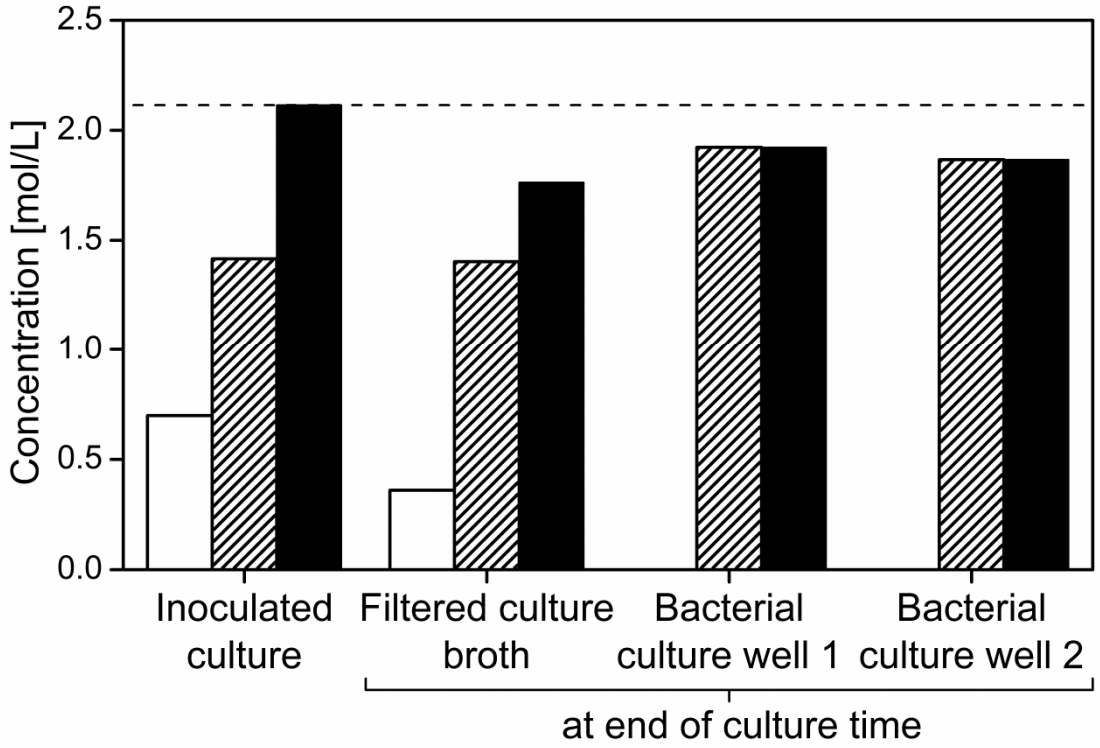


Figure 32: Concentration changes during vinegar fermentation in Flowerplate with conventional gas-permeable seal. Parallel fermentations with typical experimental parameters were conducted in the BioLector device (shaking diameter 3 mm and shaking frequency 1000 rpm) at 30 °C and 100 % relative humidity using the Flowerplate (filling volume 1000 µL) with a conventional gas-permeable seal. Concentrations of ethanol and acetic acid were determined by gas chromatography from the inoculated culture as well as the cultures at end of culture time: open columns: ethanol concentration, striped columns: acetic acid concentration, filled columns: total molar concentration (sum of ethanol and acetic acid concentration)

4.3.2 Determination of fermentation conditions in the 9 L-bioreactor for vinegar production

The fermentation conditions in the 9 L-bioreactor operated at a filling volume of 6 L were determined for one batch phase during repeated batch cultivation (figure 33). The depicted fermentation curves start at the beginning of a batch cycle, i.e. just after the preceding replenishing phase of the 9 L-bioreactor with fresh ethanol substrate. The fermentation curves end just before the initiation of the draining and replenishing phase for the next batch. The dashed vertical line indicates the time point of removal of inoculation vinegar for the microtiter plate. As far as possible, the fermentation conditions from that point on should later be resembled in the microtiter plate. Figure 33A shows the ethanol concentration. Due to the

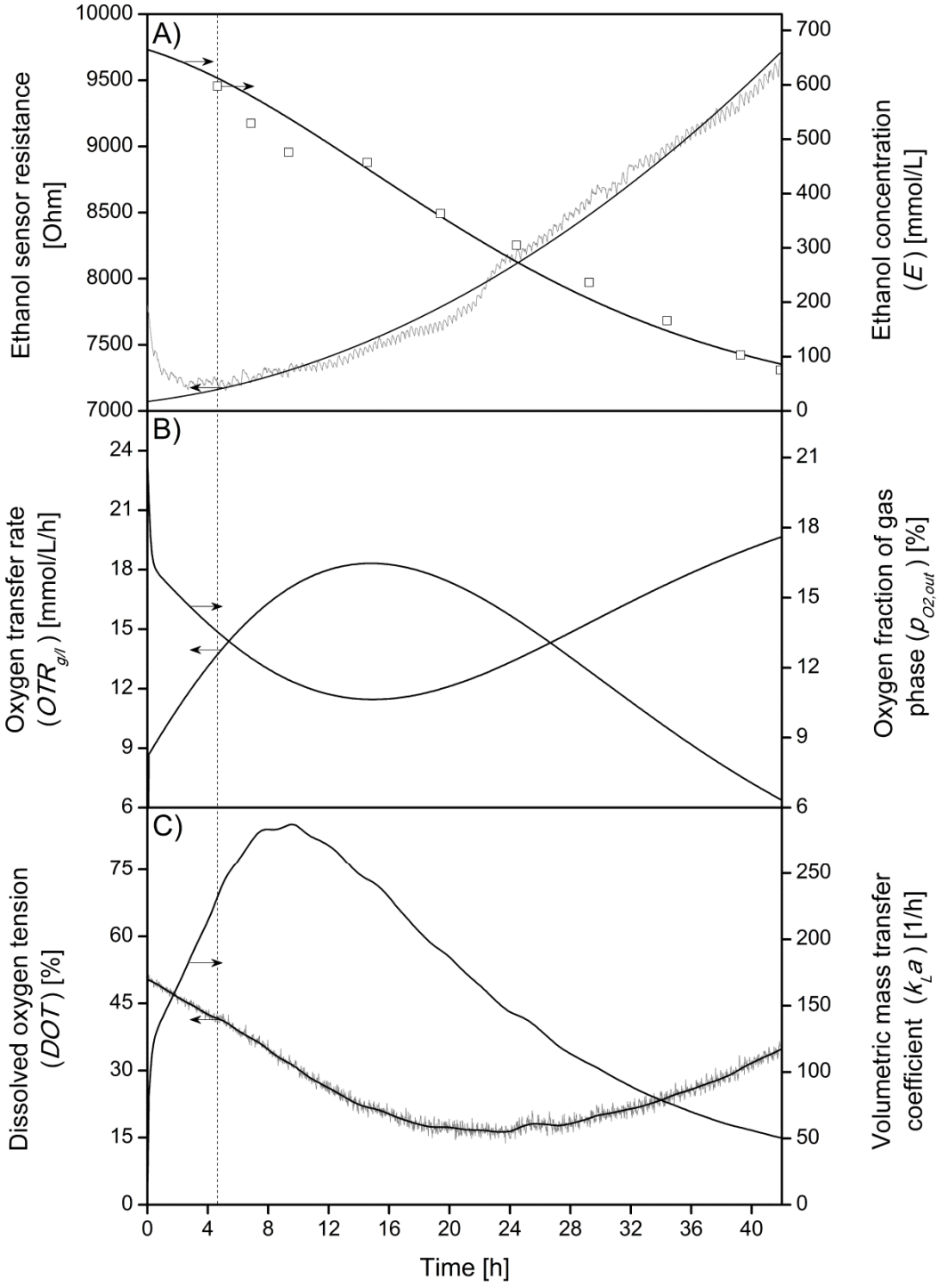


Figure 33: Determination of fermentation conditions in a 9 L-bioreactor. The 9 L-bioreactor was operated in repeated batch mode with a filling volume of 6 L. A) The ethanol concentration was measured using a semiconductor gas sensor probe. The sensor resistance (noisy line) was fitted (smooth line) and calibrated against samples drawn during fermentation (□). B) The oxygen transfer rate in the 9 L-bioreactor was obtained by differentiating the ethanol concentration. The oxygen fraction in the gas phase was approximated based on the model (figure 4#5). C) The dissolved oxygen tension was measured with a Clark-electrode (noisy line) and smoothed with a spline function (smooth line). The oxygen transfer rate and the dissolved oxygen tension permitted the calculation of the volumetric mass transfer coefficient $k_l a$ for oxygen (figure 4#7). The vertical dashed line indicates the time point for the removal of inoculation vinegar for the microtiter plate.

unsteady fermentation conditions in the beginning of the batch cycle, the ethanol sensor resistance required some time to adjust. Ethanol was continuously metabolized at concentrations from 660 mmol/L down to 87 mmol/L within 42 h. The continuous ethanol concentration curve was differentiated over time and converted into the oxygen transfer rate (figure 33B, figure 4#1, 2 and 4). This is possible, because ethanol and oxygen consumption are stoichiometrically coupled in vinegar fermentation. As the oxygen solubility of the fermentation media is extremely low, the liquid medium does not serve as a relevant oxygen reservoir. For the same reason, it can be assumed that the oxygen uptake rate of the bacteria is equivalent to the oxygen transfer rate. During the first 14.5 h, the oxygen transfer rate increased from 8.7 mmol/L/h to 18.3 mmol/L/h and then slowly decreased down to 6.4 mmol/L/h at the end of the batch (figure 33B). The decreasing oxygen transfer rate or rather the decreasing bacterial respiration activity is attributed to the increasing acetic acid concentration, which inhibits the bacteria more than the substrate ethanol does [98]. An oxygen balance of the reactor headspace based on the oxygen transfer rate and aeration rate resulted in the oxygen fraction of the gas phase (figure 33B and figure 4#5). The oxygen content in the gas phase reached its minimum of 10.6 % at 14.5 h when the oxygen transfer rate attained its maximum. The dissolved oxygen tension (figure 33C and figure 4#3) decreased from 50.4 % air saturation at 0 h to a minimum of 16.3 % at 24 h and increased again to 32.3 % at the end of fermentation. The curves of the oxygen transfer rate, oxygen fraction of the gas phase and dissolved oxygen tension were finally used to calculate the volumetric mass transfer coefficient ($k_L a$) for oxygen in the 9 L-bioreactor over fermentation time (figure 33C, figure 4#6 and 7). The maximum volumetric mass transfer coefficient was 287 h^{-1} at 9.25 h.

4.3.3 Determination of experimental parameters for vinegar fermentation in the microtiter plate

According to the design scheme (figure 4), the remaining experimental parameters – shaking frequency and area-to-height ratio (A/H) of the borehole in the microtiter plate lid – for the Flowerplate were determined. With the maximum volumetric mass transfer coefficient for oxygen from the 9 L-bioreactor of 287 h^{-1} (figure 4#9), the shaking diameter of 3 mm and the filling volume of 1200 µL, the shaking frequency resulted in 879 rpm according to equation (39) (figure 4#12). The oxygen mass transfer coefficient (k_{lid,O_2}) for the microtiter plate lid in figure 34 (figure 4#13) was approximated using the oxygen transfer rate (figure 4#4) and the oxygen partial pressure in the headspace of the 9 L-bioreactor (figure 4#5) as reference input factors. With the oxygen mass transfer coefficient (k_{lid,O_2}) for the microtiter plate lid, the area-

to-height ratio (A/H) of the borehole in the microtiter plate lid was calculated (figure 34, figure 4#15) by assuming a constant effective diffusion coefficient of oxygen in ambient air ($D_{O_{2,air}}$) of 0.204 cm²/s at 30 °C (figure 4#14). As shown in figure 34, the A/H of the borehole in the lid for vinegar fermentation in the microtiter plate under the above specified conditions should be about 0.08 mm^2/mm throughout the whole time of fermentation. Therefore, a custom-made lid with a height of 20 mm was constructed realizing centrally for one column of the microtiter plate boreholes with the A/H of 0.08 mm^2/mm (Ø 1.4 mm). Since the model provides only estimations, further columns of boreholes with A/Hs ranging from 0.06 mm^2/mm (Ø 1.2 mm) to 0.11 mm^2/mm (Ø 1.7 mm) in increments of 0.01 mm^2/mm (Ø 0.1 mm) were incorporated in the custom-made lid to compensate for model uncertainties. For curiosity, for one column of the microtiter plate by far wider boreholes with an A/H of 0.35 mm^2/mm (Ø 3.0 mm) were realized in the lid.

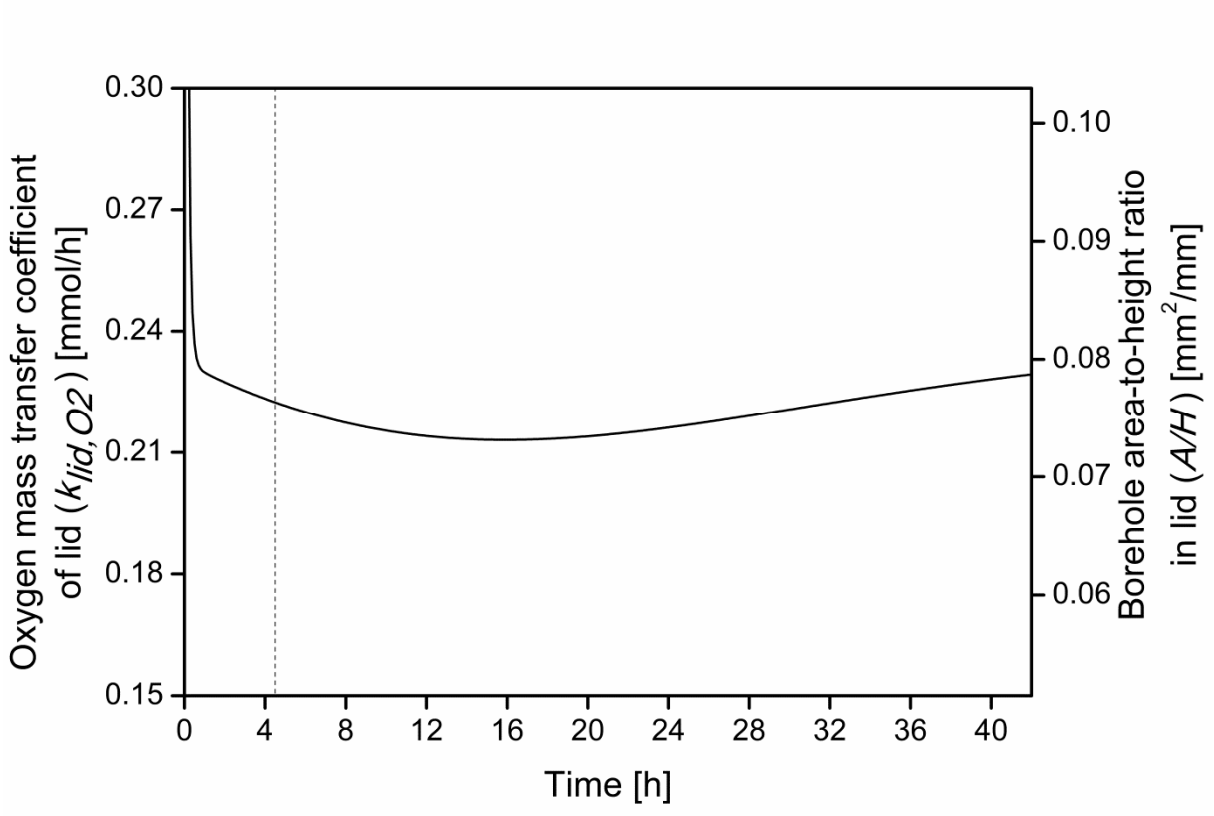


Figure 34: Calculated oxygen mass transfer coefficient for the microtiter plate lid. The oxygen mass transfer coefficient for the microtiter plate lid (k_{lid,O_2}) was calculated for the specified filling volume of 1200 µL using the oxygen transfer rate ($OTR_{g/l}$) and the oxygen partial pressure in the headspace ($p_{O_2,out}$) of the 9 L-bioreactor as reference input factors (figure 4#13, equation (32), figure 33). The A/H of the borehole in the microtiter plate lid is proportionally to the oxygen mass transfer coefficient for the lid (figure 4#14, equation (33)), and the two ordinates are correspondingly scaled to each other. Inoculation vinegar was taken from the 9 L-bioreactor after 4.5 h of a batch phase marked by the vertical dashed line.

4.3.4 Model based estimation of vinegar fermentation in Flowerplate with custom-made lid

Using the model for the microtiter plate (equations (32) to (42)) with the oxygen transfer rate from the 9 L-bioreactor as reference input, the fermentation conditions for vinegar fermentation in the Flowerplate could be predicted. Figure 35 shows the predicted curves of

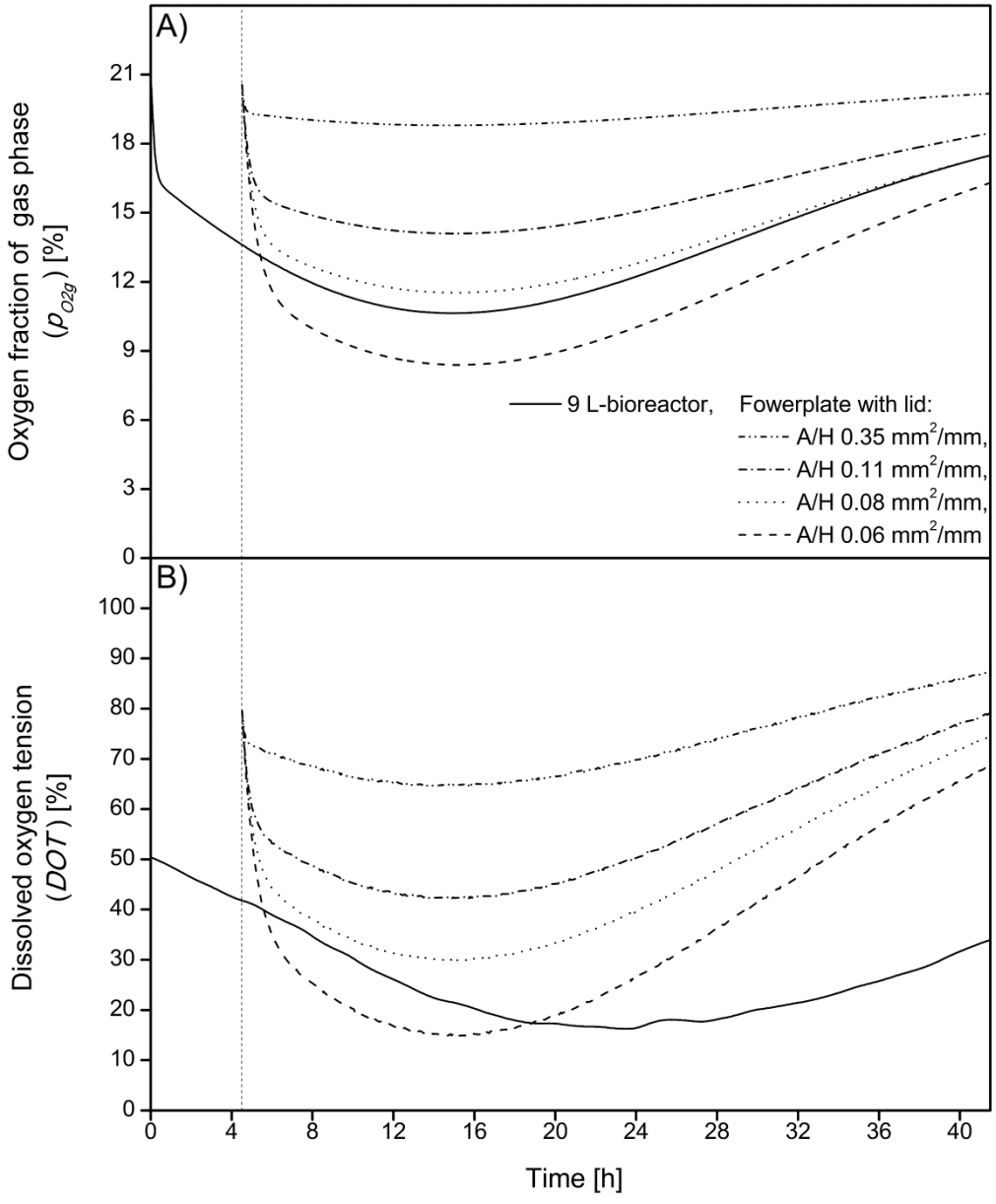


Figure 35: Predicted fermentation conditions in the Flowerplate with a custom-made lid for vinegar fermentation. The oxygen fraction of the gas phase (A) and dissolved oxygen tension (B) were calculated using the oxygen transfer rate from a 9 L-bioreactor as oxygen uptake rate of the bacteria in the Flowerplate. The experimental parameters were defined according to the scheme for the determination of the borehole dimensions in the microtiter plate lid (figure 4): shaking diameter 3 mm, filling volume 1200 µL, shaking frequency 879 rpm (volumetric mass transfer coefficient of oxygen 287 h^{-1}). Inoculation vinegar was taken from the 9 L-bioreactor after 4.5 h of a batch phase marked by the vertical dashed line.

the oxygen fractions in the gas phases ($p_{O_2,g}$) and dissolved oxygen tensions (DOT) for vinegar fermentation in the Flowerplate with the custom-made lid for the conditions determined above. Initially, the oxygen fractions in the gas phases of the Flowerplate wells were equal to that of the ambient air. Due to the oxygen transfer from the gas phase to the liquid medium the oxygen fractions in the gas phases quickly decreased within the first 1.5 h. From then on, the oxygen fractions in the gas phases of the Flowerplate wells proceeded similar to that of the 9 L-bioreactor. The greater the A/H of the borehole in the lid, the higher was the level of the oxygen fraction in the gas phase. As expected, the curve for the A/H of 0.08 mm²/mm was most similar to the curve of the 9 L-bioreactor. This value for A/H was proposed by the calculation of the oxygen mass transfer coefficient for the microtiter plate lid (figure 34). Similar to the oxygen fractions in the gas phases ($p_{O_2,g}$) the dissolved oxygen tension in the liquid phases (DOT) decreased to minimum levels at about 15 h. The greater the A/H of the borehole in the lid, the higher was the level of dissolved oxygen tension in the liquid phase. In particular, for A/Hs of 0.06 mm^2/mm to 0.08 mm^2/mm of the borehole in the lid the dissolved oxygen tension in the Flowerplate wells was in the order of magnitude of the dissolved oxygen tension in the 9 L-bioreactor. Consequently, the calculations show that fermentations in the Flowerplate with diffusive oxygen supply can be conducted under comparable conditions to a fermentation in a 9 L-bioreactor with constant convective aeration.

4.3.5 Experimental vinegar fermentation in a Flowerplate with a custom-made lid

A parallel fermentation with the custom-made lid was conducted in a BioLector device with the experimental parameters determined above. The fermentation was initiated according to the scheme depicted in figure 10 to avoid oxygen depletion during inoculation. A sufficient oxygen supply during inoculation is essential to obtain reproducible results with acetic acid bacteria (chapter 4.1). Figure 36 shows the dissolved oxygen tension measured in five wells of the Flowerplate with the A/H of the borehole in the lid of 0.08 mm^2/mm. The curves for all five wells represented by different symbols coincide with one another, thereby demonstrating the well-to-well reproducibility. The pipetting step by the automated liquid handling system, where no oxygen is delivered, was fast enough that the bacteria did not suffer from oxygen depletion. Therefore, the inoculation scheme (figure 10) designed for the Flowerplate was proven to be suitable to inoculate the Flowerplate from the 9 L-bioreactor. Since the well-to-well reproducibility was ensured, the data from different wells operated under the same conditions could be averaged and smoothed by a spline function. The splines of the

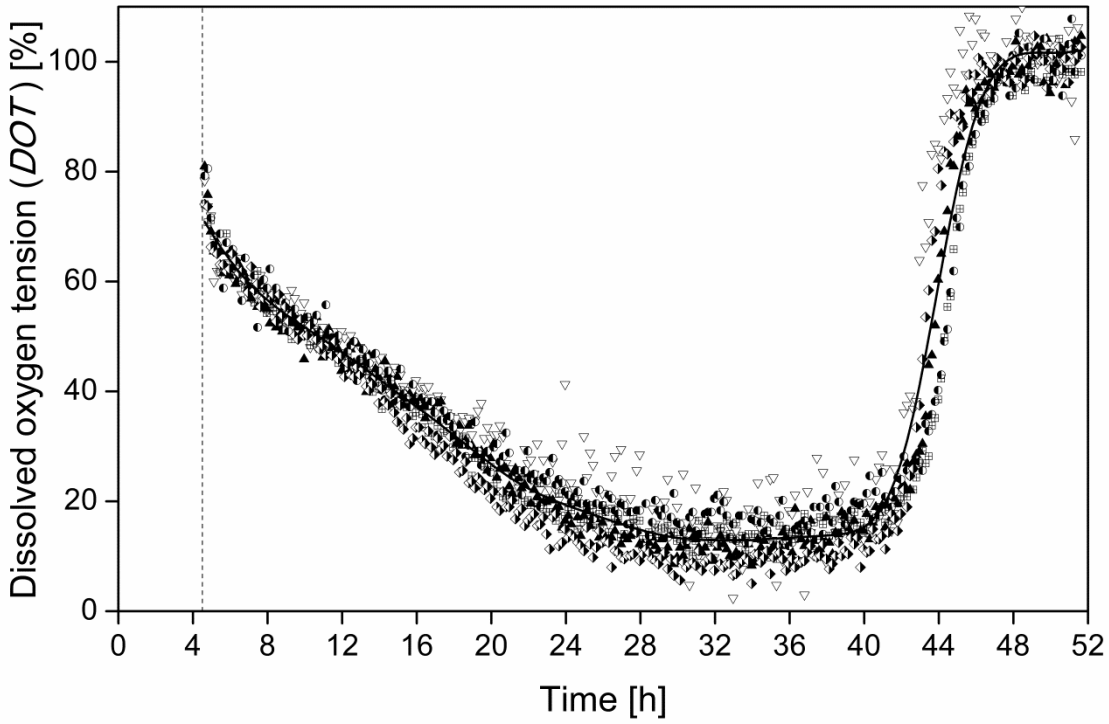


Figure 36: Dissolved oxygen tension in vinegar fermentation using a Flowerplate with a custom-made lid. Parallel fermentations with the predefined experimental parameters were conducted in a BioLector device (shaking diameter 3 mm and shaking frequency 879 rpm) at 30 °C and 100 % relative humidity using the Flowerplate (filling volume 1200 µL) with the custom-made lid. The dissolved oxygen tension was measured with a fluorescence optical method. The curves for five different wells with the A/H of the boreholes in the lid of 0.08 mm^2/mm are depicted by the symbols: ▽ well 1, ▲ well 2, ◐ well 3, ⊞ well 4 and ⬗ well 5. The measured values were averaged and smoothed with a spline function depicted as line. Inoculation vinegar was taken from the 9 L-bioreactor after 4.5 h of a batch phase marked by the vertical dashed line.

dissolved oxygen tension in the wells of the Flowerplate with the same A/H of the borehole in the lid are depicted in figure 37. The pattern of the measured curves of the dissolved oxygen tension in the wells confirmed the theory: The greater the A/H of the borehole in the lid, the higher was the dissolved oxygen tension. For the A/Hs ranging from 0.06 mm^2/mm to0.11 mm^2/mm, which were the A/Hs close to the predicted most suitable A/H of 0.08 mm^2/mm, the dissolved oxygen tension decreased over fermentation time to values between 7.5 % to 23 % air saturation, respectively. Compared to the 9 L-bioreactor the initial dissolved oxygen tension in the Flowerplate was considerably higher. This is due to the fact that the aeration rate during the transport of the inoculation vinegar was much higher than in the 9 L-bioreactor. In addition, the oxygen fraction in the headspace of the Flowerplate was initially equal to air. In contrast, the 9 L-bioreactor was operated in repeated batch mode. Hence, the gas phase in the 9 L-bioreactor was already partially depleted in oxygen which, in

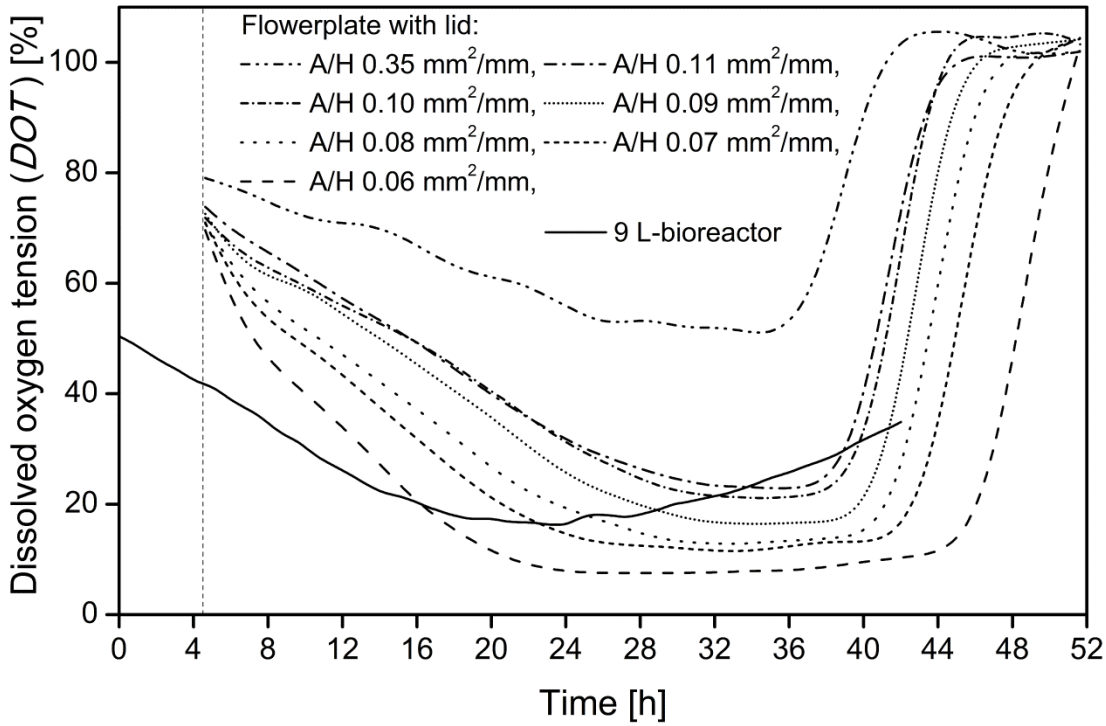


Figure 37: Smoothed dissolved oxygen tension in Flowerplate with custom-made lid for vinegar fermentation. Parallel fermentations with the predefined experimental parameters were conducted in a BioLector device (shaking diameter 3 mm and shaking frequency 879 rpm) at 30 °C and 100 % relative humidity using the Flowerplate (filling volume 1200 µL) with the custom-made lid. The dissolved oxygen tension values for the wells with the same A/H of the borehole in the lid were averaged and smoothed with splines depicted as broken lines. For comparison, the dissolved oxygen tension of the 9 L-bioreactor is depicted as solid line. Inoculation vinegar was taken from the 9 L-bioreactor after 4.5 h of a batch phase marked by the vertical dashed line.

turn, led to a lower dissolved oxygen tension. Although the detailed courses of the curves from the Flowerplate were different than the dissolved oxygen tension in the 9 L-bioreactor used to design the experiment (figure 33), these dissolved oxygen tension values were in the range of the dissolved oxygen tension in the 9 L-bioreactor. The dissolved oxygen tension for an A/H of 0.35 mm^2/mm was much higher, in the range of 80 % to 60 % air saturation. It is noticeable that the smaller the A/H of the borehole in the lid was, the earlier the lowest level of dissolved oxygen tension was reached. These minimum levels of dissolved oxygen tension also continued longer than those of the wells with greater A/Hs. The curves of the wells belonging to A/Hs of 0.06 mm^2/mm to 0.09 mm^2/mm showed obvious plateaus. These plateaus could be explained as oxygen limitations, although the level was not close to 0 % air saturation. In vinegar fermentation the biomass concentrations are generally extremely low, and the product acetic acid is inhibiting. Therefore, the dissolved oxygen tension approaches steady state already at elevated levels. Likewise, the calculations for the different A/Hs of the

borehole in the lid (figure 35) predicted lower values of the dissolved oxygen tension the smaller the A/H in the lid was. Consequently, there was less oxygen in the culture broth available for the bacteria with the smaller A/H of the borehole in the lid. As the rates of oxygen and ethanol consumption of the bacteria in vinegar fermentation are stoichiometrically coupled, the oxygen limited fermentations (figure 37, A/H of 0.06-0.09 mm^2/mm) lasted longer than the unlimited ones (figure 37, A/H of 0.10-0.11 mm^2/mm).

At the end of the experiment, the concentrations of ethanol and acetic acid were determined (figure 38A). For all the wells of the Flowerplate, ethanol was no longer present at the end of culture time. In comparison to the inoculated culture, it was obvious that most of the ethanol was converted into acetic acid. The acetic acid concentration at the end of culture time was nearly equal to the total molar concentration of the inoculated culture – the theoretically attainable upper limit of acetic acid in the fermentation without any losses. For A/Hs of the borehole in the lid between 0.06 mm^2/mm and 0.11 mm^2/mm, the attained acetic acid was greater than 95 % of this theoretical upper limit. In contrast, the attained acetic acid was only 86 % for the wells with the largest hole in the lid (A/H 0.35 mm^2/mm). Consequently, the evaporation losses especially of ethanol could be considerably minimized by the lid compared to the conventional gas-permeable seal where nearly half of the ethanol evaporated (figure 32, first and second column). The fact that nearly no medium evaporated was confirmed by the residual liquid volumes at the end of the culture time (figure 38B). The lowest residual volume was observed for the A/H of 0.35 mm^2/mm with 95 % of the initial volume. For all other A/Hs, the residual volume was about 99 % of the initial medium volume. Thus, the residual volumes substantiate the results of the ethanol and acetic acid evaporation losses. The fermentations ceased once ethanol became depleted and dissolved oxygen tension quickly increased (figure 37). These batch times are depicted in figure 38C for the various A/Hs of the borehole in the lid. The smaller the A/H, the longer lasted the fermentation. On the one hand, this can be attributed to oxygen limitation. On the other hand, especially in the case of an A/H of 0.35 mm^2/mm, the shorter batch time can also be attributed to higher evaporation losses of ethanol. Consequently, all the A/Hs of the borehole in the lid ranging from 0.08 mm^2/mm to 0.11 mm^2/mm led to dissolved oxygen tension values in the medium comparable to those of the 9 L-bioreactor. It is concluded that one of the larger A/H values of 0.09 mm^2/mm or 0.11 mm^2/mm should be chosen to avoid oxygen limited conditions. For these cases, it could be demonstrated that evaporation of ethanol and acetic acid can be considerably reduced.

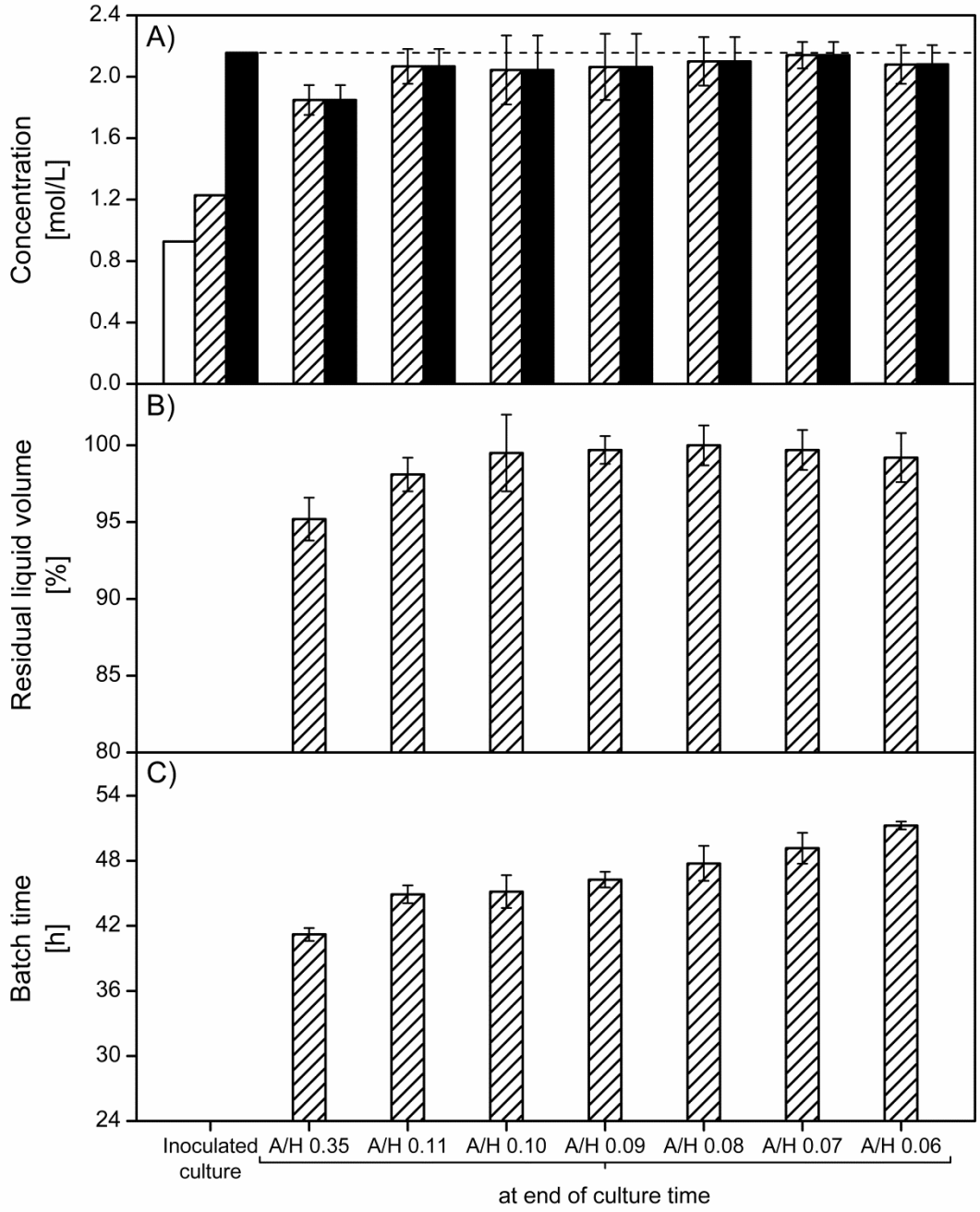


Figure 38: Final conditions in the Flowerplate with a custom-made lid for vinegar fermentation. Parallel fermentations with the predefined experimental parameters were conducted in a BioLector device (figure 37). A: The molar concentrations of ethanol (open columns) and acetic acid (striped columns) were determined by gas chromatography. The sum of the molar ethanol and acetic acid concentrations yields the total molar concentration (filled columns). B: The residual volumes were determined by the liquid level detection function of the applied automated liquid handling system. C: The batch time was defined as the time from inoculation of the Flowerplate until the dissolved oxygen tension reached 100 % air saturation plus the 4.5 h of the batch phase in the 9 L-bioreactor.

5 Conclusion

Traditional precultivation steps using pipetting are not advisable for obligatory aerobic bacteria such as acetic acid bacteria in vinegar fermentation at industrially relevant high ethanol and acetic acid concentrations. Instead, it is crucial that precultivation methods for these bacteria ensure constant oxygen supply such as via aerated bubble columns to guarantee the reproducibility of main culture experiments. As acetic acid bacteria easily die or mutate and lose certain characteristics if they are taken out of their original environment, it is essential to directly transfer them from the running precultivation to the main cultivation. In this way the diversity of the preculture is preserved in the main culture. The method with the aerated mobile bubble column described in this thesis is primarily suitable for submerged vinegar fermentation. If solid state fermentation or other technologies are used to produce vinegar, the method needs to be redesigned to be compatible with these technologies. If fermentations with obligatory aerobic bacteria other than vinegar production have to be examined, the transfer of the preculture to the main culture might need to be modified with respect to sterility requirements.

Flushing repeated batch fermentation in ShaRBS proposed in this thesis was successfully applied for parallel vinegar fermentation on small scale. Fermentation conditions, i.e. the concentrations of biomass, substrate and product, in the screening and production system were mathematically proven to be widely the same. The introduced method can also be applied to other fermentations. Until now, screening procedures for bioprocess development have focused on simple batch, fed-batch or continuous fermentation, but not on repeated batch operation mode. The main advantage of repeated batch processes are their increased productivity compared to usual batch processes because of shorter cycle times.

In contrast to fully equipped bioreactors at laboratory or pilot scale, a small-scale parallel fermentation system ought to be kept as simple as possible. Since the proposed flushing technique inherently does not require a draining pump, equipment can be saved compared to the conventional repeated batch process. Whereas in the conventional bioreactor two pumps per bioreactor are necessary for draining and filling the bioreactor, only one pump per reactor is necessary for the flushing repeated batch in ShaRBS. This simplifies the system and makes it less prone to failure. Thus, many reactors can be easily operated in parallel. Furthermore, a completely automatic operation and monitoring of the fermentations is possible due to the use of semiconductor gas sensors for the online detection of the volatile substrate ethanol. A simultaneous oxygen analysis in the headspace of the ShaRBS reactor allows for the compensation of the oxygen partial pressure dependency of the semiconductor

gas sensors. Moreover, the oxygen transfer rate can be determined during repeated batch cultivation revealing information on the bacterial activity.

Flushing repeated batch fermentations on small scale are not only valuable for screening fermentation conditions in vinegar production. In general, the repeated batch operation mode allows already in an early state of bioprocess development to actually follow the adaptation of a given microbial culture. This may lead to more robust strains and, in turn, to greater process robustness and stability.

Since the substrate ethanol and the product acetic acid easily evaporate, vinegar fermentation using microtiter plates is a challenging task. In the last part of this thesis it was shown that conventional gas-permeable seals do not sufficiently prevent evaporation of substrate and product. Using these conventional seals, the dissolved oxygen tension in the microtiter plate under the chosen operating conditions was much higher than that in a 9 L-bioreactor. The model based design of a custom-made lid with small boreholes for gas exchange yields reproducible fermentations with only minor evaporation losses. The dissolved oxygen tensions during vinegar fermentation in the microtiter plate with this lid were in the range of that of the 9 L-bioreactor. In conclusion, vinegar fermentation was successfully scaled down to the microliter scale, providing a platform for high-throughput investigations. The adapted diffusion model for gas exchange through the sterile barrier of a shake flask proved to be well-suited for microtiter plates. Thus, the demonstrated strategy may serve as a model for the scale-down of other fermentations involving volatile compounds.

6 Outlook

The small scale cultivation methods and systems established within this thesis are appropriate to study the effects of diverse influence factors on the activity of acetic acid bacteria in vinegar fermentation in high throughput. The degree of parallelism, especially in microtiter plates, allows for investigations following the rules of design of experiments. Such experiments would not only reveal the effect of a single influence factor on the microorganisms but also synergistic effects of different influence factors. As already outlined in the discussion (chapter 4.2.3), flushing repeated batch fermentation can also be applied to study adaptation phenomena, long-term physiology and genetics in vinegar and other fermentations.

Acetic acid bacteria suffered from oxygen depletion during typical inoculation procedures. The mobile bubble column was established as effective method to avoid oxygen depletion during the transfer of precultures. However, the method proved to be suitable when the preculture was taken from the 9 L-bioreactor at the beginning of a batch cycle. At this time point, the ethanol concentration is high and the acetic acid as well as the biomass concentrations are low. It will be of great interest to characterize the susceptibility of acetic acid bacteria to oxygen depletion throughout one batch cycle, i.e. in dependency of different concentrations of ethanol and acetic acid as well as dissolved oxygen tension. Shut off experiments in the bubble column are suggested for that purpose. If the inoculation according to the aerated inoculation scheme proves to be suitable at the end of a batch cycle in the 9 L-bioreactor one single batch as a kind of a repeated batch, i.e. one part of fermentation medium is inoculated with two parts of preculture, would also be possible in the RAMOS device.

Although the semiconductor gas sensors on ShaRBS proved to be suitable to conduct repeated batch vinegar fermentation, these sensors have the drawback, that they are sensitive to the oxygen partial pressure in the headspace of the reactors. Co-monitoring of the oxygen partial pressure with electrochemical oxygen sensors is one option to compensate this effect, but this implicates susceptibility to errors in the measurement of the oxygen partial pressure. Thus, the outliers in the oxygen partial pressure were also found in the ethanol signal (figure 29). Moreover, the semiconductor gas sensors are temperature-sensitive. If the system is not built up in a temperature-controlled room or if temperature shifts should be investigated, a temperature compensation needs to be implemented. Therefore, more specific infrared sensors might be considered as an alternative to the semiconductor gas sensors. According to the manufacturer's information, commercially available infrared sensors are prone to corrosion in the presence of acetic acid and with that only suitable to a limited extent for vinegar fermentation. Custom-made (infrared) sensors might ultimately be the best but most expensive and cumbersome solution.

The oxygen analysis of the ShaRBS does not only allow the characterization of the bacterial respiration activity, but also the identification of the maximum oxygen transfer capacities of the ShaRBS in vinegar fermentation. Starting at low shaking frequency with high liquid filling volume the bacteria are cultivated until oxygen limitation is reached. Then, the shaking frequency is increased stepwise to adjust to higher oxygen transfer capacities (at reduced filling volumes) whenever oxygen limitation is reached. Afterwards, the gas/liquid mass transfer coefficient ($k_L a$) in correlation to the shaking frequency (and liquid filling volume) can be determined from the measured maximum oxygen transfer rates and oxygen partial

pressures by assuming a dissolved oxygen concentration close to zero during oxygen limitation (equation (38)).

Finally, since the ethanol concentration is determined reliably by considering the oxygen partial pressure compensation, repeated fed-batch vinegar fermentation could be addressed in the ShaRBS. Repeated fed-batch fermentation is the industrially predominant operation mode in spirit vinegar fermentation, because higher acetic acid concentrations are achieved than in repeated batch mode. Thus, it is worthwhile to imitate repeated fed-batch also on small scale to study the effect of diverse influence factors at increased acetic acid concentrations meaning at increased stress of the bacteria.

7 Appendix

7.1 Recapitulation of the used models for vinegar fermentation

To describe vinegar fermentation two kinetic models from literature were adopted and combined. The model of Romero et al. [98] was used to calculate the growth of the acetic acid bacteria. The model of Gomez and Cantero [99] was used to compute the consumption of ethanol and formation of acetic acid. The growth rate (μ) of the acetic acid bacteria is given by equation (I):

$$\mu = \mu_{max}\left(\frac{E}{E + K_{SE} + \left(\frac{E}{K_{IE}}\right)^2}\right)\left(\frac{1 + \frac{A}{K_{SA}}}{1 + \left(\frac{A}{K_{IA}}\right)^3}\right)\left(\frac{\frac{O}{K_{SO}}}{1 + \left(\frac{O}{K_{IO}}\right)^3}\right) \tag{I}$$

with the maximal growth rate μ_{max}, the ethanol concentration E, the ethanol saturation constant K_{SE}, the ethanol inhibition constant K_{IE}, the acetic acid concentration A, the acetic acid activation constant K_{SA}, the acetic acid inhibition constant K_{IA}, the oxygen concentration O, the oxygen activation constant K_{SO} and the oxygen inhibition constant K_{IO}. By assuming the optimal dissolved oxygen concentration (O_{opt}), the term for the influence of oxygen in equation (I) can be calculated to O_{max} and can be included into the maximal growth rate μ^*_{max} (equation (II)). The values of all the model parameters are given in Table 3.

$$\begin{aligned}\mu &= \mu_{max}\left(\frac{E}{E + K_{SE} + \left(\frac{E}{K_{IE}}\right)^2}\right)\left(\frac{1 + \frac{A}{K_{SA}}}{1 + \left(\frac{A}{K_{IA}}\right)^3}\right)O_{max} \\ &= \mu^*_{max}\left(\frac{E}{E + K_{SE} + \left(\frac{E}{K_{IE}}\right)^2}\right)\left(\frac{1 + \frac{A}{K_{SA}}}{1 + \left(\frac{A}{K_{IA}}\right)^3}\right)\end{aligned} \tag{II}$$

Table 3: Parameters of the model for vinegar fermentation

Symbol		Ref.	Symbol		Ref.	Symbol		Ref.
K_{IA}	17.9 g/L	[99]	K_{SE}	21.1 g/L	[99]	O_{opt}	1.55 mg/L	[98]
K_{IE}	2.83 g/L	[99]	K_{SO}	0.372 mg/L	[99]	O_{max}	2.785	
K_{IO}	1.96 mg/L	[99]	μ_{max}	0.22 h^{-1}	[98]	Y'_{XE}	7.2 mg/g	[99]
K_{SA}	12.6 g/L	[99]	μ^*_{max}	0.61 h^{-1}	[98]	Y_{EA}	0.769 g/g	[99]

The change of the biomass concentration X can be described by equation (III):

$$\frac{dX}{dt} = \mu \cdot X \tag{III}$$

Upon neglecting both, formation of byproducts such as ethyl acetate and assimilation, the rate of fermentative ethanol consumption is calculated according to the following equation (IV):

$$\frac{dE}{dt} = -\frac{1}{Y'_{XE}}\left(\frac{dX}{dt}\right) = -\frac{1}{Y'_{XE}} \cdot \mu \cdot X \tag{IV}$$

where Y'_{XE} is the yield coefficient for biomass from ethanol. Likewise, the fermentative acetic acid formation rate is given by equation (V):

$$\frac{dA}{dt} = \frac{1}{Y_{EA}}\left(-\frac{dE}{dt}\right) = \frac{1}{Y_{EA}} \cdot \frac{1}{Y'_{XE}} \cdot \mu \cdot X \tag{V}$$

where Y_{EA} is the stoichiometric coefficient for the conversion of ethanol into acetic acid.

7.2 Concentration changes due to filling a reactor

During the filling phase of a conventional bioreactor operated in repeated batch mode two aspects that lead to concentration changes of a specific compound in the culture broth must be considered: first, the addition of this specific compound via the feed solution, and second, the dilution of this compound by the volume change. By neglecting any volume contraction or dilatation because of physicochemical properties, the concentration c of any compound in the mixture of the residual culture broth after draining and the addition of feed solution can be calculated as follows (equation (VI)):

$$c = \frac{c_0 \cdot V_0 + c_f \cdot V_f}{V_0 + V_f} \tag{VI}$$

with c_0 and c_f the concentration of the compound in the residual culture broth and feed solution, respectively, as well as V_0 and V_f the volume of the residual culture broth and added feed solution, respectively. The volume of added feed solution can be described by the product of the filling rate F and the time period of filling (equation (VII)). Thereby, the time period of filling is the difference of the actual time t and the time point t_0 when the feed pump is started.

$$V_f = F \cdot (t - t_0) \tag{VII}$$

Insertion of equation (VII) into equation (VI) leads to a function of time for the concentration of any compound in the reactor during the filling phase (equation (VIII)):

$$c = \frac{c_0 \cdot V_0 + c_f \cdot F \cdot (t - t_0)}{V_0 + F \cdot (t - t_0)} \tag{VIII}$$

Differentiation of equation (VIII) results in equation (IX) which consequently describes the concentration changes of any compound during the filling of the reactor with feed solution.

$$\frac{dc}{dt} = \frac{F \cdot V_0 \cdot (c_f - c_0)}{(V_0 + F \cdot (t - t_0))^2} \tag{IX}$$

With respect to the maximum filling volume V_{max} of the reactor, the dilution rate D (equation (X)) and the relative filling volume V_{rel} of the reactor (equation (XI)), equation (IX) can be rewritten to equation (1) as follows:

$$D = \frac{F}{V_{max}} \tag{X}$$

$$V_{rel} = \frac{V}{V_{max}} \tag{XI}$$

$$\frac{dc}{dt} = \frac{D \cdot V_{rel,0} \cdot (c_f - c_0)}{\left(V_{rel,0} + D \cdot (t - t_0)\right)^2} \tag{1}$$

with V the absolute filling volume of the reactor and $V_{rel,0}$ the relative filling volume at the end of the draining phase when the feed pump is started.

7.3 Calculation of diffusion coefficient of oxygen in air

To calculate the borehole dimensions in the microtiter plate lid (equation (33)) the diffusion coefficient of oxygen in air needs to be known. The diffusion coefficient D_i of a component i in a multicomponent gas mixture depends on the composition of the gas mixture and can be calculated by means of the binary diffusion coefficients D_{ij} of the component i with respect to each component j of the mixture as follows [106, 109, 110, 113]:

$$D_i = \frac{p_{abs} - p_i}{\sum_{j=2}^{N} \frac{p_j}{D_{ij}}} \tag{XII}$$

Here, p_i and p_j are the partial pressures of the components i and j, respectively. The term N is the number of components in the mixture. For the diffusion coefficient of oxygen in air, equation (XII) yields:

$$D_{O_2,air} = \frac{p_{abs} - p_{O_2,air}}{\frac{p_{CO_2,air}}{D_{O_2,CO_2}} + \frac{p_{N_2,air}}{D_{O_2,N_2}}} \tag{XIII}$$

with $p_{CO_2,air}$ and $p_{N_2,air}$ being the partial pressure of carbon dioxide and nitrogen, respectively. The terms D_{O_2,CO_2} and D_{O_2,N_2} denote the binary diffusion coefficients of oxygen with respect to carbon dioxide and nitrogen, respectively. The binary diffusion coefficients can be calculated based on the molecular characteristics of the two components as follows [108, 112]:

$$D_{ij} = \frac{0.001858 \cdot \sqrt{T^3 \cdot \frac{M_i + M_j}{M_i M_j}}}{p_{abs} \cdot \sigma_{ij}^2 \cdot \Omega_{D_{ij}}^*} \tag{XIV}$$

Here, M_i and M_j denote the molecular weights in g/mol of component i and j, respectively. The term σ_{ij} is the characteristic length in Å of the intermolecular potential between component i and j that can be obtained from the geometric mean of the zero energy collision diameters σ_i and σ_j in Å of component i and j, respectively (equation (XV)). The term $\Omega_{D_{ij}}^*$ signifies the reduced dimensionless diffusion collision integral between component i and j and can be calculated using equation (XX).

$$\sigma_{ij} = \sqrt{\sigma_i \cdot \sigma_j} \tag{XV}$$

The zero energy collision diameter σ_i of any component i can be described by the following equation:

$$\sigma_i = \sqrt[3]{\frac{1.585 \cdot V_{lb,i}}{1 + 1.3 \cdot \delta_i^2}} \tag{XVI}$$

with $V_{lb,i}$ being the molar volume of the component i in the liquid state at the normal boiling point in cm^3/mol and δ_i being the dimensionless polarity parameter of component i. The

molar volume of component i in the liquid state at the normal boiling point is the inverse of the molar density $\rho_{lb,i}$ at the normal boiling point (equation (XVII)) that can be calculated according to equation (XVIII) [112].

$$V_{lb,i} = \frac{1}{\rho_{lb,i}} \tag{XVII}$$

$$\rho_{lb,i} = \frac{C_{1,i}}{C_{2,i}^{\left[1+\left(1-\frac{T_{b,i}}{C_{3,i}}\right)^{C_{4,i}}\right]}} \tag{XVIII}$$

The constants $C_{1,i}$ to $C_{4,i}$ for each component can be found in Perry's Chemical Engineers' Handbook [112]. The polarity parameter δ_i in equation (XVI) is given as follows:

$$\delta_i = 1.94 \cdot 10^3 \cdot \frac{\mu_i^2}{V_{lb,i} \cdot T_{b,i}} \tag{XIX}$$

where $T_{b,i}$ is the normal boiling point in Kelvin and μ_i is the dipole moment in Debyes of component i. The normal boiling points are available from the Handbook of Chemistry and Physics [111]. Here, the components of interest, i.e. oxygen, carbon dioxide and nitrogen, are nonpolar. Therefore, the dipole moment and, in turn, the dimensionless polarity parameter become zero. Furthermore, the reduced dimensionless diffusion collision integral $\Omega_{D_{ij}}^*$ between component i and j is equal to the dimensionless diffusion collision integral $\Omega_{D_{ij}}$ between component i and j (equations (XX) to (XXII)):

$$\Omega_{D_{ij}}^* = \Omega_{D_{ij}} + 0.19 \cdot \frac{\delta_{ij}^2}{T_{ij}^*} \tag{XX}$$

$$\Omega_{D_{ij}} = \left(44.54 \cdot {T_{ij}^*}^{-4.909} + 1.911 \cdot {T_{ij}^*}^{-1.575}\right)^{0.10} \tag{XXI}$$

$$\delta_{ij} = \sqrt{\delta_i \cdot \delta_j} \tag{XXII}$$

The dimensionless polarity parameter δ_{ij} between component i and j can be well approximated using the geometric mean of the dimensionless polarity parameters δ_i and δ_j [108]. The term T_{ij}^* denotes the reduced temperature and can be calculated as follows:

$$T_{ij}^{*} = \frac{T}{1.18 \cdot \sqrt{T_{b,i} \cdot \left(1 + 1.3 \cdot \delta_i^2\right) \cdot T_{b,j} \cdot \left(1 + 1.3 \cdot \delta_j^2\right)}} \quad \text{(XXIII)}$$

8 References

1) Ebner H., Follmann H. and Sellmer S. "Vinegar" in "Biotechnology", Rehm H.-J., Reed G., Pühler A. and Stadler P. (eds.) Wiley-VCH, Weinheim, Germany, 1995: vol. 9 pp. 579-591

2) Stratford M. "Traditional Preservatives - Organic Acids" in "Encyclopedia of Food Microbiology", Robinson R. K. (ed.) Academic Press, London, United Kingdom, 1999: vol. 1-3 pp. 1729-1737

3) Surekha M. and Reddy S. M. "Preservatives / Classification and Properties" in "Encyclopedia of Food Microbiology", Robinson R. K. (ed.) Academic Press, London, United Kingdom, 1999: vol. 1-3 pp. 1710-1717

4) "Verordnung über den Verkehr mit Essig und Essigessenz" Bundesgesetzblatt Teil I from 04/25/1972, p. 732 (in German)

5) Solieri L. and Giudici P. (eds.) "Vinegars of the World" Springer, Milan, Italy, 2009

6) Hromatka O. and Ebner H. "Untersuchungen über die Essiggärung. I. Fesselgärung und Durchlüftungsverfahren" Enzymologia, 1949: 13 (6) 369-387 (in German)

7) Sievers M. and Swings J. "Family II. Acetobacteriaceae" in "Bergey's Manual of Systematic Bacteriology, Volume Two: The Proteobacteria", Garrity G. M., Brenner D. J., Krieg N. R. and Staley J. R. (eds.) Springer, New York, New York, U.S.A., 2005: vol. 2 (Part C) pp. 41-54

8) Hromatka O. and Ebner H. "Untersuchungen über die Essiggärung. II. Sauerstoffmangel der Fesselgärung" Enzymologia, 1950: 14 (2) 96-106 (in German)

9) Hromatka O. and Ebner H. "Untersuchungen über die Essiggärung. III. Über den Einfluss der Belüftung auf die submerse Gärung" Enzymologia, 1951: 15 (2) 57-69 (in German)

10) Hromatka O., Ebner H. and Csoklich C. "Untersuchungen über die Essiggärung. IV. Über den Einfluss einer vollständigen Unterbrechung der Belüftung auf die submerse Gärung" Enzymologia, 1951: 15 (3) 134-153 (in German)

11) Hromatka O. and Exner W. "Untersuchungen über die Essiggärung. VIII. Weitere Erkenntnisse über die Unterbrechung der Belüftung" Enzymologia, 1962: 25 (1) 37-51 (in German)

12) Ebner H., Follmann H. and Sellmer S. "Vinegar" in "Ullmann's Encyclopedia of Industrial Chemistry", Wiley-VCH, Weinheim, Germany, 1996: vol. A 27 pp. 403-418

13) Ebner H. and Sellmer-Wilsberg S. "Vinegar, Acetic Acid Production" in "Encyclopedia of Bioprocess Technology - Fermentation, Biocatalysis, and Bioseparation", Flickinger M. C. and Drew S. W. (eds.) John Wiley and Sons, Weinheim, Germany, 1999: vol. 1-5 pp. 2637-2647

14) Ebner H., Follmann H. and Sellmer S. "Vinegar" in "Ullmann's Encyclopedia of Industrial Chemistry", Wiley-VCH, Weinheim, Germany, 2001: Electronic Release

15) Mesa M. M., Caro I. and Cantero D. "Viability reduction of *Acetobacter aceti* due to the absence of oxygen in submerged cultures" Biotechnology Progress, 1996: 12 (5) 709-712

16) Muraoka H., Watabe Y. and Ogasawara N. "Effect of Oxygen Deficiency on Acid Production and Morphology of Bacterial Cells in Submerged Acetic Fermentation by *Acetobacter aceti*" Journal of Fermentation Technology, 1982: 60 (3) 171-180

17) Entani E., Ohmori S., Masai H. and Suzuki K. I. "*Acetobacter Polyoxogenes* Sp. Nov., a New Species of an Acetic Acid Bacterium Useful for Producing Vinegar with High Acidity" Journal of General and Applied Microbiology, 1985: 31 (5) 475-490

18) Kittelmann M., Stamm W. W., Follmann H. and Trüper H. G. "Isolation and Classification of Acetic Acid Bacteria from High Percentage Vinegar Fermentations" Applied Microbiology and Biotechnology, 1989: 30 (1) 47-52

19) Sievers M., Sellmer S. and Teuber M. "*Acetobacter europaeus* sp. nov., a Main Component of Industrial Vinegar Fermenters in Central Europe" Systematic and Applied Microbiology, 1992: 15 (3) 386-392

20) Sokollek S. J., Hertel C. and Hammes W. P. "Cultivation and preservation of vinegar bacteria" Journal of Biotechnology, 1998: 60 (3) 195-206

21) Beppu T. "Genetic organization of *Acetobacter* for acetic acid fermentation" Antonie Van Leeuwenhoek, 1993: 64 (2) 121-135

22) De Vero L., Gullo M. and Giudici P. "Acetic acid bacteria, biotechnological applications" in "Encyclopedia of Industrial Biotechnology, Bioprocess, Bioseparation, and Cell Technology", Flickinger M. C. (ed.) John Wiley and Sons, Hoboken, New Jersey, U.S.A., 2010: vol. 1-7 pp. 9-25

23) Asai T. "Acetic Acid Bacteria: Classification and Biochemical Activities" University of Tokyo Press, Tokyo, Japan, 1968: pp. 1-343

24) Cook K. E. and Colvin J. R. "Evidence for a Beneficial Influence of Cellulose Production on Growth of *Acetobacter xylinum* in Liquid Medium" Current Microbiology, 1980: 3 (4) 203-205

25) Steel R. and Walker T. K. "Celluloseless Mutants of Certain *Acetobacter* Species" Journal of General Microbiology, 1957: 17 (1) 12-18

26) Kulka D. and Walker T. K. "The Ketogenic Activities of *Acetobacter* Species in a Glucose Medium" Archives of Biochemistry and Biophysics, 1954: 50 (1) 169-179

27) Steel R. and Walker T. K. "A Comparative Study of Cellulose-Producing Cultures and Celluloseless Mutants of Certain *Acetobacter* Spp." Journal of General Microbiology, 1957: 17 (2) 445-452

28) Ohmori S., Uozumi T. and Beppu T. "Loss of Acetic Acid Resistance and Ethanol Oxidizing Ability in an *Acetobacter* Strain" Agricultural and Biological Chemistry, 1982: 46 (2) 381-389

29) Takemura H., Horinouchi S. and Beppu T. "Novel Insertion Sequence Is*1380* from *Acetobacter pasteurianus* Is Involved in Loss of Ethanol-Oxidizing Ability" Journal of Bacteriology, 1991: 173 (22) 7070-7076

30) Kondo K. and Horinouchi S. "Characterization of an Insertion Sequence, IS*12528*, from *Gluconobacter suboxydans*" Applied and Environmental Microbiology, 1997: 63 (3) 1139-1142

31) Kondo K. and Horinouchi S. "A new insertion sequence IS*1452* from *Acetobacter pasteurianus*" Microbiology, 1997: 143 539-546

32) Greenberg D. E., Porcella S. F., Zelazny A. M., Virtaneva K., Sturdevant D. E., Kupko III J. J., Barbian K. D., Babar A., Dorward D. W. and Holland S. M. "Genome Sequence Analysis of the Emerging Human Pathogenic Acetic Acid Bacterium *Granulibacter bethesdensis*" Journal of Bacteriology, 2007: 189 (23) 8727-8736

33) Prust C., Hoffmeister M., Liesegang H., Wiezer A., Fricke W. F., Ehrenreich A., Gottschalk G. and Deppenmeier U. "Complete genome sequence of the acetic acid bacterium Gluconobacter oxydans" Nature Biotechnology, 2005: 23 (2) 195-200

34) Azuma Y., Hosoyama A., Matsutani M., Furuya N., Horikawa H., Harada T., Hirakawa H., Kuhara S., Matsushita K., Fujita N. and Shirai M. "Whole-genome analyses reveal genetic instability of *Acetobacter pasteurianus*" Nucleic Acids Research, 2009: 37 (17) 5768-5783

35) Siguier P., Perochon J., Lestrade L., Mahillon J. and Chandler M. "ISfinder: the reference centre for bacterial insertion sequences" Nucleic Acids Research, 2006: 34 D32-D36

36) Iversen T. G., Standal R., Pedersen T. and Coucheron D. H. "IS*1032* from *Acetobacter xylinum*, a New Mobile Insertion Sequence" Plasmid, 1994: 32 (1) 46-54

37) Valla S., Coucheron D. H. and Kjosbakken J. "*Acetobacter xylinum* Contains Several Plasmids: Evidence for Their Involvement in Cellulose Formation" Archives of Microbiology, 1983: 134 (1) 9-11

38) Gullo M., Mamlouk D., De Vero L. and Giudici P. "*Acetobacter pasteurianus* strain AB0220: Cultivability and Phenotypic Stability Over 9 Years of Preservation" Current Microbiology, 2012: 64 (6) 576-580

39) Anastassiadis S. and Rehm H.-J. "Citric acid production from glucose by yeast *Candida oleophila* ATCC 20177 under batch, continuous and repeated batch cultivation" Electronic Journal of Biotechnology, 2006: 9 (1) 26-39

40) Arzumanov T. E., Shishkanova N. V. and Finogenova T. V. "Biosynthesis of citric acid by *Yarrowia lipolytica* repeat-batch culture on ethanol" Applied Microbiology and Biotechnology, 2000: 53 (5) 525-529

41) Rywińska A. and Rymowicz W. "High-yield production of citric acid by *Yarrowia lipolytica* on glycerol in repeated-batch bioreactors" Journal of Industrial Microbiology and Biotechnology, 2010: 37 (5) 431-435

42) Zhao B., Wang L., Li F., Hua D., Ma C., Ma Y. and Xu P. "Kinetics of D-lactic acid production by *Sporolactobacillus* sp. strain CASD using repeated batch fermentation" Bioresource Technology, 2010: 101 (16) 6499-6505

43) Madhavan A., Tamalampudi S., Srivastava A., Fukuda H., Bisaria V. S. and Kondo A. "Alcoholic fermentation of xylose and mixed sugars using recombinant *Saccharomyces cerevisiae* engineered for xylose utilization" Applied Microbiology and Biotechnology, 2009: 82 (6) 1037-1047

44) Naritomi T., Kouda T., Yano H., Yoshinaga F., Shigematsu T., Moriumura S. and Kida K. "Influence of broth exchange ratio on bacterial cellulose production by repeated-batch culture" Process Biochemistry, 2002: 38 (1) 41-47

45) Jin I.-H., Jung D.-Y., Son C.-W., Kim S.-K., Gao W., Chung C.-H. and Lee J.-W. "Enhanced Production of Heteropolysaccharide-7 by *Beijerinckia indica* HS-2001 in Repeated Batch Culture with Optimized Substitution of Culture Medium" Biotechnology and Bioprocess Engineering, 2011: 16 (2) 245-255

46) Khanna S. and Srivastava A. K. "Repeated batch cultivation of *Ralstonia eutropha* for poly (β-hydroxybutyrate) production" Biotechnology Letters, 2005: 27 (18) 1401-1403

47) Masuda M., Das S. K., Fujihara S., Hatashita M. and Sakurai A. "Production of cordycepin by a repeated batch culture of a *Cordyceps militaris* mutant obtained by proton beam irradiation" Journal of Bioscience and Bioengineering, 2011: 111 (1) 55-60

48) Zhang W., Jin M. F., Yu X. J. and Yuan Q. "Enhanced anthocyanin production by repeated-batch culture of strawberry cells with medium shift" Applied Microbiology and Biotechnology, 2001: 55 (2) 164-169

49) Damir O., Mladen P., Božidar S. and Srđan N. "Cultivation of the bacterium *Azotobacter chroococcum* for preparation of biofertilizers" African Journal of Biotechnology, 2011: 10 (16) 3104-3111

50) Betts J. I. and Baganz F. "Miniature bioreactors: current practices and future opportunities" Microbial Cell Factories, 2006: 5 (1) 21

51) Büchs J. "Introduction to advantages and problems of shaken cultures" Biochemical Engineering Journal, 2001: 7 (2) 91-98

52) Fernandes P. and Cabral J. M. S. "Microlitre/millilitre shaken bioreactors in fermentative and biotransformation processes - a review" Biocatalysis and Biotransformation, 2006: 24 (4) 237-252

53) Kumar S., Wittmann C. and Heinzle E. "Minibioreactors" Biotechnology Letters, 2004: 26 (1) 1-10

54) Marques M. P. C., Cabral J. M. S. and Fernandes P. "High Throughput in Biotechnology: From Shake-Flasks to Fully Instrumented Microfermentors" Recent patents on biotechnology, 2009: 3 (2) 124-140

55) Weuster-Botz D. "Parallel Reactor Systems for Bioprocess Development" in "Technology Transfer in Biotechnology", Kragl U. (ed.) Springer-Verlag, Berlin, Germany, 2005: vol. 92 pp. 125-143

56) Duetz W. A. "Microtiter plates as mini-bioreactors: miniaturization of fermentation methods" Trends in Microbiology, 2007: 15 (10) 469-475

57) Anderlei T. and Büchs J. "Device for sterile online measurement of the oxygen transfer rate in shaking flasks" Biochemical Engineering Journal, 2001: 7 (2) 157-162

58) Anderlei T., Zang W., Papaspyrou M. and Büchs J. "Online respiration activity measurement (OTR, CTR, RQ) in shake flasks" Biochemical Engineering Journal, 2004: 17 (3) 187-194

59) Dale R. F., Amsz J., Shu P., Peppler H. J. and Rudert F. J. "A Continuous Feeding Assembly for Laboratory Fermentations" Applied Microbiology, 1953: 1 (2) 68-69

60) Weuster-Botz D., Altenbach-Rehm J. and Arnold M. "Parallel substrate feeding and pH-control in shaking-flasks" Biochemical Engineering Journal, 2001: 7 (2) 163-170

61) Ruottinen M., Bollok M., Kögler M., Neubauer A., Krause M., Hämäläinen E. R., Myllyharju J., Vasala A. and Neubauer P. "Improved production of human type II procollagen in the yeast *Pichia pastoris* in shake flasks by a wireless-controlled fed-batch system" Bmc Biotechnology, 2008: 8 (33) 1-12

62) van Leeuwen M., Buijs N. A. A., Canelas A. B., Oudshoorn A., Heijnen J. J. and van Gulik W. M. "The Hagen-Poiseuille pump for parallel fed-batch cultivations in microbioreactors" Chemical Engineering Science, 2009: 64 (8) 1877-1884

63) Buchenauer A., Funke M., Büchs J., Mokwa W. and Schnakenberg U. "Microbioreactors with microfluidic control and a user-friendly connection to the actuator hardware" Journal of Micromechanics and Microengineering, 2009: 19 (7 (074012)) 1-8

64) Buchenauer A., Hofmann M. C., Funke M., Büchs J., Mokwa W. and Schnakenberg U. "Micro-bioreactors for fed-batch fermentations with integrated online monitoring and microfluidic devices" Biosensors and Bioelectronics, 2009: 24 (5) 1411-1416

65) Funke M., Buchenauer A., Mokwa W., Kluge S., Hein L., Müller C., Kensy F. and Büchs J. "Bioprocess Control in Microscale: Scalable Fermentations in Disposable and User-Friendly Microfluidic Systems" Microbial Cell Factories, 2010: 9 (86) 1-13

66) Funke M., Buchenauer A., Schnakenberg U., Mokwa W., Diederichs S., Mertens A., Müller C., Kensy F. and Büchs J. "Microfluidic BioLector-Microfluidic Bioprocess Control in Microtiter Plates" Biotechnology and Bioengineering, 2010: 107 (3) 497-505

67) Harms P., Kostov Y., French J. A., Soliman M., Anjanappa M., Ram A. and Rao G. "Design and Performance of a 24-Station High Throughput Microbioreactor" Biotechnology and Bioengineering, 2006: 93 (1) 6-13

68) Knorr B., Schlieker H., Hohmann H. P. and Weuster-Botz D. "Scale-down and parallel operation of the riboflavin production process with *Bacillus subtilis*" Biochemical Engineering Journal, 2007: 33 (3) 263-274

69) Kusterer A., Krause C., Kaufmann K., Arnold M. and Weuster-Botz D. "Fully automated single-use stirred-tank bioreactors for parallel microbial cultivations" Bioprocess and Biosystems Engineering, 2008: 31 (3) 207-215

70) Zhang Z., Perozziello G., Boccazzi P., Sinskey A. J., Geschke O. and Jensen K. F. "Microbioreactors for Bioprocess Development" Journal of the Association for Laboratory Automation, 2007: 12 (3) 143-151

71) Altenbach-Rehm J., Nell C., Arnold M. and Weuster-Botz D. "Parallel Bubble Columns with Fed-Batch Technique for Microbial Process Development on a Small Scale" Chemical Engineering and Technology, 1999: 22 (12) 1051-1058

72) Dilsen S., Paul W., Herforth D., Sandgathe A., Altenbach-Rehm J., Freudl R., Wandrey C. and Weuster-Botz D. "Evaluation of parallel operated small-scale bubble columns for microbial process development using *Staphylococcus carnosus*" Journal of Biotechnology, 2001: 88 (1) 77-84

73) Puskeiler R., Kaufmann K. and Weuster-Botz D. "Development, Parallelization, and Automation of a Gas-Inducing Milliliter-Scale Bioreactor for High-Throughput Bioprocess Design (HTBD)" Biotechnology and Bioengineering, 2005: 89 (5) 512-523

74) Puskeiler R., Kusterer A., John G. T. and Weuster-Botz D. "Miniature bioreactors for automated high-throughput bioprocess design (HTBD): reproducibility of parallel fed-batch cultivations with *Escherichia coli*" Biotechnology and Applied Biochemistry, 2005: 42 227-235

75) Gerhardt P. and Gallup D. M. "Dialysis Flask for Concentrated Culture of Microorganisms" Journal of Bacteriology, 1963: 86 (5) 919-929

76) O'Sullivan C. Y. and Pirt S. J. "Penicillin Production by Lysine Auxotrophs of *Penicillium chrysogenum*" Journal of General Microbiology, 1973: 76 (1) 65-75

77) Pirt S. J. "The Diffusion Capsule, a Novel Device for Addition of a Solute at a Constant Rate to a Liquid Medium - Its Application to Metabolic Regulation" Biochemical Journal, 1971: 121 (2) 293-297

78) Bähr C., Leuchtle B., Lehmann C., Becker J., Jeude M., Peinemann F., Arbter R. and Büchs J. "Dialysis shake flask for effective screening in fed-batch mode" Biochemical Engineering Journal, 2012: 69 182-195

79) Tyrrell E. A., Mac Donald R. E. and Gerhardt P. "Biphasic System for Growing Bacteria in Concentrated Culture" Journal of Bacteriology, 1958: 75 (1) 1-4

80) Jeude M., Dittrich B., Niederschulte H., Anderlei T., Knocke C., Klee D. and Büchs J. "Fed-Batch Mode in Shake Flasks by Slow-Release Technique" Biotechnology and Bioengineering, 2006: 95 (3) 433-445

81) Scheidle M., Dittrich B., Klinger J., Ikeda H., Klee D. and Büchs J. "Controlling pH in shake flasks using polymer-based controlled-release discs with pre-determined release kinetics" Bmc Biotechnology, 2011: 11 (1) 25

82) Panula-Perälä J., Šiurkus J., Vasala A., Wilmanowski R., Casteleijn M. G. and Neubauer P. "Enzyme controlled glucose auto-delivery for high cell density cultivations in microplates and shake flasks" Microbial Cell Factories, 2008: 7 (1) 31

83) Krause M., Ukkonen K., Haataja T., Ruottinen M., Glumoff T., Neubauer A., Neubauer P. and Vasala A. "A novel fed-batch based cultivation method provides high cell-density and improves yield of soluble recombinant proteins in shaken cultures" Microbial Cell Factories, 2010: 9 (1) 11

84) Walther I., van der Schoot B. H., Jeanneret S., Arquint P., de Rooij N. F., Gass V., Bechler B., Lorenzi G. and Cogoli A. "Development of a miniature bioreactor for continuous culture in a space laboratory" Journal of Biotechnology, 1994: 38 (1) 21-32

85) Akgün A., Maier B., Preis D., Roth B., Klingelhöfer R. and Büchs J. "A Novel Parallel Shaken Bioreactor System for Continuous Operation" Biotechnology Progress, 2004: 20 (6) 1718-1724

86) Akgün A., Müller C., Engmann R. and Büchs J. "Application of an improved continuous parallel shaken bioreactor system for three microbial model systems" Bioprocess and Biosystems Engineering, 2008: 31 (3) 193-205

87) Huber R., Ritter D., Hering T., Hillmer A. K., Kensy F., Müller C., Wang L. and Büchs J. "Robo-Lector - a novel platform for automated high-throughput cultivations in microtiter plates with high information content" Microbial Cell Factories, 2009: 8 (42) 1-15

88) Huber R., Roth S., Rahmen N. and Büchs J. "Utilizing high-throughput experimentation to enhance specific productivity of an *E.coli* T7 expression system by phosphate limitation" Bmc Biotechnology, 2011: 11 (22) 1-11

89) Kensy F., Zang E., Faulhammer C., Tan R. K. and Büchs J. "Validation of a high-throughput fermentation system based on online monitoring of biomass and fluorescence in continuously shaken microtiter plates" Microbial Cell Factories, 2009: 8 (1) 31

90) Samorski M., Müller-Newen G. and Büchs J. "Quasi-Continuous Combined Scattered Light and Fluorescence Measurements: A Novel Measurement Technique for Shaken Microtiter Plates" Biotechnology and Bioengineering, 2005: 92 (1) 61-68

91) Funke M., Diederichs S., Kensy F., Müller C. and Büchs J. "The Baffled Microtiter Plate: Increased Oxygen Transfer and Improved Online Monitoring in Small Scale Fermentations" Biotechnology and Bioengineering, 2009: 103 (6) 1118-1128

92) Fernandes P., Carvalho F. and Marques M. P. C. "Miniaturization in Biotechnology: Speeding up the Development of Bioprocesses" Recent patents on biotechnology, 2011: 5 (3) 160-173

93) Zimmermann H. F., John G. T., Trauthwein H., Dingerdissen U. and Huthmacher K. "Rapid Evaluation of Oxygen and Water Permeation through Microplate Sealing Tapes" Biotechnology Progress, 2003: 19 (3) 1061-1063

94) Arain S., Weiss S., Heinzle E., John G. T., Krause C. and Klimant I. "Gas sensing in microplates with optodes: Influence of oxygen exchange between sample, air, and plate material" Biotechnology and Bioengineering, 2005: 90 (3) 271-280

95) Duetz W. A., Kühner M. and Lohser R. "Microbial and cell growth in microtiter plates" Genetic Engineering News, 2006: 26 (11) 44

96) Perlman D. "Cell culture plate with oxygen and carbon dioxide-permeable waterproof sealing membrane" US5858770, 1999

97) Duetz W. A., Rüedi L., Hermann R., O'Connor K., Büchs J. and Witholt B. "Methods for Intense Aeration, Growth, Storage, and Replication of Bacterial Strains in Microtiter Plates" Applied and Environmental Microbiology, 2000: 66 (6) 2641-2646

98) Romero L. E., Gómez J. M., Caro I. and Cantero D. "A kinetic model for growth of *Acetobacter aceti* in submerged culture" The Chemical Engineering Journal and the Biochemical Engineering Journal, 1994: 54 (1) B15-B24

99) Gómez J. M. and Cantero D. "Kinetics of substrate consumption and product formation in closed acetic fermentation systems" Bioprocess Engineering, 1998: 18 (6) 439-444

100) Kohl D. "Surface Processes in the Detection of Reducing Gases with SnO_2-Based Devices" Sensors and Actuators, 1989: 18 (1) 71-113

101) Kohl D. "Function and applications of gas sensors" Journal of Physics D: Applied Physics, 2001: 34 (19) R125-R149

102) Morrison S. R. "Semiconductor Gas Sensors" Sensors and Actuators, 1982: 2 (4) 329-341

103) Anderlei T. "Entwicklung einer Meßanlage zur Online-Bestimmung der Atmungsaktivität von mikrobiellen Kulturen in geschüttelten Bioreaktoren" RWTH Aachen University, Aachen, Germany, 2001 (in German)

104) Beitz W. and Küttner K.-H. (eds.) "Dubbel - Taschenbuch für den Maschinenbau" Springer, Berlin, Germany, 1995 (in German)

105) Hansen S., Hariskos I., Luchterhand B. and Büchs J. "Development of a modified Respiration Activity Monitoring System for accurate and highly resolved measurement of respiration activity in shake flask fermentations" Journal of biological engineering, 2012: 6 (11) 1-12

106) Amoabediny G. and Büchs J. "Modelling and advanced understanding of unsteady-state gas transfer in shaking bioreactors" Biotechnology and Applied Biochemistry, 2007: 46 57-67

107) Mrotzek C., Anderlei T., Henzler H. J. and Büchs J. "Mass transfer resistance of sterile plugs in shaking bioreactors" Biochemical Engineering Journal, 2001: 7 (2) 107-112

108) Brokaw R. S. "Predicting Transport Properties of Dilute Gases" Industrial and Engineering Chemistry Process Design and Development, 1969: 8 (2) 240-253

109) Fairbanks D. F. and Wilke C. R. "Diffusion Coefficients in Multicomponent Gas Mixtures" Industrial and Engineering Chemistry, 1950: 42 (3) 471-475

110) Henzler H. J. and Schedel M. "Suitability of the Shaking Flask for Oxygen-Supply to Microbiological Cultures" Bioprocess Engineering, 1991: 7 (3) 123-131

111) Lide D. R. "Handbook of Chemistry and Physics" Baysinger G., Craig N. C., Koetzle T. F., Kuchitsu K., Lin C. C., Smith A. L. and Frederikse H. P. R. (eds.) CRC Press, New York, New York, U.S.A., 1999:

112) Perry R. H. and Green D. W. "Perry's Chemical Engineers' Handbook" Perry R. H., Green D. W. and Maloney J. O. (eds.) McGraw-Hill, New York, New York, U.S.A., 1997:

113) Wilke C. R. "Diffusional Properties of Multicomponent Gases" Chemical Engineering Progress, 1950: 46 (2) 95-104

114) Wilhelm E., Battino R. and Wilcock R. J. "Low-Pressure Solubility of Gases in Liquid Water" Chemical Reviews, 1977: 77 (2) 219-262

115) Rischbieter E., Schumpe A. and Wunder V. "Gas Solubilities in Aqueous Solutions of Organic Substances" Journal of Chemical and Engineering Data, 1996: 41 (4) 809-812

116) Maier U. and Büchs J. "Characterisation of the gas-liquid mass transfer in shaking bioreactors" Biochemical Engineering Journal, 2001: 7 (2) 99-106

117) Seletzky J. M., Noak U., Fricke J., Welk E., Eberhard W., Knocke C. and Büchs J. "Scale-Up From Shake Flasks to Fermenters in Batch and Continuous Mode With *Corynebacterium glutamicum* on Lactic Acid Based on Oxygen Transfer and pH" Biotechnology and Bioengineering, 2007: 98 (4) 800-811

118) Bar R., Gainer J. L. and Kirwan D. J. "An Unusual Pattern of Product Inhibition: Batch Acetic Acid Fermentation" Biotechnology and Bioengineering, 1987: 29 (6) 796-798

119) Ito T., Sota H., Honda H., Shimizu K. and Kobayashi T. "Efficient acetic acid production by repeated fed-batch fermentation using two fermentors" Applied Microbiology and Biotechnology, 1991: 36 (3) 295-299

120) Jiménez-Hornero J. E., Santos-Dueñas I. M. and García-García I. "Optimization of biotechnological processes. The acetic acid fermentation. Part III: Dynamic optimization" Biochemical Engineering Journal, 2009: 45 (1) 22-29

121) Kruppa R. K. and Vortmeyer D. "Transient growth- and product-formation kinetics of acetic acid bacteria" Bioprocess Engineering, 1999: 20 (6) 545-551

122) Nanba A., Tamura A. and Nagai S. "Synergistic Effects of Acetic Acid and Ethanol on the Growth of *Acetobacter* sp." Journal of Fermentation Technology, 1984: 62 (6) 501-505

123) Park Y. S., Ohtake H., Fukaya M., Okumura H., Kawamura Y. and Toda K. "Effects of Dissolved Oxygen and Acetic Acid Concentrations on Acetic Acid Production in Continuous Culture of *Acetobacter aceti*" Journal of Fermentation and Bioengineering, 1989: 68 (2) 96-101

124) Sengun I. Y. and Karabiyikli S. "Importance of acetic acid bacteria in food industry" Food Control, 2011: 22 (5) 647-656

125) Yamada Y. and Yukphan P. "Genera and species in acetic acid bacteria" International Journal of Food Microbiology, 2008: 125 (1) 15-24

126) Saeki A., Taniguchi M., Matsushita K., Toyama H., Theeragool G., Lotong N. and Adachi O. "Microbiological Aspects of Acetate Oxidation by Acetic Acid Bacteria, Unfavorable Phenomena in Vinegar Fermentation" Bioscience, Biotechnology and Biochemistry, 1997: 61 (2) 317-323

127) Emde F. "Vorrichtung zum Messen zumindest eines flüchtigen Bestandteils einer wässrigen Lösung, insbesondere zum Messen von Alkohol" WO2007/033395, 2007 (in German)

128) Heider M., Hofschneider J., Schallenberger W., Nodes F. and Kempe E. "Measurement of volatile constituents of a culture medium" US4404284, 1983

129) Guarna M. M., Lesnicki G. J., Tam B. M., Robinson J., Radziminski C. Z., Hasenwinkle D., Boraston A., Jervis E., MacGillivray R. T. A., Turner R. F. B. and Kilburn D. G. "On-line Monitoring and Control of Methanol Concentration in Shake-Flask Cultures of *Pichia pastoris*" Biotechnology and Bioengineering, 1997: 56 (3) 279-286

130) Mathur A. and Chand S. "Model-based evaluation of plasmid segregational instability in repeated batch culture with recombinant *Escherichia coli*" Chemical Engineering Journal, 2009: 153 (1-3) 227-230

131) Huang W.-C., Chen S.-J. and Chen T.-L. "Production of hyaluronic acid by repeated batch fermentation" Biochemical Engineering Journal, 2008: 40 (3) 460-464

Lebenslauf

Persönliche Daten

Name:	Schlepütz
Vorname:	Tino
Geburtstag:	20. Januar 1982
Geburtsort:	Simmerath
Staatsangehörigkeit:	Deutsch

Ausbildung

2001	Abitur am Burgau Gymnasium, Stadt Düren
2002 – 2005	Bachelorstudium Biotechnologie / molekulare Biotechnologie an der RWTH Aachen University
2005 – 2007	Masterstudium Biotechnologie / molekulare Biotechnologie an der RWTH Aachen University

Berufstätigkeit

Seit 2007	Wissenschaftlicher Mitarbeiter bei der Aachener Verfahrenstechnik - Bioverfahrenstechnik